

# Corso di Complementi di Gasdinamica

Tommaso Astarita  
[astarita@unina.it](mailto:astarita@unina.it)  
[www.docenti.unina.it](http://www.docenti.unina.it)



Complementi di Gasdinamica – T Astarita – Modulo 14 del 5/12/17

## MOTI IN CONDOTTI

### Applicazioni:

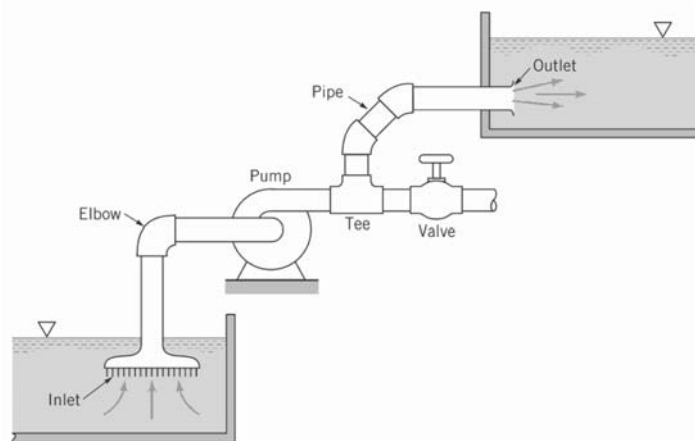
- The Alaskan pipeline carries crude oil almost 800 miles across Alaska.
- Natural systems of “pipes” that carry blood throughout our body and air into and out of our lungs.
- Water pipes in our homes and the distribution system that delivers the water from the city well to the house.
- Numerous hoses and pipes carry hydraulic fluid or other fluids to various components of vehicles and machines.
- The air quality within our buildings is maintained at comfortable levels by the distribution of conditioned (heated, cooled, humidified /dehumidified ) air through a maze of pipes and ducts.



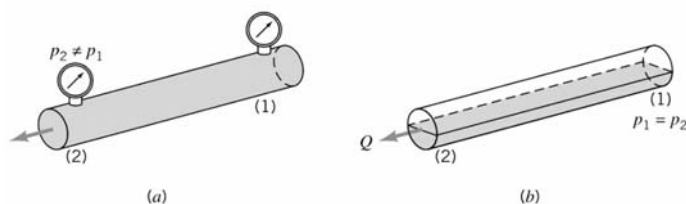
Complementi di Gasdinamica – T Astarita

# MOTI IN CONDOTTI

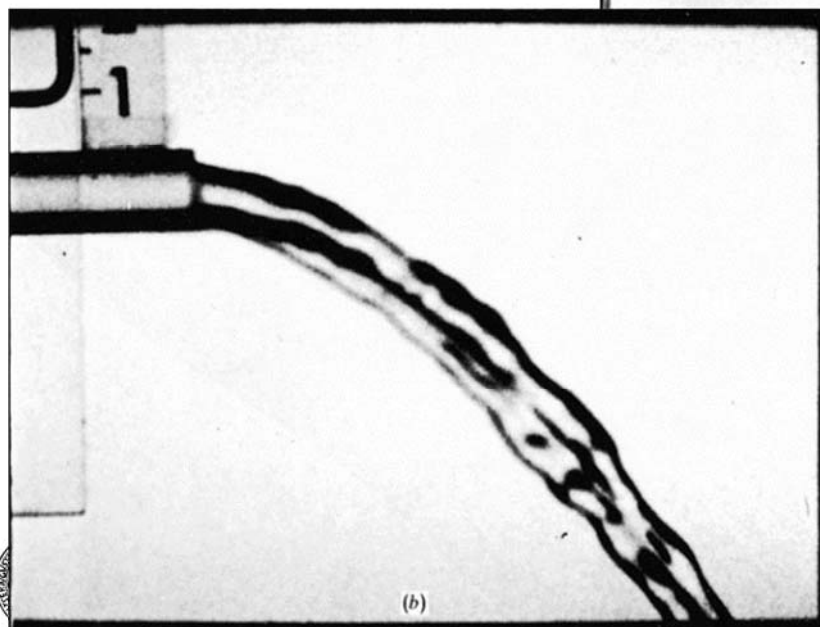
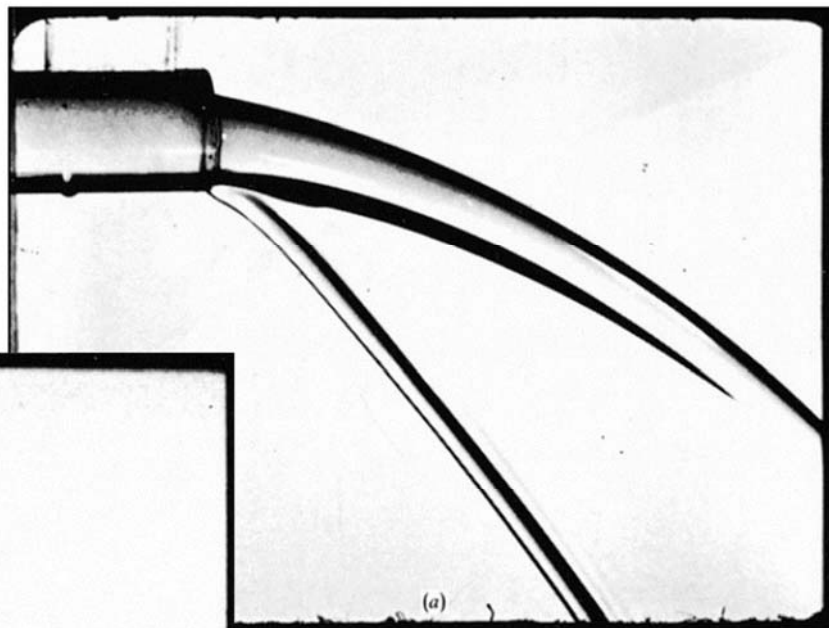
The transport of a fluid in a closed conduit (commonly called a pipe if it is of round cross section or a duct if it is not round) is extremely important in our daily operations.



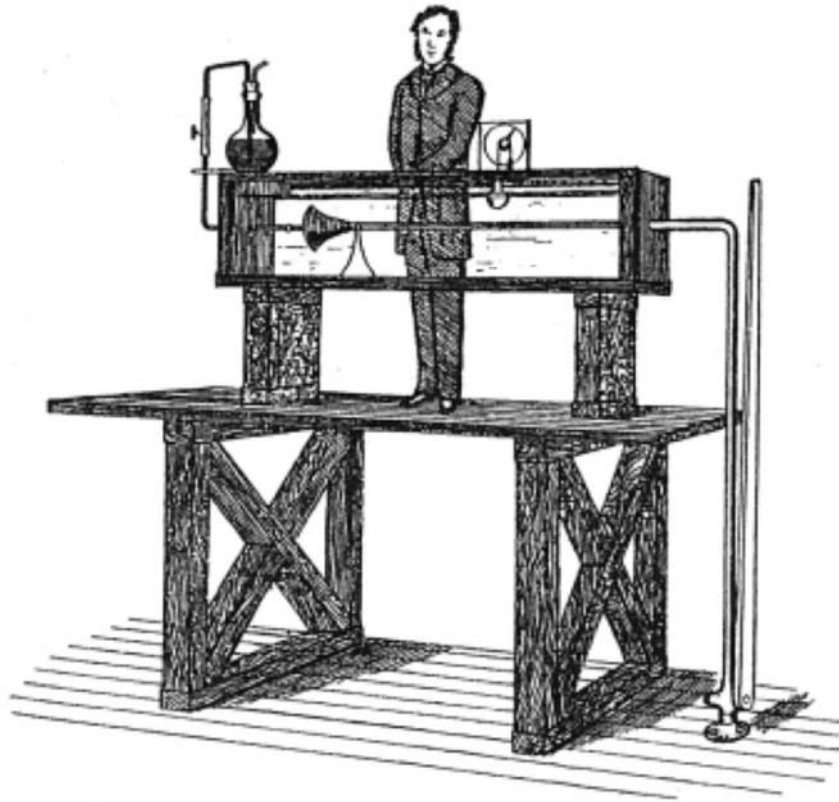
- a) Pipe flow
- b) Open channel flow



## MOTO LAMINARE - MOTO TURBOLENTO



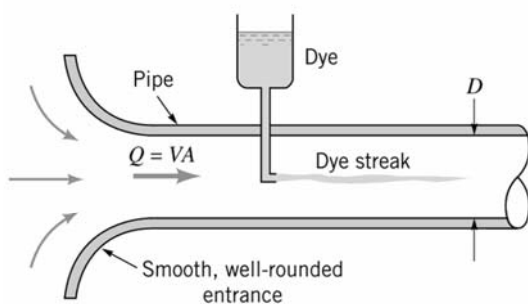
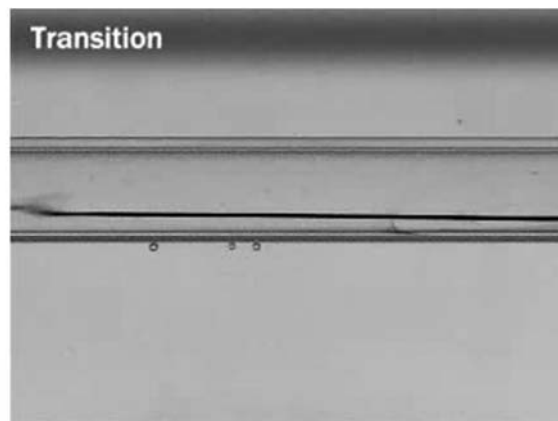
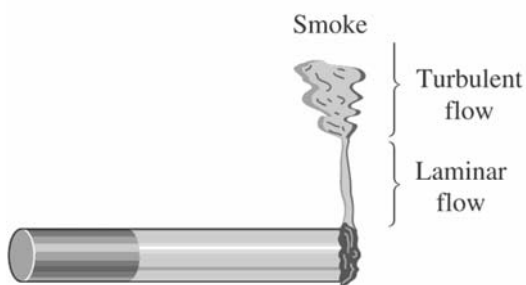
# MOTO LAMINARE - MOTO TURBOLENTO



Esperimento di Reynolds



# MOTO LAMINARE - MOTO TURBOLENTO



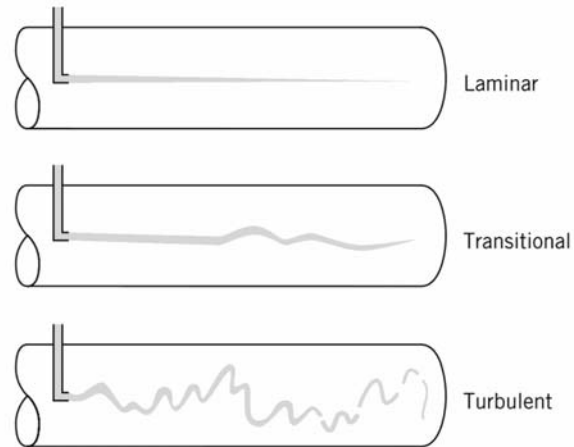
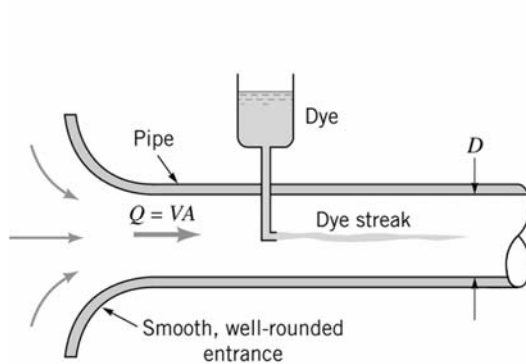
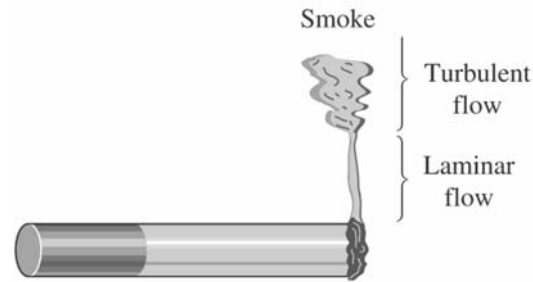
(a)



(b)



# MOTO LAMINARE - MOTO TURBOLENTO



(a)

(b)



Complementi di Gasdinamica – T Astarita

7

# MOTO LAMINARE - MOTO TURBOLENTO

- $0 < Re < 1$ : highly viscous laminar “creeping” motion
- $1 < Re < 100$ : laminar, strong Reynolds-number dependence
- $100 < Re < 10^3$ : laminar, boundary-layer theory useful
- $10^3 < Re < 10^4$ : transition to turbulence
- $10^4 < Re < 10^6$ : turbulent, moderate Reynolds-number dependence
- $10^6 < Re < \infty$ : turbulent, slight Reynolds-number dependence

These are representative ranges which vary somewhat with flow geometry, surface roughness, and the level of fluctuations in the inlet stream. The great majority of our analyses are concerned with laminar flow or with turbulent flow, and one should not normally design a flow operation in the transition region.



Complementi di Gasdinamica – T Astarita

8



# MOTO LAMINARE - MOTO TURBOLENTO

## EXAMPLE 6.1

The accepted transition Reynolds number for flow in a circular pipe is  $Re_{d,crit} \approx 2300$ . For flow through a 5-cm-diameter pipe, at what velocity will this occur at 20°C for (a) airflow and (b) water flow?

### Solution

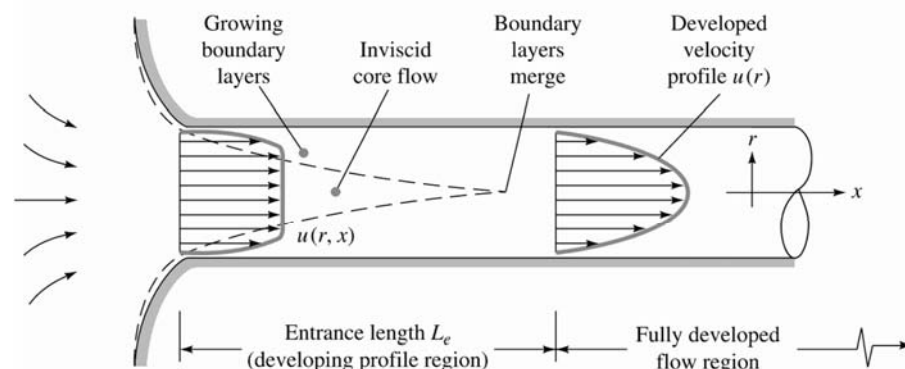
Almost all pipe-flow formulas are based on the *average* velocity  $V = Q/A$ , not centerline or any other point velocity. Thus transition is specified at  $\rho Vd/\mu \approx 2300$ . With  $d$  known, we introduce the appropriate fluid properties at 20°C from Tables A.3 and A.4:

(a) Air:  $\frac{\rho Vd}{\mu} = \frac{(1.205 \text{ kg/m}^3)V(0.05 \text{ m})}{1.80 \text{ E-5 kg/(m} \cdot \text{s)}} = 2300 \quad \text{or} \quad V \approx 0.7 \frac{\text{m}}{\text{s}}$

(b) Water:  $\frac{\rho Vd}{\mu} = \frac{(998 \text{ kg/m}^3)V(0.05 \text{ m})}{0.001 \text{ kg/(m} \cdot \text{s)}} = 2300 \quad \text{or} \quad V = 0.046 \frac{\text{m}}{\text{s}}$

These are very low velocities, so most engineering air and water pipe flows are turbulent, not laminar. We might expect laminar duct flow with more viscous fluids such as lubricating oils or glycerin.

## LUNGHEZZA D'INGRESSO

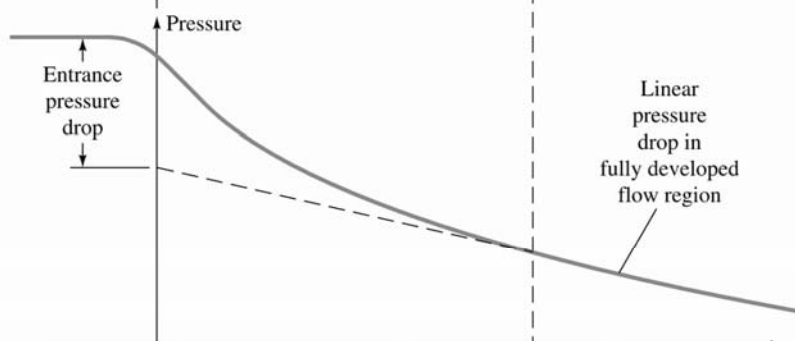


$$L_e = f(d, V, \rho, \mu)$$

$$\frac{L_e}{d} = g\left(\frac{\rho Vd}{\mu}\right) = g(Re)$$

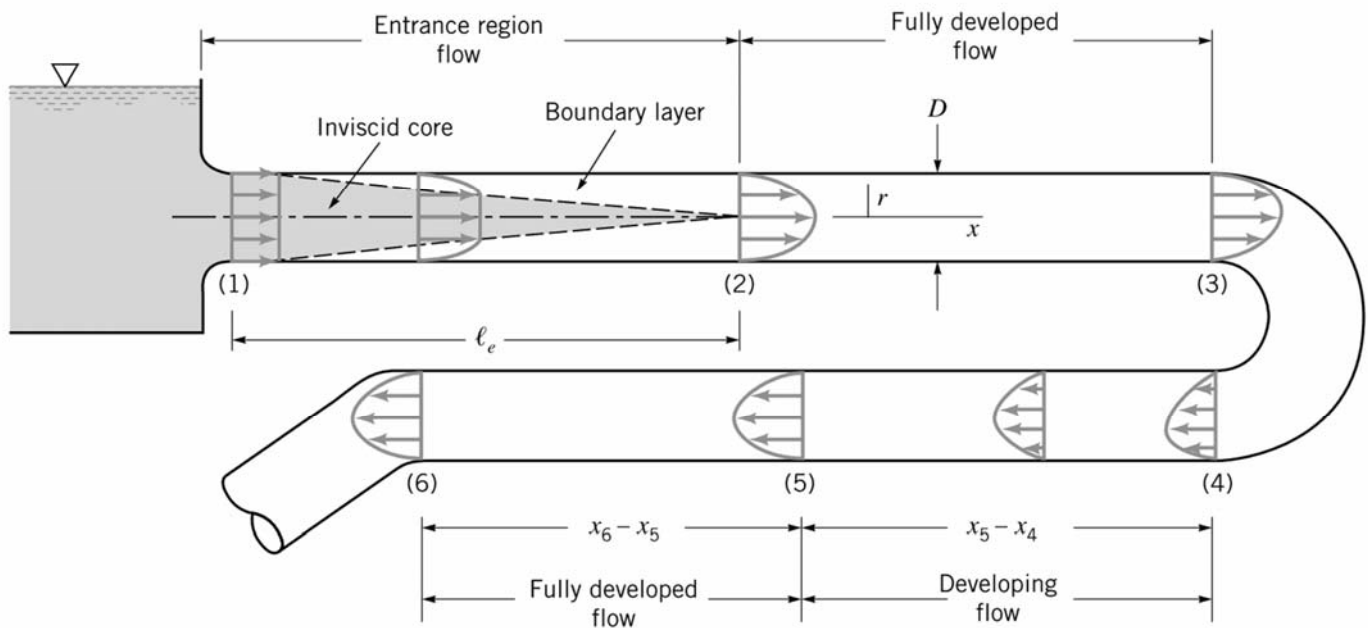
$$\frac{L_e}{d} \approx 0.06 Re \quad \text{laminar}$$

$$\frac{L_e}{d} \approx 4.4 Re_d^{1/6} \quad \text{turbulent}$$



$Re_d$	4000	$10^4$	$10^5$	$10^6$	$10^7$	$10^8$
$L_e/d$	18	20	30	44	65	95

# Lunghezza d'ingresso



# Lunghezza d'ingresso

## EXAMPLE 6.2

A  $\frac{1}{2}$ -in-diameter water pipe is 60 ft long and delivers water at 5 gal/min at 20°C. What fraction of this pipe is taken up by the entrance region?

## Solution

Convert

$$Q = (5 \text{ gal/min}) \frac{0.00223 \text{ ft}^3/\text{s}}{1 \text{ gal/min}} = 0.0111 \text{ ft}^3/\text{s}$$

The average velocity is

$$V = \frac{Q}{A} = \frac{0.0111 \text{ ft}^3/\text{s}}{(\pi/4)[(\frac{1}{2}/12) \text{ ft}]^2} = 8.17 \text{ ft/s}$$

From Table 1.4 read for water  $\nu = 1.01 \times 10^{-6} \text{ m}^2/\text{s} = 1.09 \times 10^{-5} \text{ ft}^2/\text{s}$ . Then the pipe Reynolds number is

$$\text{Re}_d = \frac{Vd}{\nu} = \frac{(8.17 \text{ ft/s})[(\frac{1}{2}/12) \text{ ft}]}{1.09 \times 10^{-5} \text{ ft}^2/\text{s}} = 31,300$$



## Lunghezza d'ingresso

$$\text{Re}_d = \frac{Vd}{\nu} = \frac{(8.17 \text{ ft/s})(\frac{1}{2}/12) \text{ ft}}{1.09 \times 10^{-5} \text{ ft}^2/\text{s}} = 31,300$$

This is greater than 4000; hence the flow is fully turbulent, and Eq. (6.6) applies for entrance length

$$\frac{L_e}{d} \approx 4.4 \text{Re}_d^{1/6} = (4.4)(31,300)^{1/6} = 25$$

The actual pipe has  $L/d = (60 \text{ ft})/[(\frac{1}{2}/12) \text{ ft}] = 1440$ . Hence the entrance region takes up the fraction

$$\frac{L_e}{L} = \frac{25}{1440} = 0.017 = 1.7\% \quad \text{Ans.}$$

This is a very small percentage, so that we can reasonably treat this pipe flow as essentially fully developed.



## CONSERVAZIONE DELLA MASSA E BILANCIO DELLA QM

$$\dot{m} = \rho VA = \text{cost}$$

Per flusso incompressibile e sezione costante si ha  $V = \text{cost}$ .

$$\dot{m}(V_2 - V_1) + p_1 A_1 n_1 + p_2 A_2 n_2 + S = \underline{m}g$$

Ricordando che:

$$S_x = \tau_w \rho \Delta L$$

Proiettando sull'asse  $x$  ( $\Delta V = 0$ ):

$$\cancel{\dot{m}\Delta V} + A\Delta p + \rho g A \Delta z + \tau_w \rho \Delta L = 0$$

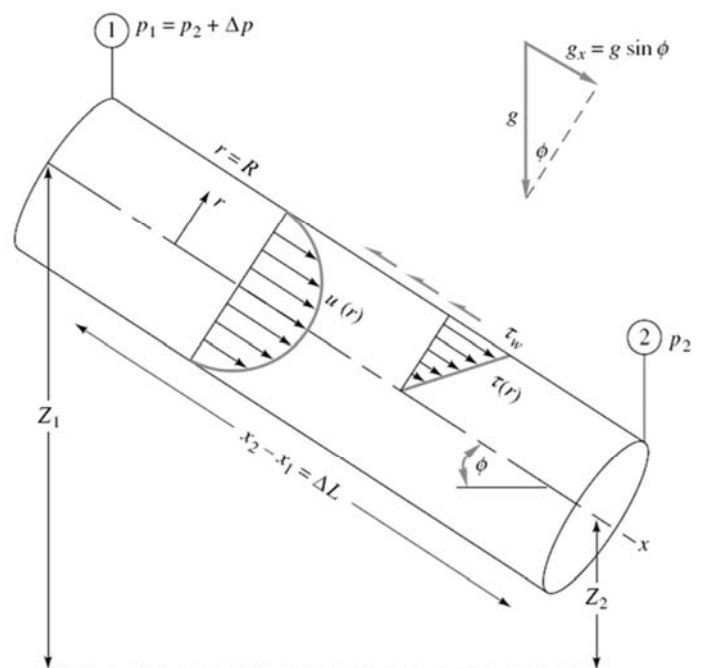
Dividendo per  $A$  e indicando con

$D_e = 4A/\rho$  il diametro equivalente:

$$\Delta p + \rho g \Delta z + 4\tau_w \frac{\Delta L}{D_e} = 0$$

Ovvero:

$$\frac{\Delta p}{\rho g} + \Delta z = -\frac{4\tau_w}{\rho g} \frac{\Delta L}{D_e} = -h_f$$



## Perdite di carico distribuite

$$\frac{\Delta p}{\rho g} + \Delta z = -\frac{4\tau_w}{\rho g D_e} \Delta L = -h_f$$

Da un'analisi dimensionale del fenomeno si vede che:

$$\tau_p = F(\rho, V, \mu, D_e, \varepsilon)$$

Mediante il **Teorema di Buckingham** si ottiene:

$$f = \frac{8\tau_w}{\rho V^2} = f\left(Re, \frac{\varepsilon}{D_e}\right) \quad Re = \frac{\rho V D_e}{\mu}$$

$f$  coefficiente di Darcy (diverso da quello di Fanning). Sostituendo  $L$  nella relazione precedente si trova:

$$h_f = f \frac{L}{D_e} \frac{V^2}{2g}$$

Nel seguito si utilizzerà al posto del simbolo  $D_e$   $D$  oppure  $d$ .



## MOTO IN CONDOTTI

Lungo un tubo di flusso vale la relazione di Bernoulli generalizzata:

$$\frac{p_1}{\rho g} + \frac{V_1^2}{2g} + z_1 = \frac{p_2}{\rho g} + \frac{V_2^2}{2g} + z_2 + h_2 = \frac{p_3}{\rho g} + \frac{V_3^2}{2g} + z_3 + h_3$$

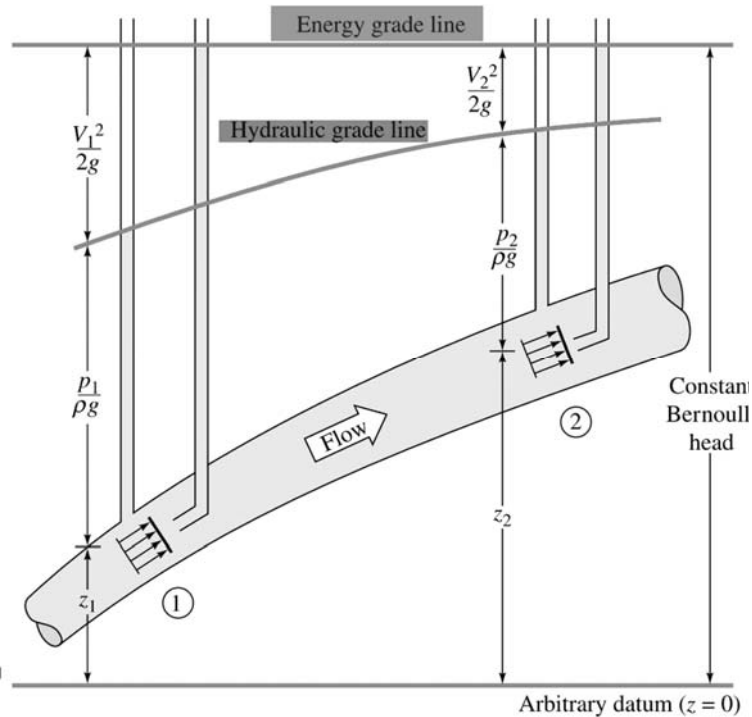
A useful visual interpretation of Bernoulli's equation is to sketch two grade lines of a flow. The **energy grade line (EGL)** shows the height of the total Bernoulli constant  $h_0 = z + p/\gamma + V^2/(2g)$ . In frictionless flow with no work or heat transfer, Eq. (3.77), the EGL has constant height. The **hydraulic grade line (HGL)** shows the height corresponding to elevation and pressure head  $z + p/\gamma$ , that is, the EGL minus the velocity head  $V^2/(2g)$ . The HGL is the height to which liquid would rise in a piezometer tube (see Prob. 2.11) attached to the flow. In an open-channel flow the HGL is identical to the free surface of the water.



# MOTO IN CONDOTTI

Lungo un tubo di flusso vale la relazione di Bernoulli generalizzata:

$$\frac{p_1}{\rho g} + \frac{V_1^2}{2g} + z_1 = \frac{p_2}{\rho g} + \frac{V_2^2}{2g} + z_2 + h_2 = \frac{p_3}{\rho g} + \frac{V_3^2}{2g} + z_3 + h_3$$



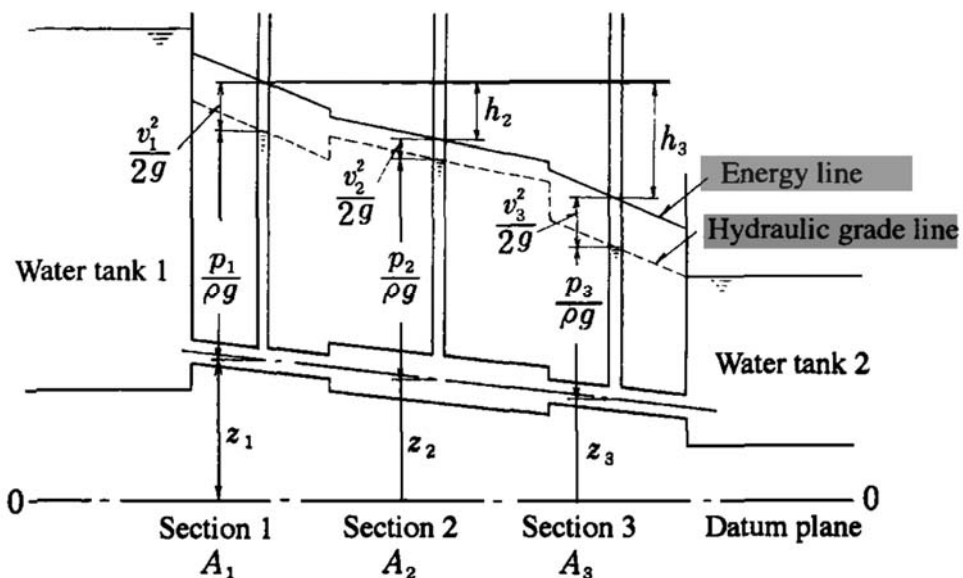
Complementi di Gasdin

17

# MOTO IN CONDOTTI

Lungo un tubo di flusso vale la relazione di Bernoulli generalizzata:

$$\frac{p_1}{\rho g} + \frac{V_1^2}{2g} + z_1 = \frac{p_2}{\rho g} + \frac{V_2^2}{2g} + z_2 + h_2 = \frac{p_3}{\rho g} + \frac{V_3^2}{2g} + z_3 + h_3$$



Complementi di Gasdinamica – T Astarita

18

## SEZIONE NON CIRCOLARE

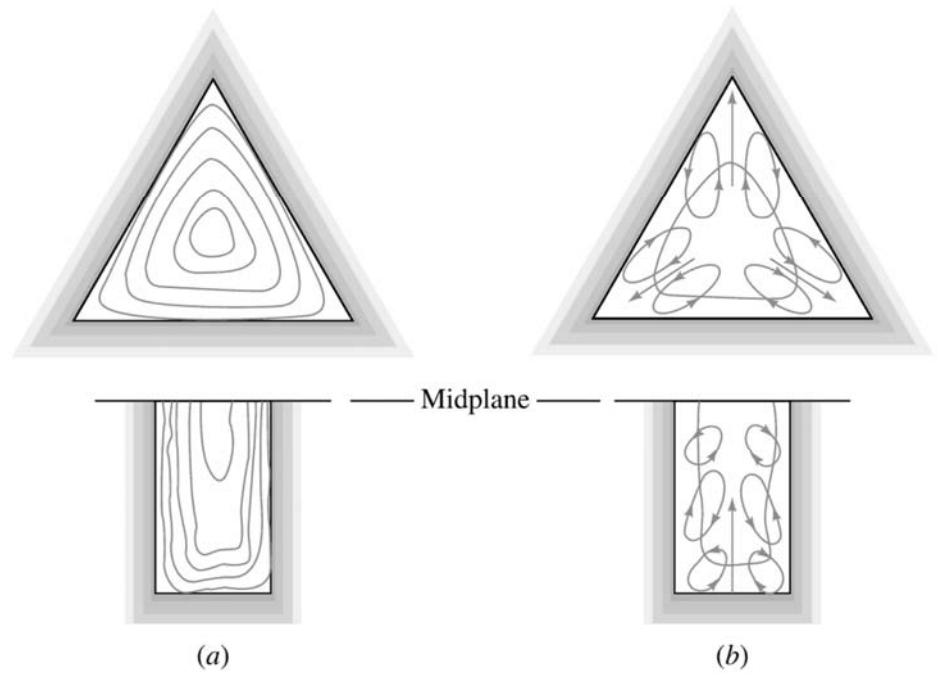
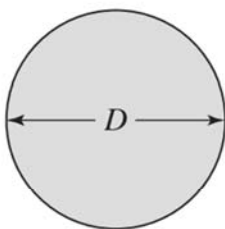


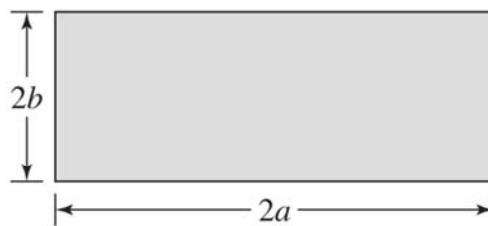
**Fig. 6.16** Illustration of secondary turbulent flow in noncircular ducts: (a) axial mean-velocity contours; (b) secondary-flow cellular motions. (After J. Nikuradse, dissertation, Göttingen, 1926.)



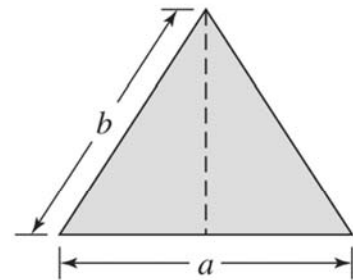
## DIAMETRO EQUIVALENTE (IDRAULICO)



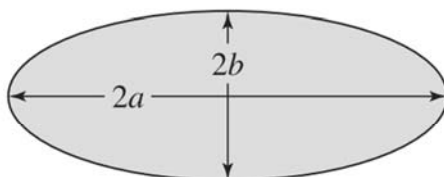
$$D_H = D$$



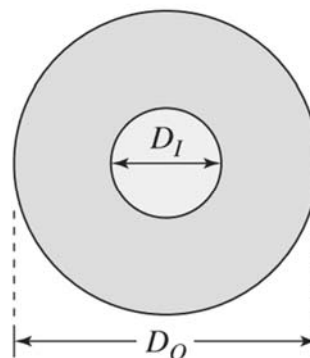
$$D_H = \frac{4ab}{a + b}$$



$$D_H = \frac{\sqrt{4a^2b^2 - a^4}}{a + 2b}$$



$$D_H \approx \frac{2\sqrt{2}(ab)}{\sqrt{a^2 + b^2}}$$



$$D_H = D_O - D_I$$



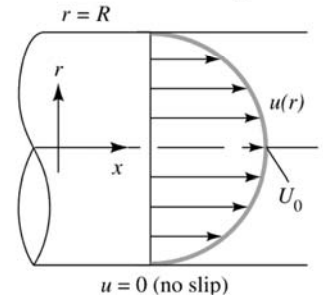
# MOTO IN CONDOTTI $\int_{CS} (\hat{h} + \frac{1}{2}V^2 + gz)\rho(\mathbf{V} \cdot \mathbf{n}) dA$

Often the flow entering or leaving a port is not strictly one-dimensional. In particular, the velocity may vary over the cross section, as in Fig. E3.4. In this case the kinetic-energy term in Eq. (3.64) for a given port should be modified by a dimensionless correction factor  $\alpha$  so that the integral can be proportional to the square of the average velocity through the port

$$\int_{\text{port}} (\frac{1}{2}V^2)\rho(\mathbf{V} \cdot \mathbf{n}) dA \equiv \alpha(\frac{1}{2}V_{av}^2)\dot{m}$$

where

$$V_{av} = \frac{1}{A} \int u dA \quad \text{for incompressible flow}$$



If the density is also variable, the integration is very cumbersome; we shall not treat this complication. By letting  $u$  be the velocity normal to the port, the first equation above becomes, for incompressible flow,

$$\frac{1}{2}\rho \int u^3 dA = \frac{1}{2}\rho\alpha V_{av}^3 A$$



or

$$\alpha = \frac{1}{A} \int \left( \frac{u}{V_{av}} \right)^3 dA \quad (3.70)$$

## MOTO IN CONDOTTI

The term  $\alpha$  is the kinetic-energy correction factor, having a value of about 2.0 for fully developed laminar pipe flow and from 1.04 to 1.11 for turbulent pipe flow. The complete incompressible steady-flow energy equation (3.69), including pumps, turbines, and losses, would generalize to

$$\left( \frac{p}{\rho g} + \frac{\alpha}{2g} V^2 + z \right)_{\text{in}} = \left( \frac{p}{\rho g} + \frac{\alpha}{2g} V^2 + z \right)_{\text{out}} + h_{\text{turbine}} - h_{\text{pump}} + h_{\text{friction}} \quad (3.71)$$

where the head terms on the right ( $h_t$ ,  $h_p$ ,  $h_f$ ) are all numerically positive. All additive terms in Eq. (3.71) have dimensions of length  $\{L\}$ . In problems involving turbulent pipe flow, it is common to assume that  $\alpha \approx 1.0$ . To compute numerical values, we can use these approximations to be discussed in Chap. 6:

Laminar flow:

$$u = U_0 \left[ 1 - \left( \frac{r}{R} \right)^2 \right]$$

from which

$$V_{av} = 0.5U_0$$

and

$$\alpha = 2.0 \quad (3.72)$$

Turbulent flow:

$$u \approx U_0 \left( 1 - \frac{r}{R} \right)^m \quad m \approx \frac{1}{7}$$



# MOTO IN CONDOTTI

from which, in Example 3.4,

$$V_{av} = \frac{2U_0}{(1+m)(2+m)}$$

Substituting into Eq. (3.70) gives

$$\alpha = \frac{(1+m)^3(2+m)^3}{4(1+3m)(2+3m)} \quad (3.73)$$

and numerical values are as follows:

Turbulent flow:	$m$	$\frac{1}{5}$	$\frac{1}{6}$	$\frac{1}{7}$	$\frac{1}{8}$	$\frac{1}{9}$
	$\alpha$	1.106	1.077	1.058	1.046	1.037

These values are only slightly different from unity and are often neglected in elementary turbulent-flow analyses. However,  $\alpha$  should never be neglected in laminar flow.



For either laminar or turbulent flow, the continuity equation in cylindrical coordinates is given by (App. D)

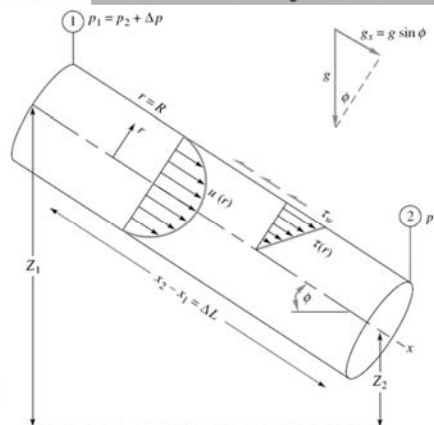
$$\frac{1}{r} \frac{\partial}{\partial r}(rv_r) + \frac{1}{r} \frac{\partial}{\partial \theta}(v_\theta) + \frac{\partial u}{\partial x} = 0 \quad (6.31)$$

We assume that there is no swirl or circumferential variation,  $v_\theta = \partial/\partial\theta = 0$ , and fully developed flow:  $u = u(r)$  only. Then Eq. (6.31) reduces to

$$\frac{1}{r} \frac{\partial}{\partial r}(rv_r) = 0$$

or  $rv_r = \text{const} \quad (6.32)$

But at the wall,  $r = R$ ,  $v_r = 0$  (no slip); therefore (6.32) implies that  $v_r = 0$  everywhere. Thus in fully developed flow there is only one velocity component,  $u = u(r)$ .





# MOTO IN CONDOTTI

The momentum differential equation in cylindrical coordinates now reduces to

$$\rho u \frac{\partial u}{\partial x} = -\frac{dp}{dx} + \rho g_x + \frac{1}{r} \frac{\partial}{\partial r} (r\tau) \quad (6.33)$$

where  $\tau$  can represent either laminar or turbulent shear. But the left-hand side vanishes because  $u = u(r)$  only. Rearrange, noting from Fig. 6.10 that  $g_x = g \sin \phi$ :

$$\frac{1}{r} \frac{\partial}{\partial r} (r\tau) = \frac{d}{dx} (p - \rho g x \sin \phi) = \frac{d}{dx} (p + \rho g z) \quad (6.34)$$

Since the left-hand side varies only with  $r$  and the right-hand side varies only with  $x$ , it follows that both sides must be equal to the same constant.<sup>2</sup> Therefore we can integrate Eq. (6.34) to find the shear distribution across the pipe, utilizing the fact that  $\tau = 0$  at  $r = 0$

$$\tau = \frac{1}{2} r \frac{d}{dx} (p + \rho g z) = (\text{const})(r) \quad (6.35)$$

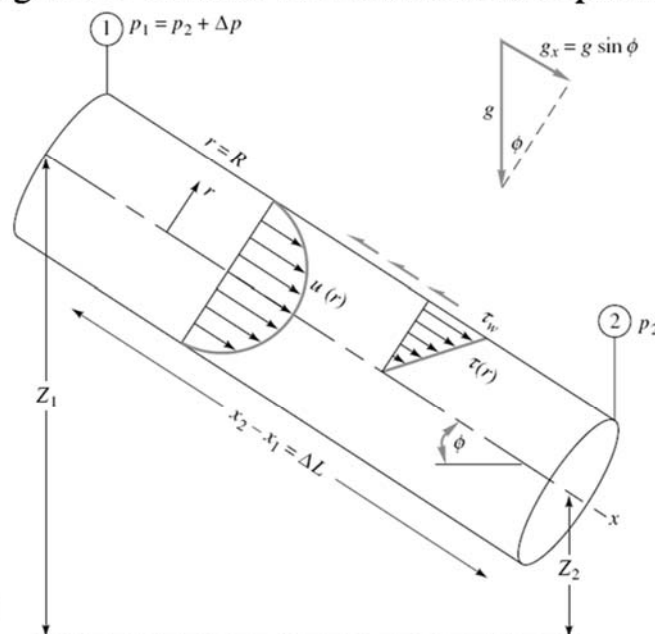


# MOTO IN CONDOTTI

Thus the shear varies linearly from the centerline to the wall, for either laminar or turbulent flow. This is also shown in Fig. 6.10. At  $r = R$ , we have the wall shear

$$\tau_w = \frac{1}{2} R \frac{\Delta p + \rho g \Delta z}{\Delta L} \quad (6.36)$$

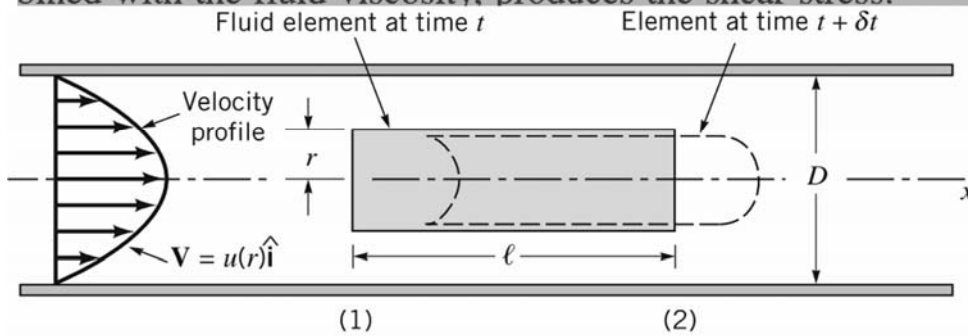
which is identical with our momentum relation (6.27). We can now complete our study of pipe flow by applying either laminar or turbulent assumptions to fill out Eq. (6.35).



## MOTI IN CONDOTTI

### 8.2.1 From $F = ma$ Applied Directly to a Fluid Element

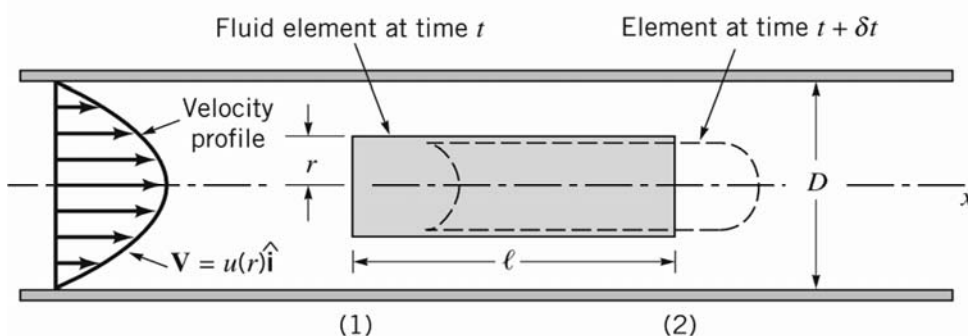
We consider the fluid element at time  $t$  as is shown in Fig. 8.7. It is a circular cylinder of fluid of length  $\ell$  and radius  $r$  centered on the axis of a horizontal pipe of diameter  $D$ . Because the velocity is not uniform across the pipe, the initially flat ends of the cylinder of fluid at time  $t$  become distorted at time  $t + \delta t$  when the fluid element has moved to its new location along the pipe as shown in the figure. If the flow is fully developed and steady, the distortion on each end of the fluid element is the same, and no part of the fluid experiences any acceleration as it flows. The local acceleration is zero ( $\partial \mathbf{V} / \partial t = 0$ ) because the flow is steady, and the convective acceleration is zero ( $\mathbf{V} \cdot \nabla \mathbf{V} = u \partial u / \partial x \hat{\mathbf{i}} = 0$ ) because the flow is fully developed. Thus, every part of the fluid merely flows along its pathline parallel to the pipe walls with constant velocity, although neighboring particles have slightly different velocities. The velocity varies from one pathline to the next. This velocity variation, combined with the fluid viscosity, produces the shear stress.



■ FIGURE 8.7  
Motion of a cylindrical  
fluid element within a pipe.

## MOTI IN CONDOTTI

If gravitational effects are neglected, the pressure is constant across any vertical cross section of the pipe, although it varies along the pipe from one section to the next. Thus, if the pressure is  $p = p_1$  at section (1), it is  $p_2 = p_1 - \Delta p$  at section (2). We anticipate the fact that the pressure decreases in the direction of flow so that  $\Delta p > 0$ . A shear stress,  $\tau$ , acts on the surface of the cylinder of fluid. This viscous stress is a function of the radius of the cylinder,  $\tau = \tau(r)$ .



■ FIGURE 8.7  
Motion of a cylindrical  
fluid element within a pipe.

## MOTI IN CONDOTTI

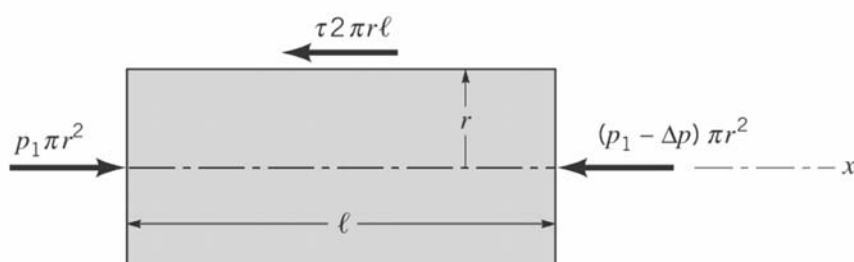
As was done in fluid statics analysis (Chapter 2), we isolate the cylinder of fluid as is shown in Fig. 8.8 and apply Newton's second law,  $F_x = ma_x$ . In this case even though the fluid is moving, it is not accelerating, so that  $a_x = 0$ . Thus, fully developed horizontal pipe flow is merely a balance between pressure and viscous forces—the pressure difference acting on the end of the cylinder of area  $\pi r^2$ , and the shear stress acting on the lateral surface of the cylinder of area  $2\pi r\ell$ . This force balance can be written as

$$(p_1)\pi r^2 - (p_1 - \Delta p)\pi r^2 - (\tau)2\pi r\ell = 0$$

which can be simplified to give

$$\frac{\Delta p}{\ell} = \frac{2\tau}{r} \quad (8.3)$$

$$\tau = \frac{1}{2}r \frac{d}{dx}(p + \rho g z) \quad (6.35)$$



■ FIGURE 8.8 Free-body diagram of a cylinder of fluid.



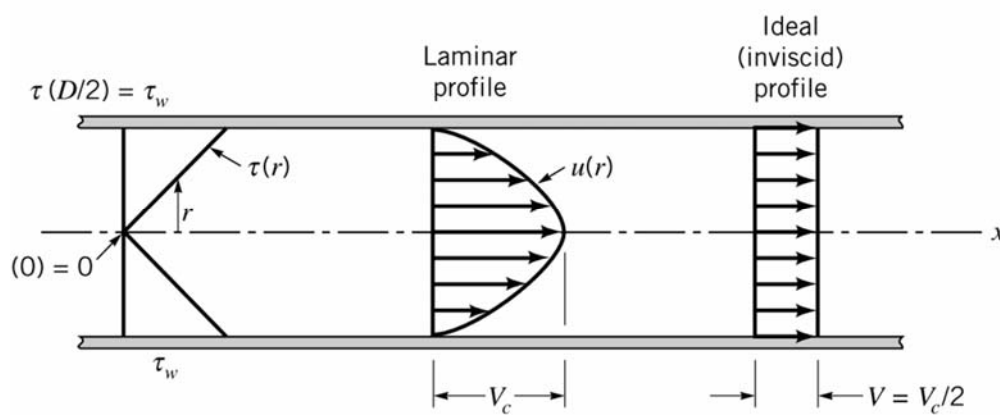
## MOTI IN CONDOTTI

Equation 8.3 represents the basic balance in forces needed to drive each fluid particle along the pipe with constant velocity. Since neither  $\Delta p$  nor  $\ell$  are functions of the radial coordinate,  $r$ , it follows that  $2\tau/r$  must also be independent of  $r$ . That is,  $\tau = Cr$ , where  $C$  is a constant. At  $r = 0$  (the centerline of the pipe) there is no shear stress ( $\tau = 0$ ). At  $r = D/2$  (the pipe wall) the shear stress is a maximum, denoted  $\tau_w$ , the *wall shear stress*. Hence,  $C = 2\tau_w/D$  and the shear stress distribution throughout the pipe is a linear function of the radial coordinate

$$\frac{\Delta p}{l} = \frac{2\tau}{r} \quad (8.3)$$

$$\tau = \frac{2\tau_w r}{D} \quad (8.4)$$

## MOTI IN CONDOTTI



■ **FIGURE 8.9**  
Shear stress distribution within the fluid in a pipe (laminar or turbulent flow) and typical velocity profiles.

as is indicated in Fig. 8.9. The linear dependence of  $\tau$  on  $r$  is a result of the pressure force being proportional to  $r^2$  (the pressure acts on the end of the fluid cylinder; area =  $\pi r^2$ ) and the shear force being proportional to  $r$  (the shear stress acts on the lateral sides of the cylinder; area =  $2\pi r\ell$ ). If the viscosity were zero there would be no shear stress, and the pressure would be constant throughout the horizontal pipe ( $\Delta p = 0$ ). As is seen from Eqs. 8.3 and 8.4, the pressure drop and wall shear stress are related by

$$\frac{\Delta p}{l} = \frac{2\tau}{r} \quad (8.3)$$

$$\Delta p = \frac{4\ell\tau_w}{D} \quad (8.5)$$

(A small shear stress can produce a large pressure difference if the pipe is relatively long ( $\ell/D \gg 1$ )).

## MOTI IN CONDOTTI

Although we are discussing laminar flow, a closer consideration of the assumptions involved in the derivation of Eqs. 8.3, 8.4, and 8.5 reveals that these equations are valid for both laminar and turbulent flow. To carry the analysis further we must prescribe how the shear stress is related to the velocity. This is the critical step that separates the analysis of laminar from that of turbulent flow—from being able to solve for the laminar flow properties and not being able to solve for the turbulent flow properties without additional ad hoc assumptions. As is discussed in Section 8.3, the shear stress dependence for turbulent flow is very complex. However, for laminar flow of a Newtonian fluid, the shear stress is simply proportional to the velocity gradient, “ $\tau = \mu du/dy$ ” (see Section 1.6). In the notation associated with our pipe flow, this becomes

$$\tau = -\mu \frac{du}{dr} \quad (8.6)$$

The negative sign is included to give  $\tau > 0$  with  $du/dr < 0$  (the velocity decreases from the pipe centerline to the pipe wall).

$$\frac{\Delta p}{L} = \frac{2\tau}{r} \quad (8.3)$$

$$\text{MOTO LAMINARE} \quad \tau = \frac{1}{2} r \frac{d}{dx} (p + \rho g z) \quad (6.35)$$

Note in Eq. (6.35) that the HGL slope  $d(p + \rho g z)/dx$  is *negative* because both pressure and height drop with  $x$ . For laminar flow,  $\tau = \mu du/dr$ , which we substitute in Eq. (6.35)

$$\mu \frac{du}{dr} = \frac{1}{2} r K \quad K = \frac{d}{dx} (p + \rho g z) \quad (6.37)$$

Integrate once

$$u = \frac{1}{4} r^2 \frac{K}{\mu} + C_1 \quad (6.38)$$

The constant  $C_1$  is evaluated from the no-slip condition at the wall:  $u = 0$  at  $r = R$

$$0 = \frac{1}{4} R^2 \frac{K}{\mu} + C_1 \quad (6.39)$$

or  $C_1 = -\frac{1}{4} R^2 K/\mu$ . Introduce into Eq. (6.38) to obtain the exact solution for laminar fully developed pipe flow

$$u = u_{\max} \left( 1 - \frac{r^2}{R^2} \right) \quad u = \frac{1}{4\mu} \left[ -\frac{d}{dx} (p + \rho g z) \right] (R^2 - r^2) \quad (6.40)$$



Complementi di Gasdinamica – T Astarita

33

## MOTO LAMINARE

The laminar-flow profile is thus a paraboloid falling to zero at the wall and reaching a maximum at the axis

$$u_{\max} = \frac{R^2}{4\mu} \left[ -\frac{d}{dx} (p + \rho g z) \right] \quad \frac{R^2}{4\mu} \frac{\Delta p}{L} \quad (6.41)$$

It resembles the sketch of  $u(r)$  given in Fig. 6.10.

The laminar distribution (6.40) is called *Hagen-Poiseuille flow* to commemorate the experimental work of G. Hagen in 1839 and J. L. Poiseuille in 1940, both of whom established the pressure-drop law, Eq. (6.1). The first theoretical derivation of Eq. (6.40) was given independently by E. Hagenbach and by F. Neumann around 1859.

Other pipe-flow results follow immediately from Eq. (6.40). The volume flow is

$$\begin{aligned} Q &= \int_0^R u \, dA = \int_0^R u_{\max} \left( 1 - \frac{r^2}{R^2} \right) 2\pi r \, dr \\ &= \frac{1}{2} u_{\max} \pi R^2 = \frac{\pi R^4}{8\mu} \left[ -\frac{d}{dx} (p + \rho g z) \right] \quad \frac{\pi R^4}{8\mu} \frac{\Delta p}{L} \quad (6.42) \end{aligned}$$

Thus the average velocity in laminar flow is one-half the maximum velocity



Complementi di Gasdinamica – T Astarita

34

$$u_{\max} = \frac{R^2}{4\mu} \frac{\Delta p}{L}$$

## MOTO LAMINARE

$$\tau = \frac{1}{2} r \frac{d}{dx} (p + \rho g z) \quad (6.35)$$

$$V = \frac{Q}{A} = \frac{Q}{\pi R^2} = \frac{1}{2} u_{\max} \quad (6.43)$$

For a horizontal tube ( $\Delta z = 0$ ), Eq. (6.42) is of the form predicted by Hagen's experiment, Eq. (6.1):

$$u_{\max} L = \frac{R^2}{4\mu} \Delta p \rightarrow \Delta p = \frac{4\mu u_{\max} L}{R^2} \quad \Delta p = \frac{8\mu L Q}{\pi R^4} \quad \Delta p = \frac{8\mu V L}{R^2} = \frac{32\mu V L}{d^2} \quad (6.44)$$

The wall shear is computed from the wall velocity gradient

$$u = u_{\max} \left( 1 - \frac{r^2}{R^2} \right) \quad \tau_w = \left| \mu \frac{du}{dr} \right|_{r=R} = \frac{2\mu u_{\max}}{R} = \frac{1}{2} R \left| \frac{d}{dx} (p + \rho g z) \right| = \frac{R}{2} \frac{\Delta p}{L} \quad (6.45)$$

This gives an exact theory for laminar Darcy friction factor

$$f = \frac{8\tau_w}{\rho V^2} = \frac{8(8\mu V/d)}{\rho V^2} = \frac{64\mu}{\rho V d} \quad \tau_w = \frac{8\mu V}{d}$$

or

$$f_{\text{lam}} = \frac{64}{\text{Re}_d} \quad (6.46)$$

$$h_{f,\text{lam}} = \frac{64\mu}{\rho V d} \frac{L}{d} \frac{V^2}{2g} = \frac{32\mu L V}{\rho g d^2} = \frac{128\mu L Q}{\pi \rho g d^4} \quad (6.47)$$



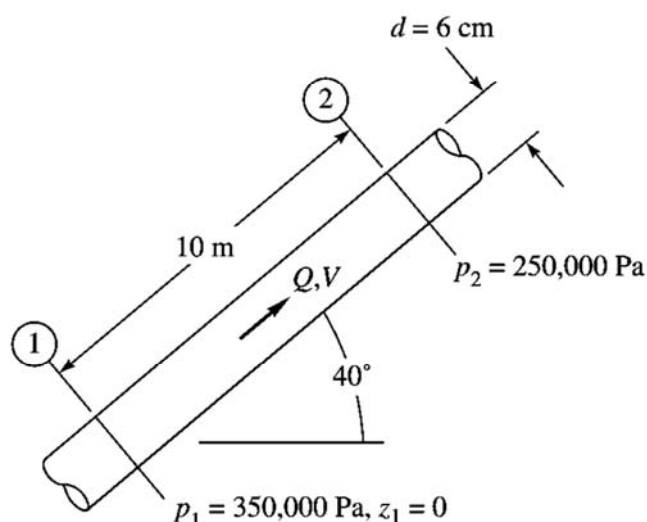
Complementi di

35

## MOTO LAMINARE

### EXAMPLE 6.4

An oil with  $\rho = 900 \text{ kg/m}^3$  and  $\nu = 0.0002 \text{ m}^2/\text{s}$  flows upward through an inclined pipe as shown in Fig. E6.4. The pressure and elevation are known at sections 1 and 2, 10 m apart. Assuming



steady laminar flow, (a) verify that the flow is up, (b) compute  $h_f$  between 1 and 2, and compute (c)  $Q$ , (d)  $V$ , and (e)  $\text{Re}_d$ . Is the flow really laminar?



Complementi di Gasdinamica – T Astarita

36

# MOTO LAMINARE

## Solution

**Part (a)** For later use, calculate

$$\mu = \rho\nu = (900 \text{ kg/m}^3)(0.0002 \text{ m}^2/\text{s}) = 0.18 \text{ kg}/(\text{m} \cdot \text{s})$$

$$z_2 = \Delta L \sin 40^\circ = (10 \text{ m})(0.643) = 6.43 \text{ m}$$

The flow goes in the direction of falling HGL; therefore compute the hydraulic grade-line height at each section

$$\text{HGL}_1 = z_1 + \frac{p_1}{\rho g} = 0 + \frac{350,000}{900(9.807)} = 39.65 \text{ m}$$

$$\text{HGL}_2 = z_2 + \frac{p_2}{\rho g} = 6.43 + \frac{250,000}{900(9.807)} = 34.75 \text{ m}$$

The HGL is lower at section 2; hence the flow is from 1 to 2 as assumed.

*Ans. (a)*

**Part (b)** The head loss is the change in HGL:

$$h_f = \text{HGL}_1 - \text{HGL}_2 = 39.65 \text{ m} - 34.75 \text{ m} = 4.9 \text{ m}$$

*Ans. (b)*

Half the length of the pipe is quite a large head loss.



# MOTO LAMINARE

**Part (c)** We can compute  $Q$  from the various laminar-flow formulas, notably Eq. (6.47)

$$Q = \frac{\pi \rho g d^4 h_f}{128 \mu L} = \frac{\pi(900)(9.807)(0.06)^4(4.9)}{128(0.18)(10)} = 0.0076 \text{ m}^3/\text{s}$$

*Ans. (c)*

**Part (d)** Divide  $Q$  by the pipe area to get the average velocity

$$V = \frac{Q}{\pi R^2} = \frac{0.0076}{\pi(0.03)^2} = 2.7 \text{ m/s}$$

*Ans. (d)*

**Part (e)** With  $V$  known, the Reynolds number is

$$\text{Re}_d = \frac{Vd}{\nu} = \frac{2.7(0.06)}{0.0002} = 810$$

*Ans. (e)*

This is well below the transition value  $\text{Re}_d = 2300$ , and so we are fairly certain the flow is laminar.

Notice that by sticking entirely to consistent SI units (meters, seconds, kilograms, newtons) for all variables we avoid the need for any conversion factors in the calculations.





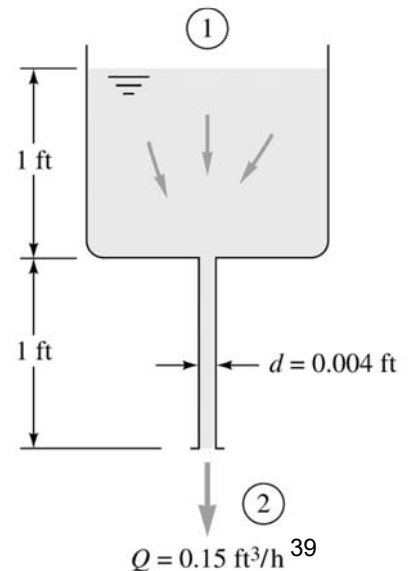
# MOTO LAMINARE

## EXAMPLE 6.5

A liquid of specific weight  $\rho g = 58 \text{ lbf/ft}^3$  flows by gravity through a 1-ft tank and a 1-ft capillary tube at a rate of  $0.15 \text{ ft}^3/\text{h}$ , as shown in Fig. E6.5. Sections 1 and 2 are at atmospheric pressure. Neglecting entrance effects, compute the viscosity of the liquid.

## Solution

Apply the steady-flow energy equation (6.24), including the correction factor  $\alpha$ :



Complementi di Gasdinamica – T Astarita

$$\frac{p_1}{\rho g} + \frac{\alpha_1 V_1^2}{2g} + z_1 = \frac{p_2}{\rho g} + \frac{\alpha_2 V_2^2}{2g} + z_2 + h_f$$

The average exit velocity  $V_2$  can be found from the volume flow and the pipe size:

$$V_2 = \frac{Q}{A_2} = \frac{Q}{\pi R^2} = \frac{(0.15/3600) \text{ ft}^3/\text{s}}{\pi(0.002 \text{ ft})^2} \approx 3.32 \text{ ft/s}$$

Meanwhile  $p_1 = p_2 = p_a$ , and  $V_1 \approx 0$  in the large tank. Therefore, approximately,

$$h_f \approx z_1 - z_2 - \alpha_2 \frac{V_2^2}{2g} = 2.0 \text{ ft} - 2.0 \frac{(3.32 \text{ ft/s})^2}{2(32.2 \text{ ft/s}^2)} \approx 1.66 \text{ ft}$$

where we have introduced  $\alpha_2 = 2.0$  for laminar pipe flow from Eq. (3.72). Note that  $h_f$  includes the entire 2-ft drop through the system and not just the 1-ft pipe length.

With the head loss known, the viscosity follows from our laminar-flow formula (6.47):

$$h_f = 1.66 \text{ ft} = \frac{32\mu LV}{\rho g d^2} = \frac{32\mu(1.0 \text{ ft})(3.32 \text{ ft/s})}{(58 \text{ lbf/ft}^3)(0.004 \text{ ft})^2} = 114,500 \mu$$

or

$$\mu = \frac{1.66}{114,500} = 1.45 \text{ E-5 slug/(ft} \cdot \text{s)} \quad \text{Ans.}$$

Note that  $L$  in this formula is the pipe length of 1 ft. Finally, check the Reynolds number:

$$\text{Re}_d = \frac{\rho V d}{\mu} = \frac{(58/32.2 \text{ slug/ft}^3)(3.32 \text{ ft/s})(0.004 \text{ ft})}{1.45 \text{ E-5 slug/(ft} \cdot \text{s)}} = 1650 \quad \text{laminar}$$

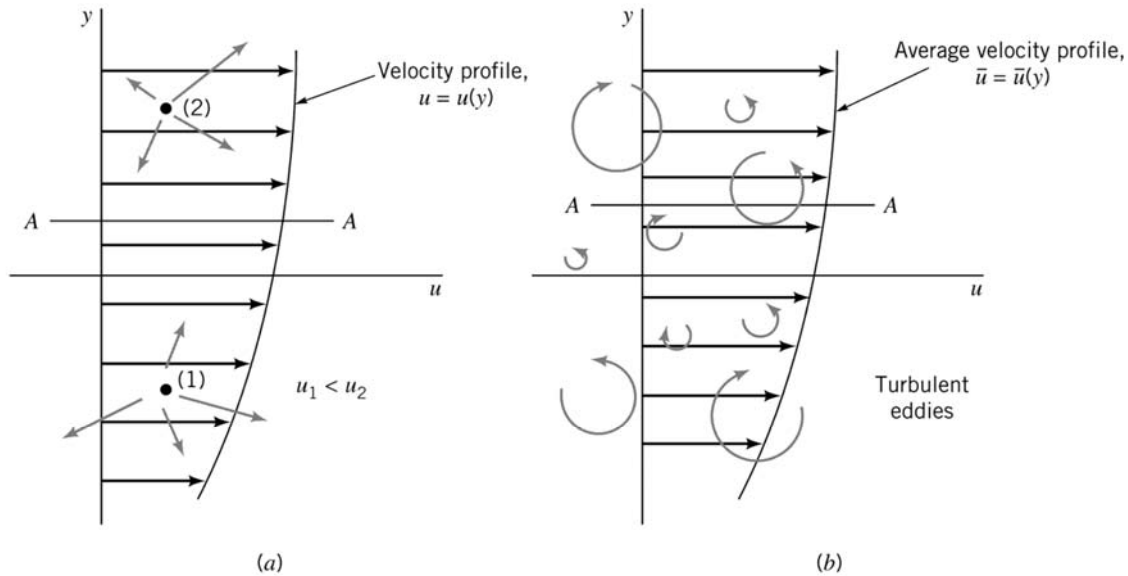


Since this is less than 2300, we conclude that the flow is indeed laminar. Actually, for this head loss, there is a *second* (turbulent) solution, as we shall see in Example 6.8.



# MOTO TURBOLENTO

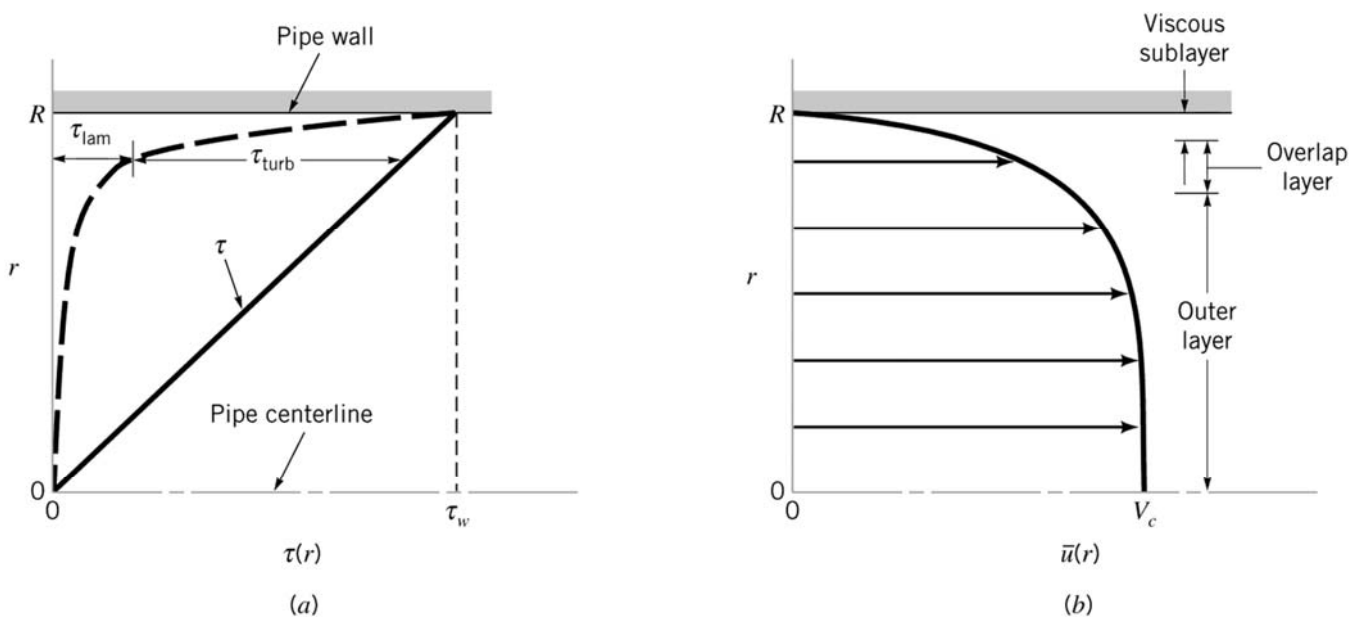
$$\tau = \mu \frac{\partial \bar{u}}{\partial y} - \rho \overline{u'v'} = \tau_{\text{lam}} + \tau_{\text{turb}}$$



■ **FIGURE 8.14** (a) Laminar flow shear stress caused by random motion of molecules. (b) Turbulent flow as a series of random, three-dimensional eddies.

# MOTO TURBOLENTO

$$\tau = \mu \frac{\partial \bar{u}}{\partial y} - \rho \overline{u'v'} = \tau_{\text{lam}} + \tau_{\text{turb}}$$



■ **FIGURE 8.15** Structure of turbulent flow in a pipe. (a) Shear stress. (b) Average velocity.

# MOTO TURBOLENTO

## The Logarithmic-Overlap Law

We have seen in Fig. 6.8 that there are three regions in turbulent flow near a wall:

1. Wall layer: Viscous shear dominates.
2. Outer layer: Turbulent shear dominates.
3. Overlap layer: Both types of shear are important.

From now on let us agree to drop the overbar from velocity  $\bar{u}$ . Let  $\tau_w$  be the wall shear stress, and let  $\delta$  and  $U$  represent the thickness and velocity at the edge of the outer layer,  $y = \delta$ .

For the wall layer, Prandtl deduced in 1930 that  $u$  must be independent of the shear-layer thickness

$$u = f(\mu, \tau_w, \rho, y) \quad (6.17)$$

By dimensional analysis, this is equivalent to



# MOTO TURBOLENTO

$$u^+ = \frac{u}{u^*} = F\left(\frac{yu^*}{\nu}\right) \quad u^* = \left(\frac{\tau_w}{\rho}\right)^{1/2} \quad (6.18)$$

Equation (6.18) is called the *law of the wall*, and the quantity  $u^*$  is termed the *friction velocity* because it has dimensions  $\{LT^{-1}\}$ , although it is not actually a flow velocity.

Subsequently, Kármán in 1933 deduced that  $u$  in the outer layer is independent of molecular viscosity, but its deviation from the stream velocity  $U$  must depend on the layer thickness  $\delta$  and the other properties

$$(U - u)_{\text{outer}} = g(\delta, \tau_w, \rho, y) \quad (6.19)$$

Again, by dimensional analysis we rewrite this as

$$\frac{U - u}{u^*} = G\left(\frac{y}{\delta}\right) \quad (6.20)$$

where  $u^*$  has the same meaning as in Eq. (6.18). Equation (6.20) is called the *velocity-defect law* for the outer layer.



Both the wall law (6.18) and the defect law (6.20) are found to be accurate for a wide variety of experimental turbulent duct and boundary-layer flows [1 to 3]. They are different in form, yet they must overlap smoothly in the intermediate layer. In 1937 C. B. Millikan showed that this can be true only if the overlap-layer velocity varies logarithmically with  $y$ :

$$\frac{u}{u^*} = \frac{1}{\kappa} \ln \frac{yu^*}{\nu} + B \quad \text{overlap layer} \quad (6.21)$$

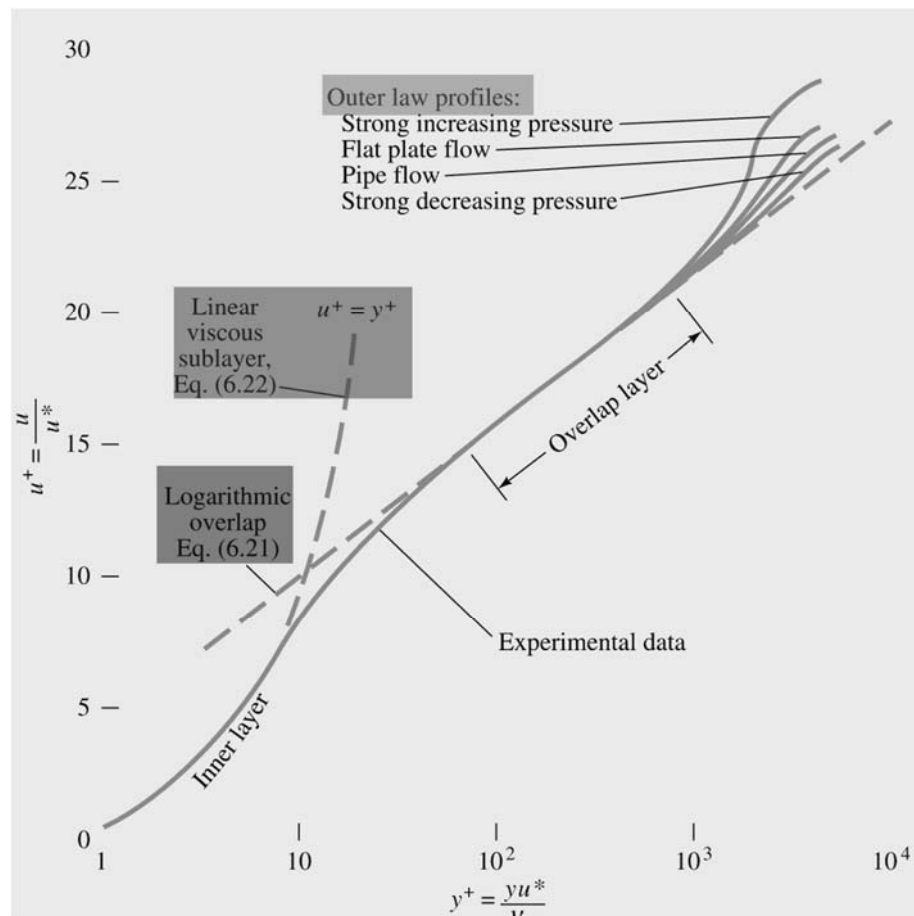
Over the full range of turbulent smooth wall flows, the dimensionless constants  $\kappa$  and  $B$  are found to have the approximate values  $\kappa \approx 0.41$  and  $B \approx 5.0$ . Equation (6.21) is called the **logarithmic-overlap layer**.

Thus by dimensional reasoning and physical insight we infer that a plot of  $u$  versus  $\ln y$  in a turbulent-shear layer will show a curved wall region, a curved outer region, and a straight-line logarithmic overlap. Figure 6.9 shows that this is exactly the case. The four outer-law profiles shown all merge smoothly with the logarithmic-overlap law but have different magnitudes because they vary in external pressure gradient. The wall law is unique and follows the linear viscous relation

$$u^+ = \frac{u}{u^*} = \frac{yu^*}{\nu} = y^+ \quad (6.22)$$

from the wall to about  $y^+ = 5$ , thereafter curving over to merge with the logarithmic law at about  $y^+ = 30$ .

## MOTO TURBOLENTO



# MOTO TURBOLENTO

Believe it or not, Fig. 6.9, which is nothing more than a shrewd correlation of velocity profiles, is the basis for most existing “theory” of turbulent-shear flows. Notice that we have not solved any equations at all but have merely expressed the streamwise velocity in a neat form.

There is serendipity in Fig. 6.9: The logarithmic law (6.21), instead of just being a short overlapping link, actually approximates nearly the entire velocity profile, except for the outer law when the pressure is increasing strongly downstream (as in a diffuser). The inner-wall law typically extends over less than 2 percent of the profile and can be neglected. Thus we can use Eq. (6.21) as an excellent approximation to solve nearly every turbulent-flow problem presented in this and the next chapter.



# MOTO TURBOLENTO

For turbulent pipe flow we need not solve a differential equation but instead proceed with the logarithmic law, as in Example 6.3. Assume that Eq. (6.21) correlates the local mean velocity  $u(r)$  all the way across the pipe

$$\frac{u(r)}{u^*} \approx \frac{1}{\kappa} \ln \frac{(R - r)u^*}{\nu} + B \quad (6.48)$$

where we have replaced  $y$  by  $R - r$ . Compute the average velocity from this profile

$$\begin{aligned} V = \frac{Q}{A} &= \frac{1}{\pi R^2} \int_0^R u^* \left[ \frac{1}{\kappa} \ln \frac{(R - r)u^*}{\nu} + B \right] 2\pi r \, dr \\ &= \frac{1}{2} u^* \left( \frac{2}{\kappa} \ln \frac{Ru^*}{\nu} + 2B - \frac{3}{\kappa} \right) \end{aligned} \quad (6.49)$$

Introducing  $\kappa = 0.41$  and  $B = 5.0$ , we obtain, numerically,

$$\frac{V}{u^*} \approx 2.44 \ln \frac{Ru^*}{\nu} + 1.34 \quad u^* = \sqrt{\frac{\tau_w}{\rho}} \quad (6.50)$$

This looks only marginally interesting until we realize that  $V/u^*$  is directly related to the Darcy friction factor



$$\frac{V}{u^*} \approx 2.44 \ln \frac{Ru^*}{\nu} + 1.34 \quad \text{MOTO TURBOLENTO} \quad f = \frac{8\tau_w}{\rho V^2} \quad u^* = \sqrt{\frac{\tau_w}{\rho}}$$

$$\frac{V}{u^*} = \left( \frac{\rho V^2}{\tau_w} \right)^{1/2} = \left( \frac{8}{f} \right)^{1/2} \quad (6.51)$$

Moreover, the argument of the logarithm in (6.50) is equivalent to

$$\frac{Ru^*}{\nu} = \frac{\frac{1}{2}Vd}{\nu} \frac{u^*}{V} = \frac{1}{2} \text{Re}_d \left( \frac{f}{8} \right)^{1/2} \quad (6.52)$$

Introducing (6.52) and (6.51) into Eq. (6.50), changing to a base-10 logarithm, and rearranging, we obtain

$$\frac{1}{f^{1/2}} \approx 1.99 \log (\text{Re}_d f^{1/2}) - 1.02 \quad (6.53)$$

In other words, by simply computing the mean velocity from the logarithmic-law correlation, we obtain a relation between the friction factor and Reynolds number for turbulent pipe flow. Prandtl derived Eq. (6.53) in 1935 and then adjusted the constants slightly to fit friction data better

$$\frac{1}{f^{1/2}} = 2.0 \log (\text{Re}_d f^{1/2}) - 0.8 \quad (6.54)$$

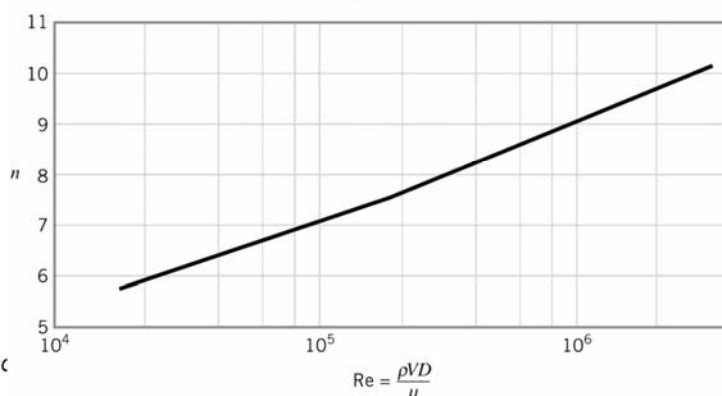


## MOTO TURBOLENTO

A number of other correlations exist for the velocity profile in turbulent pipe flow. In the central region (the outer turbulent layer) the expression  $(V_c - \bar{u})/u^* = 2.5 \ln(R/y)$ , where  $V_c$  is the centerline velocity, is often suggested as a good correlation with experimental data. Another often-used (and relatively easy to use) correlation is the empirical *power-law velocity profile*

$$\frac{\bar{u}}{V_c} = \left( 1 - \frac{r}{R} \right)^{1/n} \quad (8.31)$$

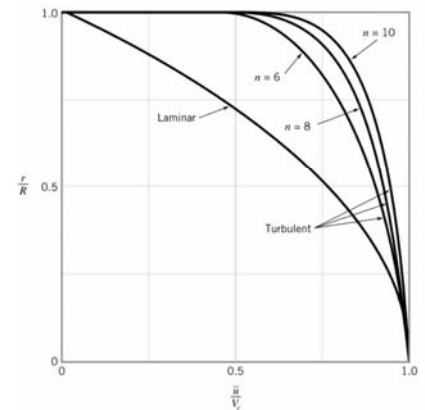
In this representation, the value of  $n$  is a function of the Reynolds number, as is indicated in Fig. 8.17. The one-seventh power-law velocity profile ( $n = 7$ ) is often used as a reasonable approximation for many practical flows. Typical turbulent velocity profiles based on this power-law representation are shown in Fig. 8.18.



## MOTO TURBOLENTO

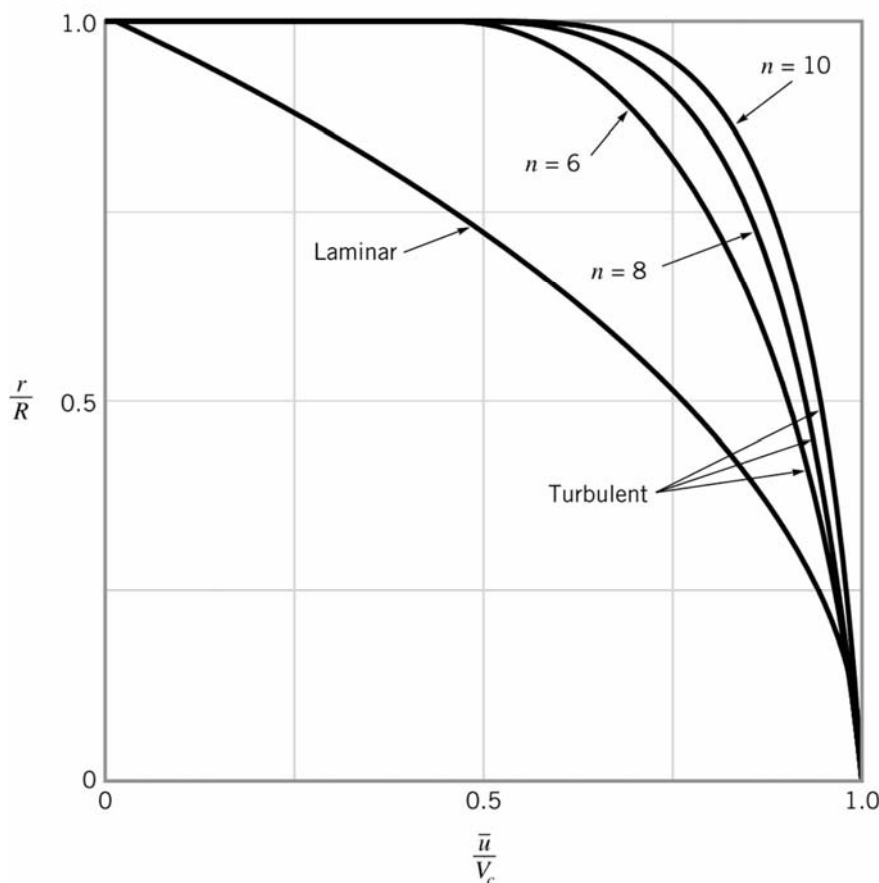
A closer examination of Eq. 8.31 shows that the power-law profile cannot be valid near the wall, since according to this equation the velocity gradient is infinite there. In addition, Eq. 8.31 cannot be precisely valid near the centerline because it does not give  $d\bar{u}/dr = 0$  at  $r = 0$ . However, it does provide a reasonable approximation to the measured velocity profiles across most of the pipe.

Note from Fig. 8.18 that the turbulent profiles are much “flatter” than the laminar profile and that this flatness increases with Reynolds number (i.e., with  $n$ ). Recall from **Chapter 3** that reasonable approximate results are often obtained by using the inviscid Bernoulli equation and by assuming a fictitious uniform velocity profile. Since most flows are turbulent and turbulent flows tend to have nearly uniform velocity profiles, the usefulness of the Bernoulli equation and the uniform profile assumption is not unexpected. Of course, many properties of the flow cannot be accounted for without including viscous effects.



Complementi di Gasdinamica – T Astarita

## MOTO TURBOLENTO



Complementi di Gasdinamica – T Astarita

$$\tau_w = \frac{8\mu V}{d}$$

## 8.4.1 The Moody Chart

A dimensional analysis treatment of pipe flow provides the most convenient base from which to consider turbulent, fully developed pipe flow. An introduction to this topic was given in Section 8.3. As is discussed in **Sections 8.2.1** and 8.2.4, the pressure drop and head loss in a pipe are dependent on the wall shear stress,  $\tau_w$ , between the fluid and pipe surface. A fundamental difference between laminar and turbulent flow is that the shear stress for turbulent flow is a function of the density of the fluid,  $\rho$ . For laminar flow, the shear stress is independent of the density, leaving the viscosity,  $\mu$ , as the only important fluid property.

Thus, the pressure drop,  $\Delta p$ , for steady, **incompressible turbulent flow** in a horizontal round pipe of diameter  $D$  can be written in functional form as

$$\Delta p = F(V, D, \ell, \varepsilon, \mu, \rho) \quad (8.32)$$

where  $V$  is the average velocity,  $\ell$  is the pipe length, and  $\varepsilon$  is a measure of the roughness of the pipe wall. It is clear that  $\Delta p$  should be a function of  $V$ ,  $D$ , and  $\ell$ . The dependence of  $\Delta p$  on the fluid properties  $\mu$  and  $\rho$  is expected because of the dependence of  $\tau$  on these parameters.



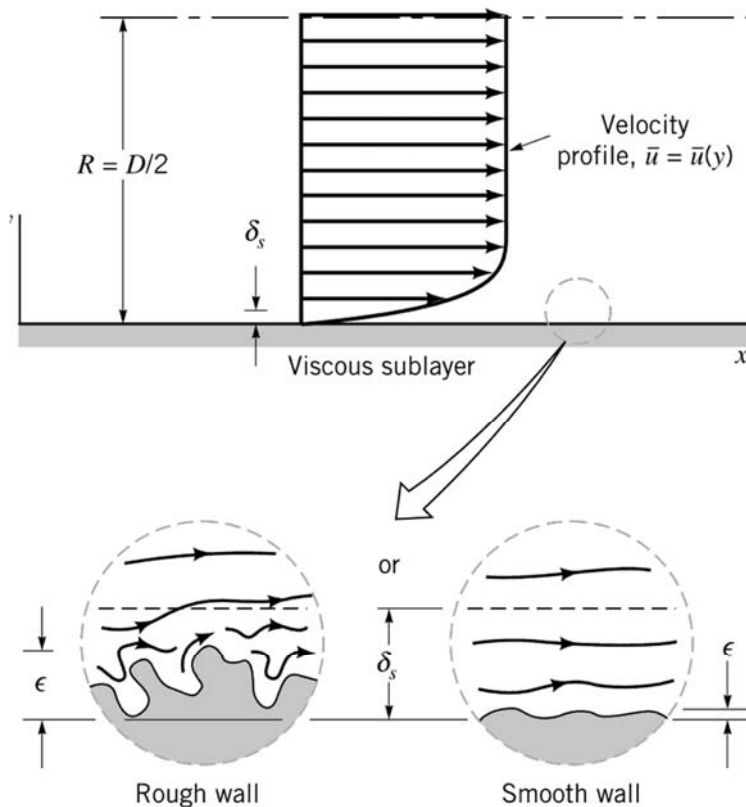
# ABACO DI MOODY

Although the pressure drop for laminar pipe flow is found to be independent of the roughness of the pipe, it is necessary to include this parameter when considering turbulent flow. As is discussed in **Section 8.3.3** and illustrated in Fig. 8.19, for turbulent flow there is a relatively thin viscous sublayer formed in the fluid near the pipe wall. In many instances this layer is very thin;  $\delta_s/D \ll 1$ , where  $\delta_s$  is the sublayer thickness. If a typical wall roughness element protrudes sufficiently far into (or even through) this layer, the structure and properties of the viscous sublayer (along with  $\Delta p$  and  $\tau_w$ ) will be different than if the wall were smooth. **Thus, for turbulent flow the pressure drop is expected to be a function of the wall roughness.** For laminar flow there is no thin viscous layer—viscous effects are important across the entire pipe. Thus, relatively small roughness elements have completely negligible effects on laminar pipe flow. **Of course, for pipes with very large wall “roughness,” ( $\varepsilon/D \gtrsim 0.1$ ), such as that in corrugated pipes, the flowrate may be a function of the “roughness.”** We will consider only typical constant diameter pipes with relative roughnesses in the range  $0 \leq \varepsilon/D \lesssim 0.05$ . Analysis of flow in corrugated pipes does not fit into the standard constant diameter pipe category, although experimental results for such pipes are available (Ref. 30).





## ABACO DI MOODY



■ FIGURE 8.19 Flow in the viscous sublayer near rough and smooth walls.

## ABACO DI MOODY

The list of parameters given in Eq. 8.32 is apparently a complete one. That is, experiments have shown that other parameters (such as surface tension, vapor pressure, etc.) do not affect the pressure drop for the conditions stated (steady, incompressible flow; round, horizontal pipe). Since there are seven variables ( $k = 7$ ) which can be written in terms of the three reference dimensions  $MLT$  ( $r = 3$ ), Eq. 8.32 can be written in dimensionless form in terms of  $k - r = 4$  dimensionless groups. As was discussed in Section 7.9.1, one such representation is

$$\frac{\Delta p}{\frac{1}{2}\rho V^2} = \tilde{\phi}\left(\frac{\rho V D}{\mu}, \frac{\ell}{D}, \frac{\epsilon}{D}\right)$$



As was done for laminar flow, the functional representation can be simplified by imposing the reasonable assumption that the pressure drop should be proportional to the pipe length. (Such a step is not within the realm of dimensional analysis. It is merely a logical assumption supported by experiments.) The only way that this can be true is if the  $\ell/D$  dependence is factored out as

$$\frac{\Delta p}{\frac{1}{2}\rho V^2} = \frac{\ell}{D} \phi\left(\text{Re}, \frac{\varepsilon}{D}\right)$$

As was discussed in Section 8.2.3, the quantity  $\Delta p D / (\ell \rho V^2 / 2)$  is termed the friction factor,  $f$ . Thus, for a horizontal pipe

$$\Delta p = f \frac{\ell}{D} \frac{\rho V^2}{2} \quad (8.33)$$

where

$$f = \phi\left(\text{Re}, \frac{\varepsilon}{D}\right)$$

For laminar fully developed flow, the value of  $f$  is simply  $f = 64/\text{Re}$ , independent of  $\varepsilon/D$ . For turbulent flow, the functional dependence of the friction factor on the Reynolds number and the relative roughness,  $f = \phi(\text{Re}, \varepsilon/D)$ , is a rather complex one that cannot, as yet, be obtained from a theoretical analysis. The results are obtained from an exhaustive set of experiments and usually presented in terms of a curve-fitting formula or the equivalent graphical form.

## ABACO DI MOODY

Nikuradse [7] simulated roughness by gluing uniform sand grains onto the inner walls of the pipes. He then measured the pressure drops and flow rates and correlated friction factor versus Reynolds number in Fig. 6.12*b*. We see that laminar friction is unaffected, but turbulent friction, after an *onset* point, increases monotonically with the roughness ratio  $\varepsilon/d$ . For any given  $\varepsilon/d$ , the friction factor becomes constant (*fully rough*) at high Reynolds numbers. These points of change are certain values of  $\varepsilon^+ = \varepsilon u^*/\nu$ :

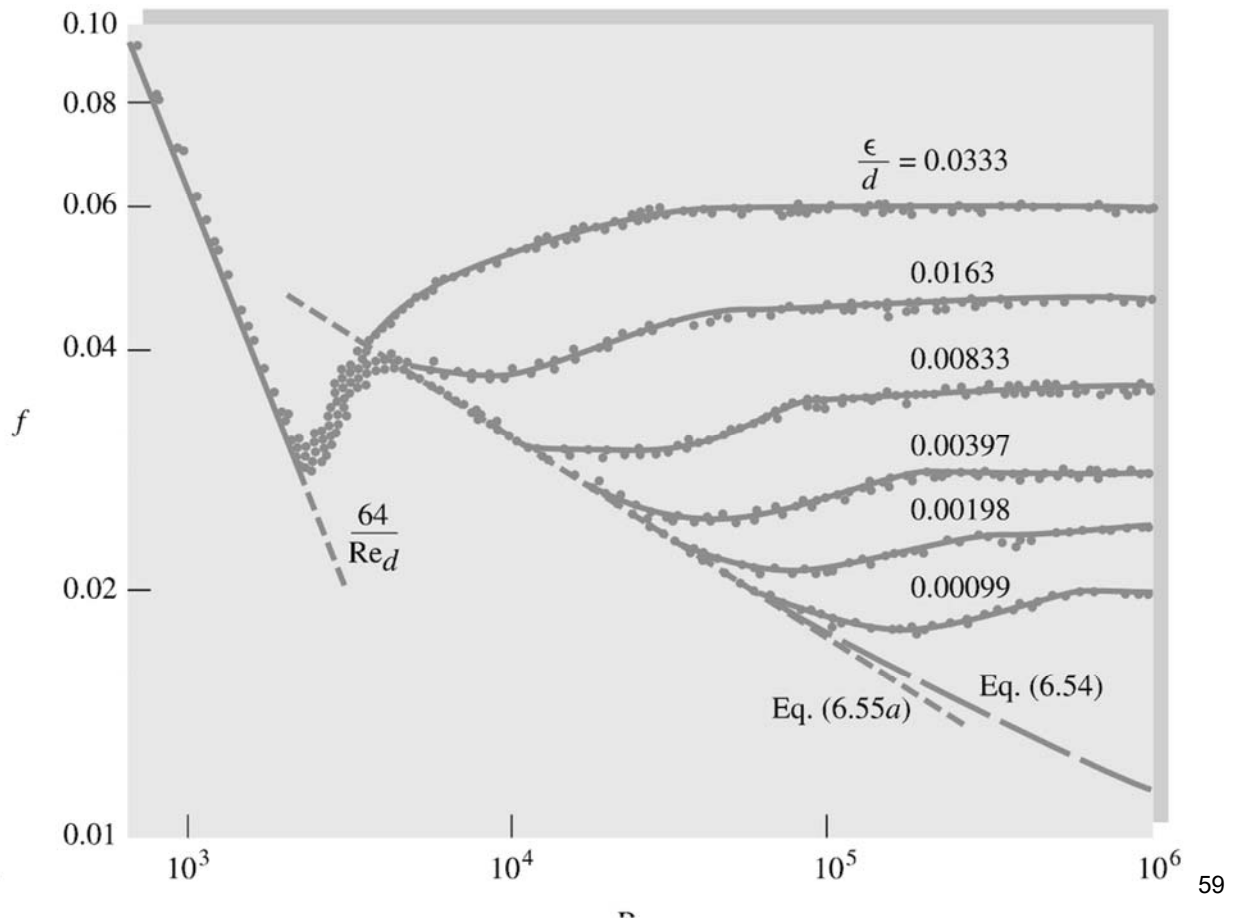
$$\frac{\varepsilon u^*}{\nu} < 5: \quad \text{hydraulically smooth walls, no effect of roughness on friction}$$

$$5 \leq \frac{\varepsilon u^*}{\nu} \leq 70: \quad \text{transitional roughness, moderate Reynolds-number effect}$$

$$\frac{\varepsilon u^*}{\nu} > 70: \quad \text{fully rough flow, sublayer totally broken up and friction independent of Reynolds number}$$



## ABACO DI MOODY



## ABACO DI MOODY

In 1939 to cover the transitionally rough range, Colebrook [9] combined the smooth-wall [Eq. (6.54)] and fully rough [Eq. (6.63)] relations into a clever interpolation formula

$$\frac{1}{f^{1/2}} = -2.0 \log \left( \frac{\epsilon/d}{3.7} + \frac{2.51}{Re_d f^{1/2}} \right) \quad (6.64)$$

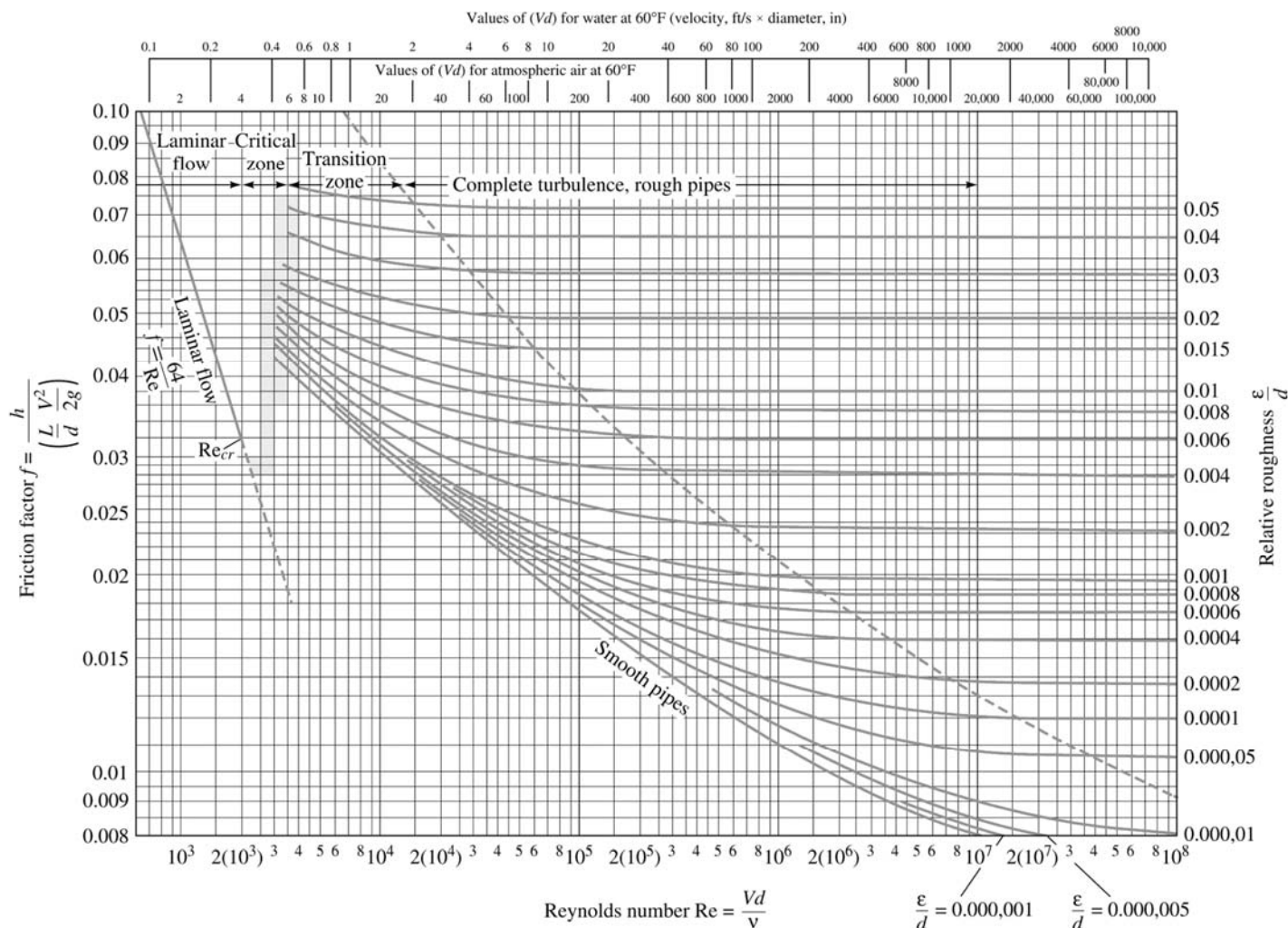
This is the accepted design formula for turbulent friction. It was plotted in 1944 by Moody [8] into what is now called the **Moody chart** for pipe friction (Fig. 6.13). The Moody chart is probably the most famous and useful figure in fluid mechanics. It is accurate to  $\pm 15$  percent for design calculations over the full range shown in Fig. 6.13. It can be used for circular and noncircular (Sec. 6.6) pipe flows and for open-channel flows (Chap. 10). The data can even be adapted as an approximation to boundary-layer flows (Chap. 7).

Equation (6.64) is cumbersome to evaluate for  $f$  if  $Re_d$  is known, although it easily yields to the EES Equation Solver. An alternate explicit formula given by Haaland [33] as

$$\frac{1}{f^{1/2}} \approx -1.8 \log \left[ \frac{6.9}{Re_d} + \left( \frac{\epsilon/d}{3.7} \right)^{1.11} \right] \quad (6.64a)$$

varies less than 2 percent from Eq. (6.64).





## TIPICHE SCABREZZE

Material	Condition	$\epsilon$		Uncertainty, %
		ft	mm	
Steel	Sheet metal, new	0.00016	0.05	± 60
	Stainless, new	0.000007	0.002	± 50
	Commercial, new	0.00015	0.046	± 30
	Riveted	0.01	3.0	± 70
	Rusted	0.007	2.0	± 50
Iron	Cast, new	0.00085	0.26	± 50
	Wrought, new	0.00015	0.046	± 20
	Galvanized, new	0.0005	0.15	± 40
	Asphalted cast	0.0004	0.12	± 50
Brass	Drawn, new	0.000007	0.002	± 50
Plastic	Drawn tubing	0.000005	0.0015	± 60
Glass	—	Smooth	Smooth	
Concrete	Smoothed	0.00013	0.04	± 60
	Rough	0.007	2.0	± 50
Rubber	Smoothed	0.000033	0.01	± 60
Wood	Stave	0.0016	0.5	± 40



## TRE POSSIBILI PROBLEMI

The Moody chart (Fig. 6.13) can be used to solve almost any problem involving friction losses in long pipe flows. However, many such problems involve considerable iteration and repeated calculations using the chart because the standard Moody chart is essentially a *head-loss chart*. One is supposed to know all other variables, compute  $Re_d$ , enter the chart, find  $f$ , and hence compute  $h_f$ . This is one of three fundamental problems which are commonly encountered in pipe-flow calculations:

1. Given  $d$ ,  $L$ , and  $V$  or  $Q$ ,  $\rho$ ,  $\mu$ , and  $g$ , compute the head loss  $h_f$  (head-loss problem).
2. Given  $d$ ,  $L$ ,  $h_f$ ,  $\rho$ ,  $\mu$ , and  $g$ , compute the velocity  $V$  or flow rate  $Q$  (flow-rate problem).
3. Given  $Q$ ,  $L$ ,  $h_f$ ,  $\rho$ ,  $\mu$ , and  $g$ , compute the diameter  $d$  of the pipe (sizing problem).



### EXAMPLE 6.6<sup>3</sup>

Compute the loss of head and pressure drop in 200 ft of horizontal 6-in-diameter asphalted cast-iron pipe carrying water with a mean velocity of 6 ft/s.

#### Solution

One can estimate the Reynolds number of water and air from the Moody chart. Look across the top of the chart to  $V \text{ (ft/s)} \times d \text{ (in)} = 36$ , and then look directly down to the bottom abscissa to find that  $Re_d(\text{water}) \approx 2.7 \times 10^5$ . The roughness ratio for asphalted cast iron ( $\epsilon = 0.0004 \text{ ft}$ ) is

$$\frac{\epsilon}{d} = \frac{0.0004}{\frac{6}{12}} = 0.0008$$

Find the line on the right side for  $\epsilon/d = 0.0008$ , and follow it to the left until it intersects the vertical line for  $Re = 2.7 \times 10^5$ . Read, approximately,  $f = 0.02$  [or compute  $f = 0.0197$  from Eq. (6.64a)]. Then the head loss is

$$h_f = f \frac{L}{d} \frac{V^2}{2g} = (0.02) \frac{200}{0.5} \frac{(6 \text{ ft/s})^2}{2(32.2 \text{ ft/s}^2)} = 4.5 \text{ ft} \quad \text{Ans.}$$

The pressure drop for a horizontal pipe ( $z_1 = z_2$ ) is

$$\Delta p = \rho g h_f = (62.4 \text{ lbf/ft}^3)(4.5 \text{ ft}) = 280 \text{ lbf/ft}^2 \quad \text{Ans.}$$



Moody points out that this computation, even for clean new pipe, can be considered accurate only to about  $\pm 10$  percent.

## Esempi (Head loss)

### EXAMPLE 6.7

Oil, with  $\rho = 900 \text{ kg/m}^3$  and  $\nu = 0.00001 \text{ m}^2/\text{s}$ , flows at  $0.2 \text{ m}^3/\text{s}$  through 500 m of 200-mm-diameter cast-iron pipe. Determine (a) the head loss and (b) the pressure drop if the pipe slopes down at  $10^\circ$  in the flow direction.

### Solution

First compute the velocity from the known flow rate

$$V = \frac{Q}{\pi R^2} = \frac{0.2 \text{ m}^3/\text{s}}{\pi(0.1 \text{ m})^2} = 6.4 \text{ m/s}$$

Then the Reynolds number is

$$\text{Re}_d = \frac{Vd}{\nu} = \frac{(6.4 \text{ m/s})(0.2 \text{ m})}{0.00001 \text{ m}^2/\text{s}} = 128,000$$

From Table 6.1,  $\epsilon = 0.26 \text{ mm}$  for cast-iron pipe. Then

$$\frac{\epsilon}{d} = \frac{0.26 \text{ mm}}{200 \text{ mm}} = 0.0013$$



Complementi di Gasdinamica – T Astarita

66

## Esempi (Head loss)

Enter the Moody chart on the right at  $\epsilon/d = 0.0013$  (you will have to interpolate), and move to the left to intersect with  $\text{Re} = 128,000$ . Read  $f \approx 0.0225$  [from Eq. (6.64) for these values we could compute  $f = 0.0227$ ]. Then the head loss is

$$h_f = f \frac{L}{d} \frac{V^2}{2g} = (0.0225) \frac{500 \text{ m}}{0.2 \text{ m}} \frac{(6.4 \text{ m/s})^2}{2(9.81 \text{ m/s}^2)} = 117 \text{ m} \quad \text{Ans. (a)}$$

From Eq. (6.25) for the inclined pipe,

$$h_f = \frac{\Delta p}{\rho g} + z_1 - z_2 = \frac{\Delta p}{\rho g} + L \sin 10^\circ$$

$$\text{or} \quad \Delta p = \rho g [h_f - (500 \text{ m}) \sin 10^\circ] = \rho g (117 \text{ m} - 87 \text{ m})$$

$$= (900 \text{ kg/m}^3)(9.81 \text{ m/s}^2)(30 \text{ m}) = 265,000 \text{ kg/(m} \cdot \text{s}^2) = 265,000 \text{ Pa} \quad \text{Ans. (b)}$$



## ESEMPI (FLOW RATE)

### EXAMPLE 6.9

Oil, with  $\rho = 950 \text{ kg/m}^3$  and  $\nu = 2 \text{ E-5 m}^2/\text{s}$ , flows through a 30-cm-diameter pipe 100 m long with a head loss of 8 m. The roughness ratio is  $\epsilon/d = 0.0002$ . Find the average velocity and flow rate.

By definition, the friction factor is known except for  $V$ :

$$f = h_f \frac{d}{L} \frac{2g}{V^2} = (8 \text{ m}) \left( \frac{0.3 \text{ m}}{100 \text{ m}} \right) \left[ \frac{2(9.81 \text{ m/s}^2)}{V^2} \right] \quad \text{or} \quad fV^2 \approx 0.471 \quad (\text{SI units})$$

To get started, we only need to guess  $f$ , compute  $V = \sqrt{0.471/f}$ , then get  $\text{Re}_d$ , compute a better  $f$  from the Moody chart, and repeat. The process converges fairly rapidly. A good first guess is the “fully rough” value for  $\epsilon/d = 0.0002$ , or  $f \approx 0.014$  from Fig. 6.13. The iteration would be as follows:



## ESEMPI (FLOW RATE)

Guess  $f \approx 0.014$ , then  $V = \sqrt{0.471/0.014} = 5.80 \text{ m/s}$  and  $\text{Re}_d = Vd/\nu \approx 87,000$ . At  $\text{Re}_d = 87,000$  and  $\epsilon/d = 0.0002$ , compute  $f_{\text{new}} \approx 0.0195$  [Eq. (6.64)].

New  $f \approx 0.0195$ ,  $V = \sqrt{0.481/0.0195} = 4.91 \text{ m/s}$  and  $\text{Re}_d = Vd/\nu = 73,700$ . At  $\text{Re}_d = 73,700$  and  $\epsilon/d = 0.0002$ , compute  $f_{\text{new}} \approx 0.0201$  [Eq. (6.64)].

Better  $f \approx 0.0201$ ,  $V = \sqrt{0.471/0.0201} = 4.84 \text{ m/s}$  and  $\text{Re}_d \approx 72,600$ . At  $\text{Re}_d = 72,600$  and  $\epsilon/d = 0.0002$ , compute  $f_{\text{new}} \approx 0.0201$  [Eq. (6.64)].

We have converged to three significant figures. Thus our iterative solution is

$$V = 4.84 \text{ m/s}$$

$$Q = V \left( \frac{\pi}{4} \right) d^2 = (4.84) \left( \frac{\pi}{4} \right) (0.3)^2 \approx 0.342 \text{ m}^3/\text{s} \quad \text{Ans.}$$

The iterative approach is straightforward and not too onerous, so it is routinely used by engineers. Obviously this repetitive procedure is ideal for a personal computer.



## ESEMPI (SIZING PROBLEM)

### EXAMPLE 6.11

Work Example 6.9 backward, assuming that  $Q = 0.342 \text{ m}^3/\text{s}$  and  $\epsilon = 0.06 \text{ mm}$  are known but that  $d$  (30 cm) is unknown. Recall  $L = 100 \text{ m}$ ,  $\rho = 950 \text{ kg/m}^3$ ,  $\nu = 2 \text{ E-5 m}^2/\text{s}$ , and  $h_f = 8 \text{ m}$ .

### Iterative Solution

First write the diameter in terms of the friction factor:

$$f = \frac{\pi^2}{8} \frac{(9.81 \text{ m/s}^2)(8 \text{ m})d^5}{(100 \text{ m})(0.342 \text{ m}^3/\text{s})^2} = 8.28d^5 \quad \text{or} \quad d \approx 0.655f^{1/5} \quad (1)$$

in SI units. Also write the Reynolds number and roughness ratio in terms of the diameter:



## ESEMPI (SIZING PROBLEM)

$$\text{Re}_d = \frac{4(0.342 \text{ m}^3/\text{s})}{\pi(2 \text{ E-5 m}^2/\text{s})d} = \frac{21,800}{d} \quad (2)$$

$$\frac{\epsilon}{d} = \frac{6 \text{ E-5 m}}{d} \quad (3)$$

Guess  $f$ , compute  $d$  from (1), then compute  $\text{Re}_d$  from (2) and  $\epsilon/d$  from (3), and compute a better  $f$  from the Moody chart or Eq. (6.64). Repeat until (fairly rapid) convergence. Having no initial estimate for  $f$ , the writer guesses  $f \approx 0.03$  (about in the middle of the turbulent portion of the Moody chart). The following calculations result:

$$f \approx 0.03 \quad d \approx 0.655(0.03)^{1/5} \approx 0.325 \text{ m}$$

$$\text{Re}_d \approx \frac{21,800}{0.325} \approx 67,000 \quad \frac{\epsilon}{d} \approx 1.85 \text{ E-4}$$

$$\text{Eq. (6.54):} \quad f_{\text{new}} \approx 0.0203 \quad \text{then} \quad d_{\text{new}} \approx 0.301 \text{ m}$$

$$\text{Re}_{d,\text{new}} \approx 72,500 \quad \frac{\epsilon}{d} \approx 2.0 \text{ E-4}$$

$$\text{Eq. (6.54):} \quad f_{\text{better}} \approx 0.0201 \quad \text{and} \quad d = 0.300 \text{ m}$$

Ans.



The procedure has converged to the correct diameter of 30 cm given in Example 6.9.



### EXAMPLE 6.12

Work Moody's problem, Example 6.6, backward to find the unknown (6 in) diameter if the flow rate  $Q = 1.18 \text{ ft}^3/\text{s}$  is known. Recall  $L = 200 \text{ ft}$ ,  $\epsilon = 0.0004 \text{ ft}$ , and  $\nu = 1.1 \text{ E-5 ft}^2/\text{s}$ .

### Solution

Write  $f$ ,  $\text{Re}_d$ , and  $\epsilon/d$  in terms of the diameter:

$$f = \frac{\pi^2}{8} \frac{gh_f d^5}{LQ^2} = \frac{\pi^2}{8} \frac{(32.2 \text{ ft/s}^2)(4.5 \text{ ft})d^5}{(200 \text{ ft})(1.18 \text{ ft}^3/\text{s})^2} = 0.642d^5 \quad \text{or} \quad d \approx 1.093f^{1/5} \quad (1)$$

$$\text{Re}_d = \frac{4(1.18 \text{ ft}^3/\text{s})}{\pi(1.1 \text{ E-5 ft}^2/\text{s})d} = \frac{136,600}{d} \quad (2)$$

$$\frac{\epsilon}{d} = \frac{0.0004 \text{ ft}}{d} \quad (3)$$

with everything in BG units, of course. Guess  $f$ ; compute  $d$  from (1),  $\text{Re}_d$  from (2), and  $\epsilon/d$  from (3); and then compute a better  $f$  from the Moody chart. Repeat until convergence. The writer traditionally guesses an initial  $f \approx 0.03$ :

$$f \approx 0.03 \quad d \approx 1.093(0.03)^{1/5} \approx 0.542 \text{ ft}$$

$$\text{Re}_d = \frac{136,600}{0.542} \approx 252,000 \quad \frac{\epsilon}{d} \approx 7.38 \text{ E-4}$$

$$f_{\text{new}} \approx 0.0196 \quad d_{\text{new}} \approx 0.498 \text{ ft} \quad \text{Re}_d \approx 274,000 \quad \frac{\epsilon}{d} \approx 8.03 \text{ E-4}$$

$$f_{\text{better}} \approx 0.0198 \quad d \approx 0.499 \text{ ft} \quad \text{Ans.}$$



Cor. Convergence is rapid, and the predicted diameter is correct, about 6 in. The slight discrepancy (0.499 rather than 0.500 ft) arises because  $h_f$  was rounded to 4.5 ft.

71

## PERDITE DI CARICO CONCENTRATE

Le perdite di carico concentrate si hanno in:

- Ingressi (o uscite) di condotti
- Variazioni di sezione repentine
- Variazioni di sezione gradual
- Curve, condotti a T, in generale tutte le connessioni di condotti
- Valvole (aperte, o parzialmente chiuse)

Coefficiente di perdita

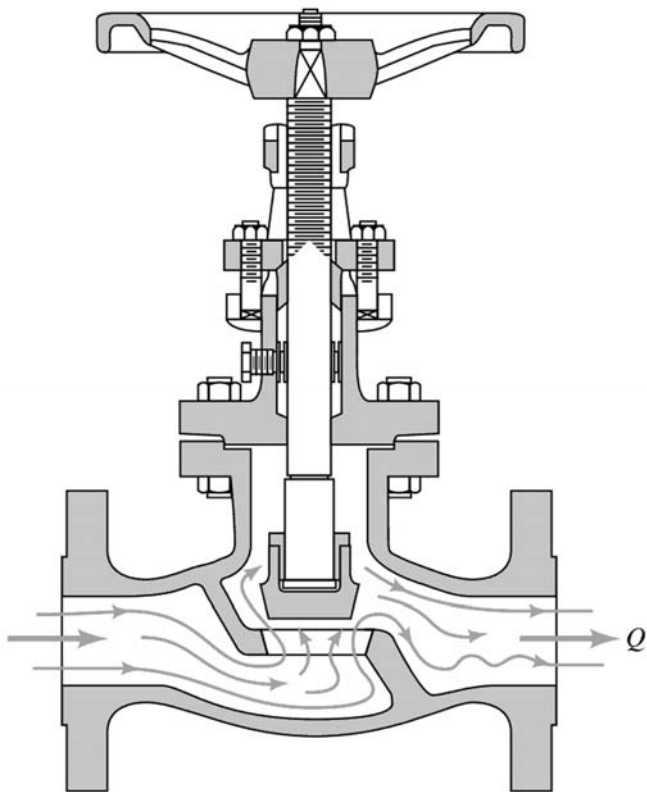
$$K = \frac{h_c}{V^2/2g} = \frac{\Delta p}{V^2/2g}$$

Oppure si utilizza una lunghezza equivalente.





# Valvole



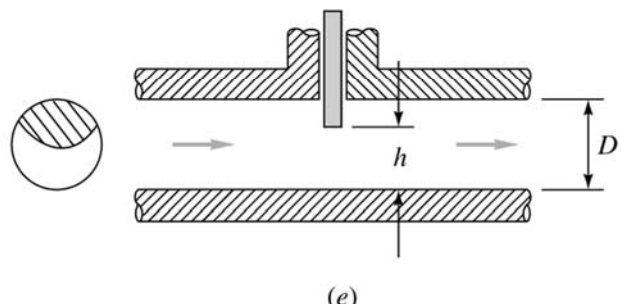
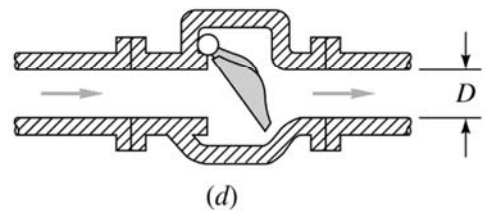
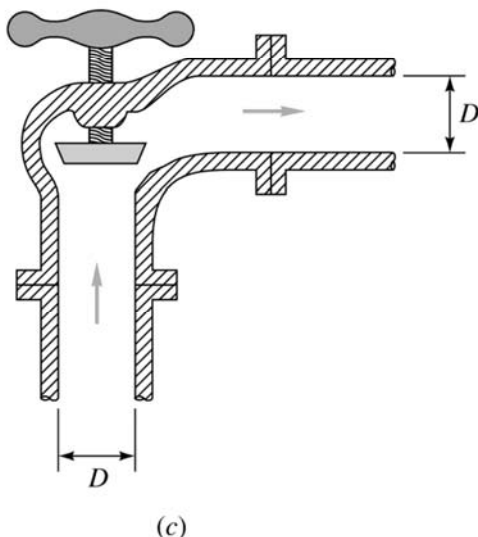
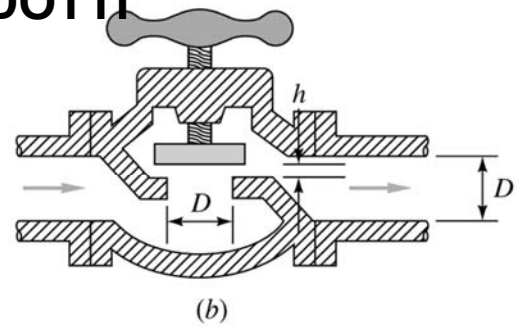
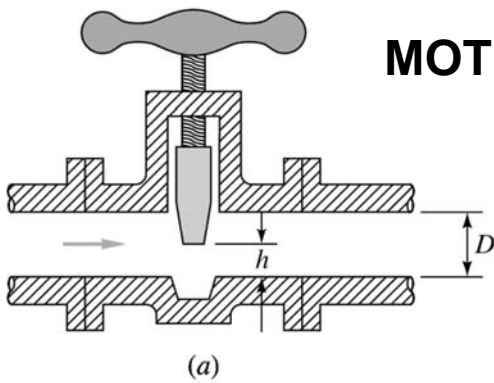
$$K = \frac{h_c}{V^2/2g} = \frac{\Delta p}{V^2/2g}$$



Complementi di Gasdinamica – T Astarita

73

## MOTI IN CONDOTTI



a/e) Valvola a saracinesca; b) Valvola a globo c) Valvola ad angolo d) Valvola a farfalla



Complementi di Gasdinamica – T Astarita

74

# VALVOLE

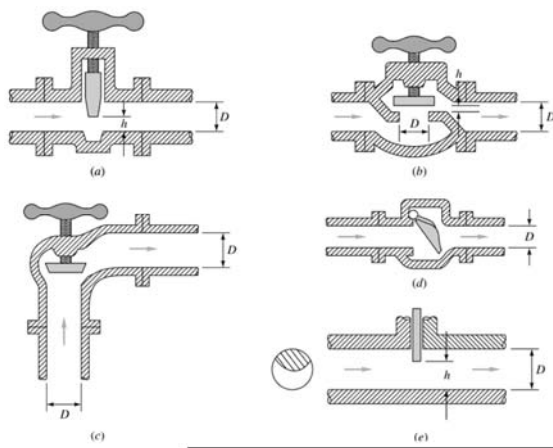


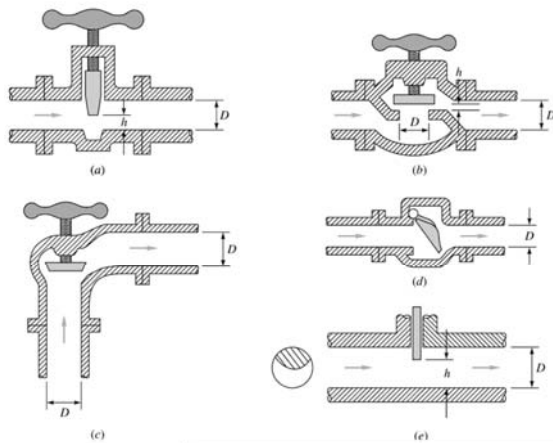
**Fig. 6.17** Typical commercial valve geometries: (a) gate valve; (b) globe valve; (c) angle valve; (d) swing-check valve; (e) disk-type gate valve.

	Nominal diameter, in									
	Screwed					Flanged				
	$\frac{1}{2}$	1	2	4		1	2	4	8	20
Valves (fully open):										
Globe	14	8.2	6.9	5.7		13	8.5	6.0	5.8	5.5
Gate	0.30	0.24	0.16	0.11		0.80	0.35	0.16	0.07	0.03
Swing check	5.1	2.9	2.1	2.0		2.0	2.0	2.0	2.0	2.0
Angle	9.0	4.7	2.0	1.0		4.5	2.4	2.0	2.0	2.0
Elbows:										
45° regular	0.39	0.32	0.30	0.29						
45° long radius						0.21	0.20	0.19	0.16	0.14
90° regular	2.0	1.5	0.95	0.64		0.50	0.39	0.30	0.26	0.21
90° long radius	1.0	0.72	0.41	0.23		0.40	0.30	0.19	0.15	0.10
180° regular	2.0	1.5	0.95	0.64		0.41	0.35	0.30	0.25	0.20
180° long radius						0.40	0.30	0.21	0.15	0.10
Tees:										
Line flow	0.90	0.90	0.90	0.90		0.24	0.19	0.14	0.10	0.07
Branch flow	2.4	1.8	1.4	1.1		1.0	0.80	0.64	0.58	0.41



Comple

75



Globe, fully open	10
Angle, fully open	2
Gate, fully open	0.15
Gate, $\frac{1}{4}$ closed	0.26
Gate, $\frac{1}{2}$ closed	2.1
Gate, $\frac{3}{4}$ closed	17
Swing check, forward flow	2
Swing check, backward flow	$\infty$
Ball valve, fully open	0.05
Ball valve, $\frac{1}{3}$ closed	5.5
Ball valve, $\frac{2}{3}$ closed	210

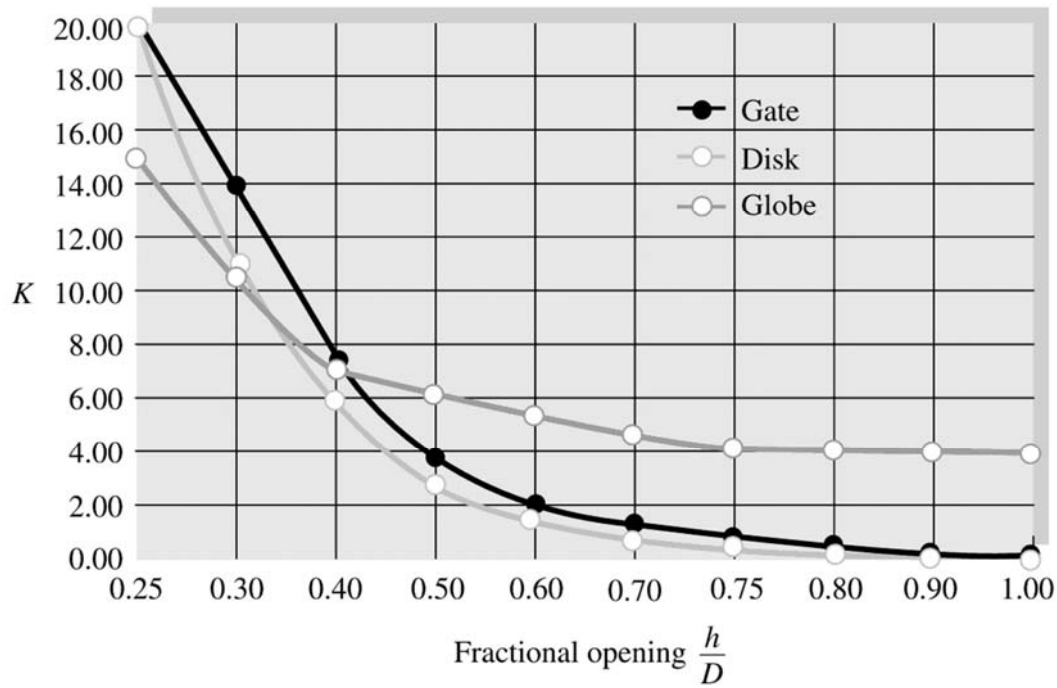
	Nominal diameter, in									
	Screwed					Flanged				
	$\frac{1}{2}$	1	2	4		1	2	4	8	20
Valves (fully open):										
Globe	14	8.2	6.9	5.7		13	8.5	6.0	5.8	5.5
Gate	0.30	0.24	0.16	0.11		0.80	0.35	0.16	0.07	0.03
Swing check	5.1	2.9	2.1	2.0		2.0	2.0	2.0	2.0	2.0
Angle	9.0	4.7	2.0	1.0		4.5	2.4	2.0	2.0	2.0
Elbows:										
45° regular	0.39	0.32	0.30	0.29						
45° long radius						0.21	0.20	0.19	0.16	0.14
90° regular	2.0	1.5	0.95	0.64		0.50	0.39	0.30	0.26	0.21
90° long radius	1.0	0.72	0.41	0.23		0.40	0.30	0.19	0.15	0.10
180° regular	2.0	1.5	0.95	0.64		0.41	0.35	0.30	0.25	0.20
180° long radius						0.40	0.30	0.21	0.15	0.10
Tees:										
Line flow	0.90	0.90	0.90	0.90		0.24	0.19	0.14	0.10	0.07
Branch flow	2.4	1.8	1.4	1.1		1.0	0.80	0.64	0.58	0.41



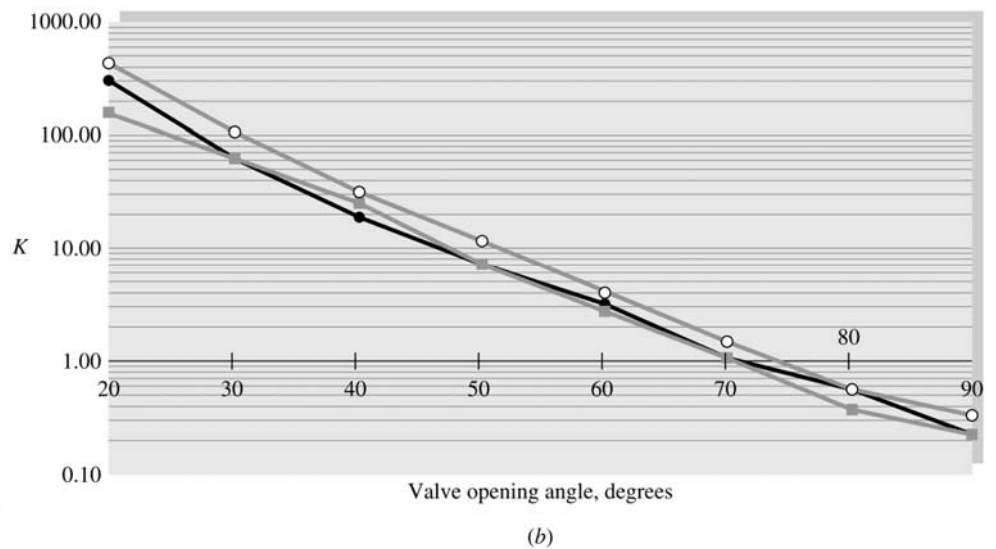
Comple

76

## VALVOLE



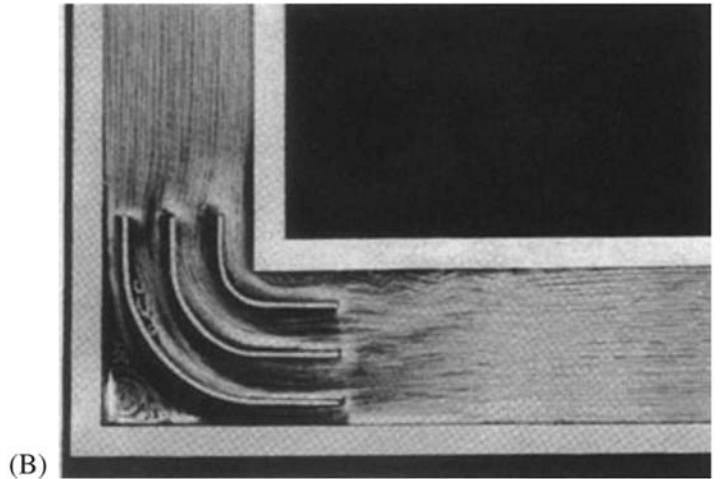
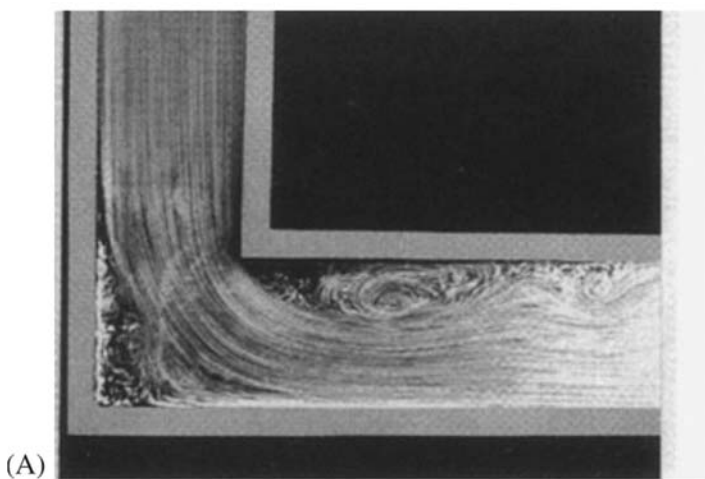
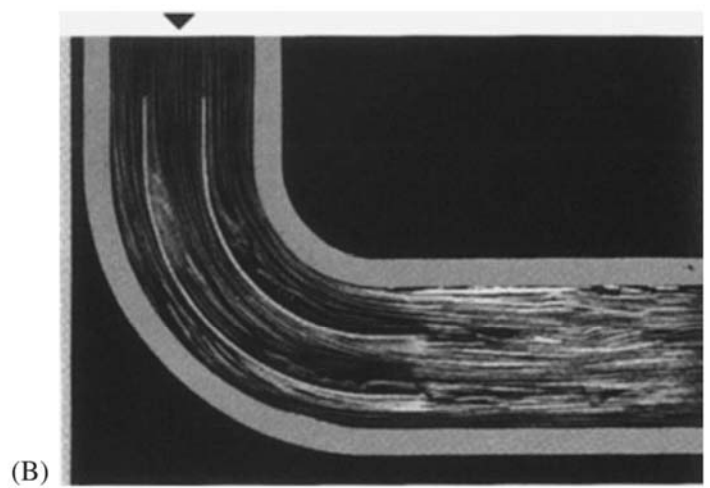
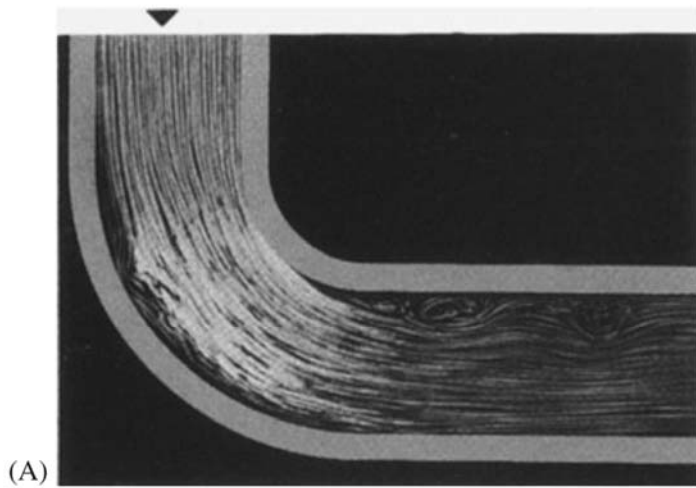
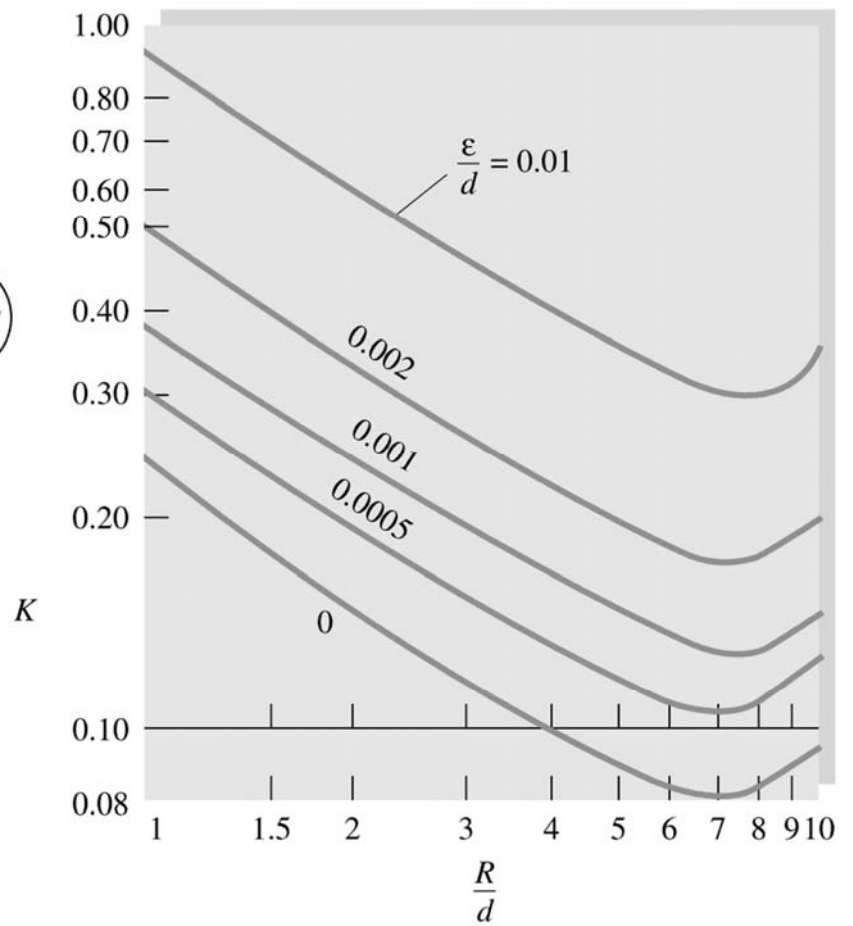
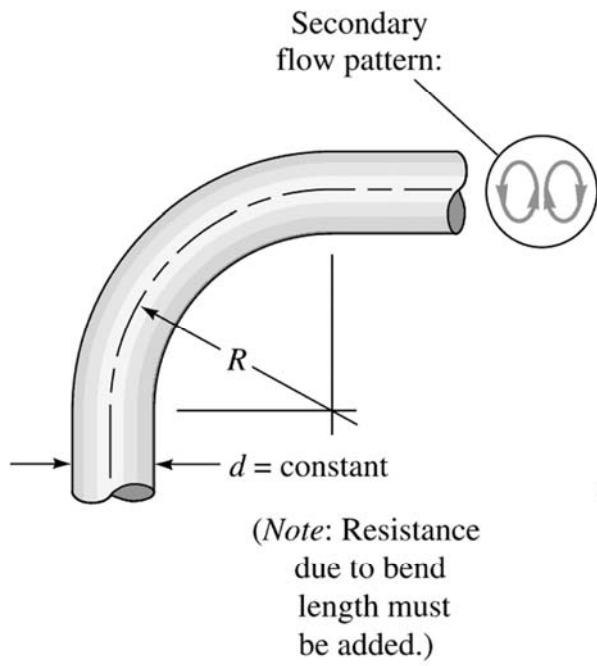
## VALVOLE

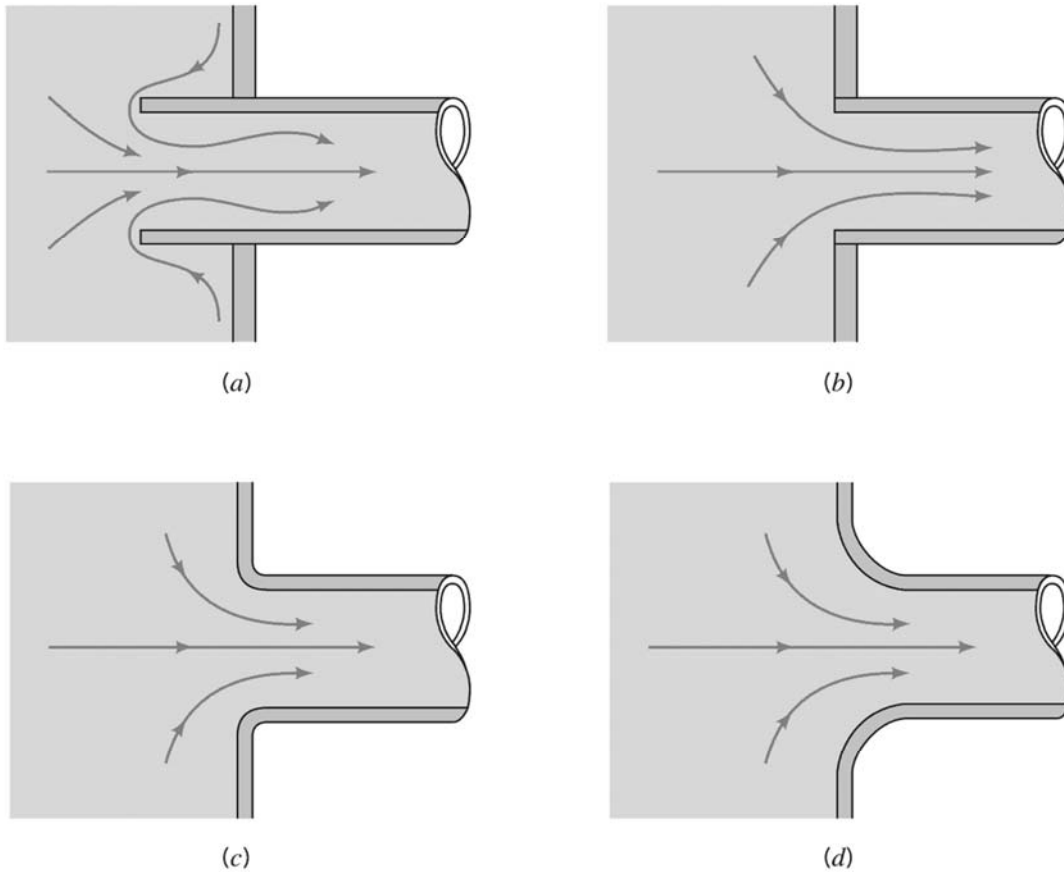


**Fig. 6.19** Performance of butterfly valves: (a) typical geometry (*courtesy of Grinnell Corp., Cranston, R.I.*); (b) loss coefficients for three different manufacturers.



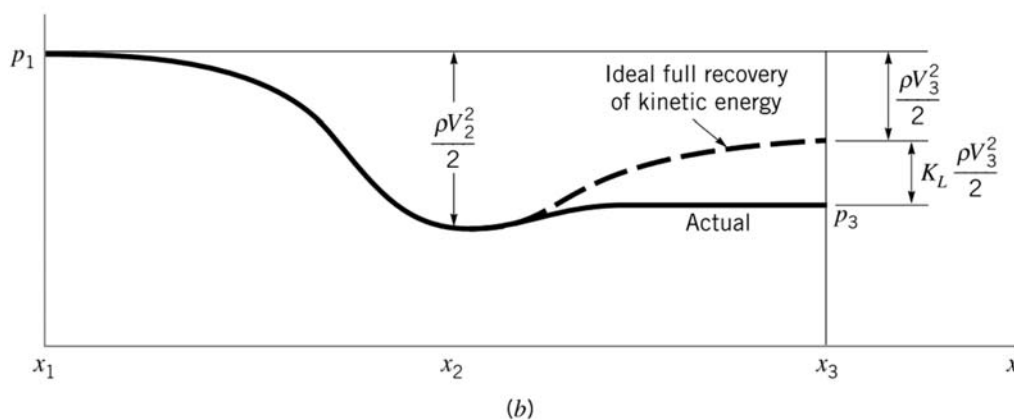
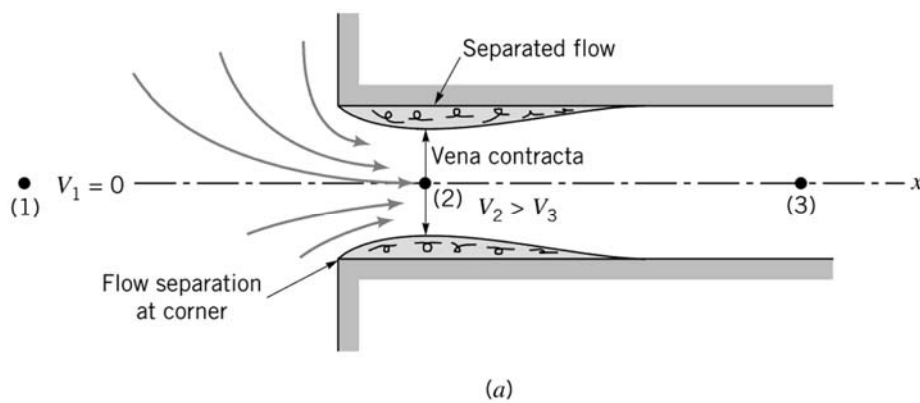
# Curve





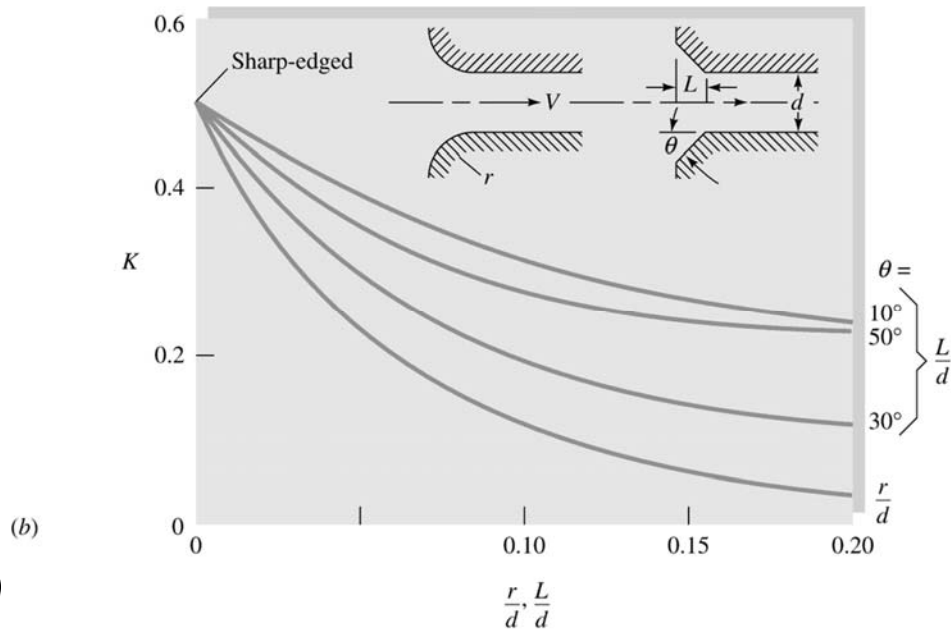
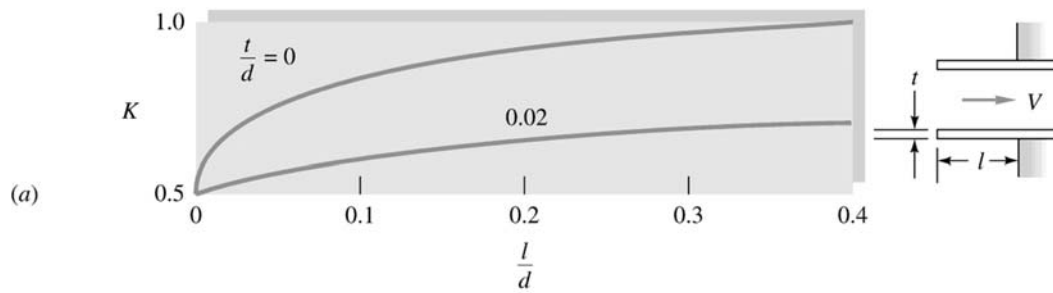
■ **FIGURE 8.22** Entrance flow conditions and loss coefficient (Refs. 28, 29). (a) Reentrant,  $K_L = 0.8$ , (b) sharp-edged,  $K_L = 0.5$ , (c) slightly rounded,  $K_L = 0.2$  (see Fig. 8.24), (d) well-rounded,  $K_L = 0.04$  (see Fig. 8.24).

## Ingressi



■ **FIGURE 8.23** Flow pattern and pressure distribution for a sharp-edged entrance.<sup>2</sup>

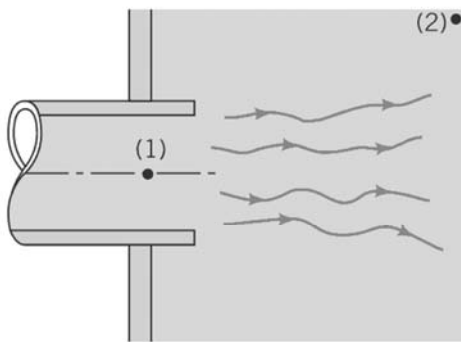
# Ingressi



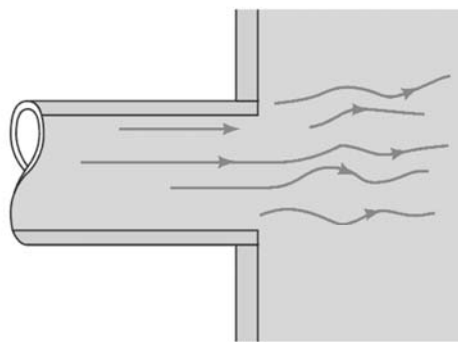
Comp

83

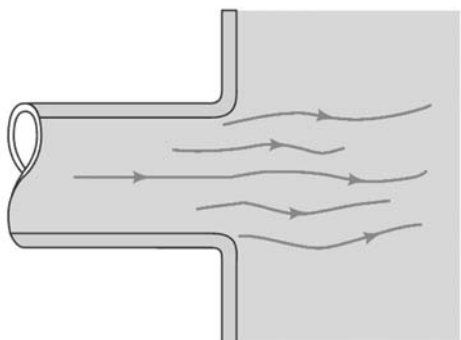
## VARIAZIONI DI SEZIONE REPENTINE



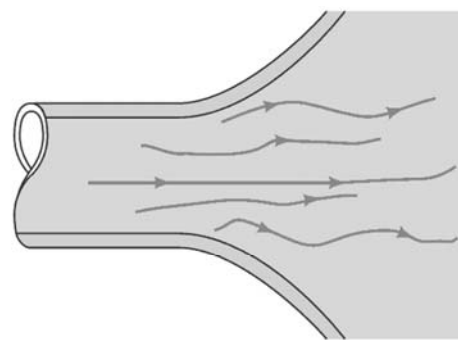
(a)



(b)



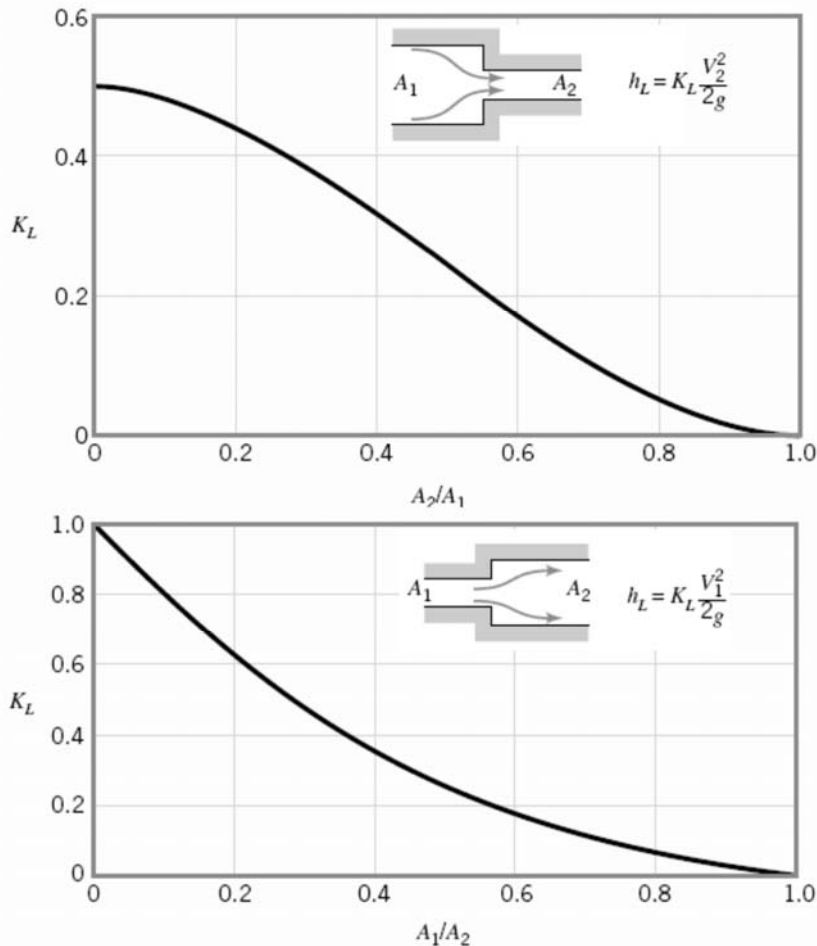
(c)



(d)

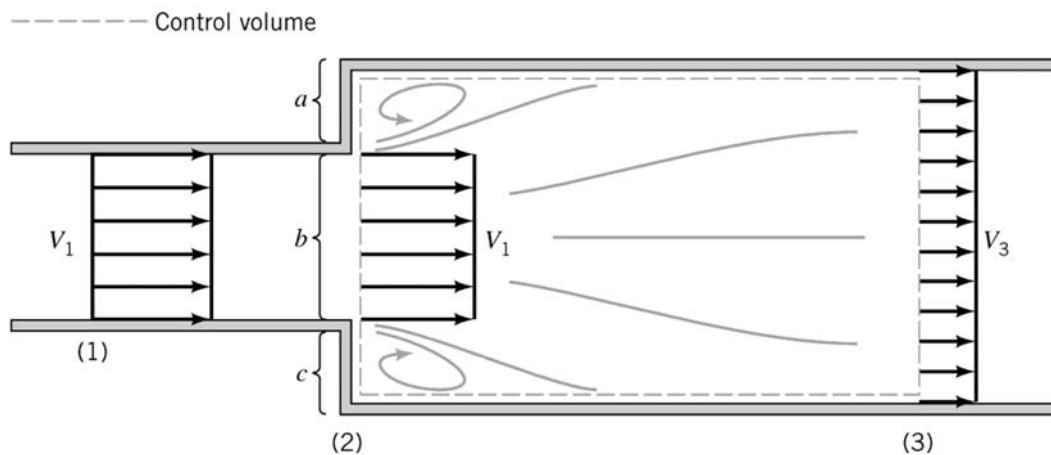


# VARIAZIONI DI SEZIONE REPENTINE



Complementi d

85



A **sudden expansion** is one of the few components (perhaps the only one) for which the loss coefficient can be obtained by means of **a simple analysis**. To do this we consider the continuity and momentum equations for the control volume shown in Fig. 8.28 and the energy equation applied between (2) and (3). We assume that the flow is uniform at sections (1), (2), and (3) and the pressure is constant across the left-hand side of the control volume ( $p_a = p_b = p_c = p_1$ ). The resulting three governing equations (**mass, momentum, and energy**) are

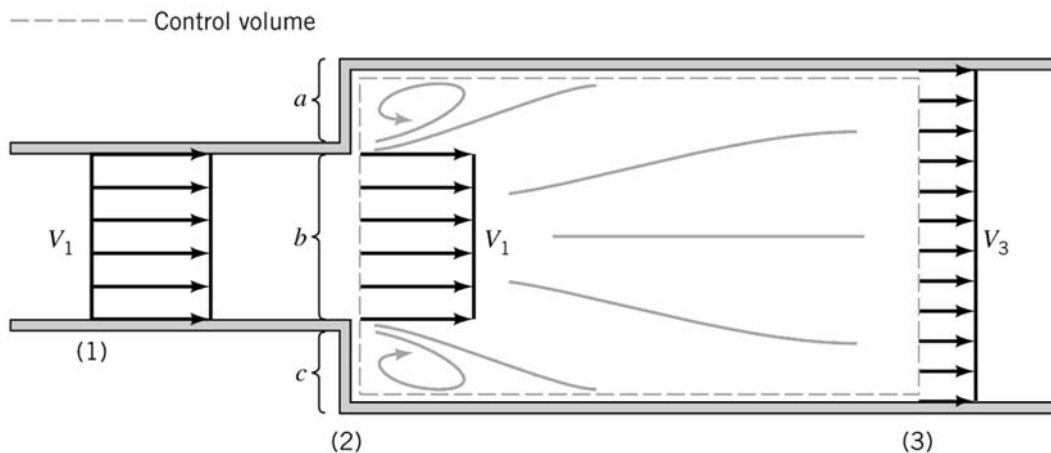
$$A_1 V_1 = A_3 V_3$$

$$p_1 A_3 - p_3 A_3 = \rho A_3 V_3 (V_3 - V_1)$$

and

$$\frac{p_1}{\gamma} + \frac{V_1^2}{2g} = \frac{p_3}{\gamma} + \frac{V_3^2}{2g} + h_L$$





$$A_1 V_1 = A_3 V_3$$

$$p_1 A_3 - p_3 A_3 = \rho A_3 V_3 (V_3 - V_1)$$

$$\frac{p_1}{\gamma} + \frac{V_1^2}{2g} = \frac{p_3}{\gamma} + \frac{V_3^2}{2g} + h_L$$

$$V_3 = \frac{A_1}{A_3} V_1 = \frac{A_1}{A_2} V_1$$

$$\frac{p_1 - p_3}{\rho} = V_3^2 - V_3 V_1$$

$$h_L = \frac{p_1 - p_3}{\rho g} + \frac{V_1^2}{2g} - \frac{V_3^2}{2g} = \frac{V_3^2}{g} - \frac{V_3 V_1}{g} + \frac{V_1^2}{2g} - \frac{V_3^2}{2g}$$

$$h_L = \frac{V_3^2}{2g} + \frac{V_1^2}{2g} - \frac{V_3 V_1}{g} = \frac{V_1^2}{2g} \left[ \left( \frac{A_1}{A_2} \right)^2 - 2 \frac{A_1}{A_2} + 1 \right] = \frac{V_1^2}{2g} \left( 1 - \frac{A_1}{A_2} \right)^2$$



## VARIAZIONI DI SEZIONE REPENTINE

These can be rearranged to give the loss coefficient,  $K_L = h_L/(V_1^2/2g)$ , as

$$K_L = \left( 1 - \frac{A_1}{A_2} \right)^2$$

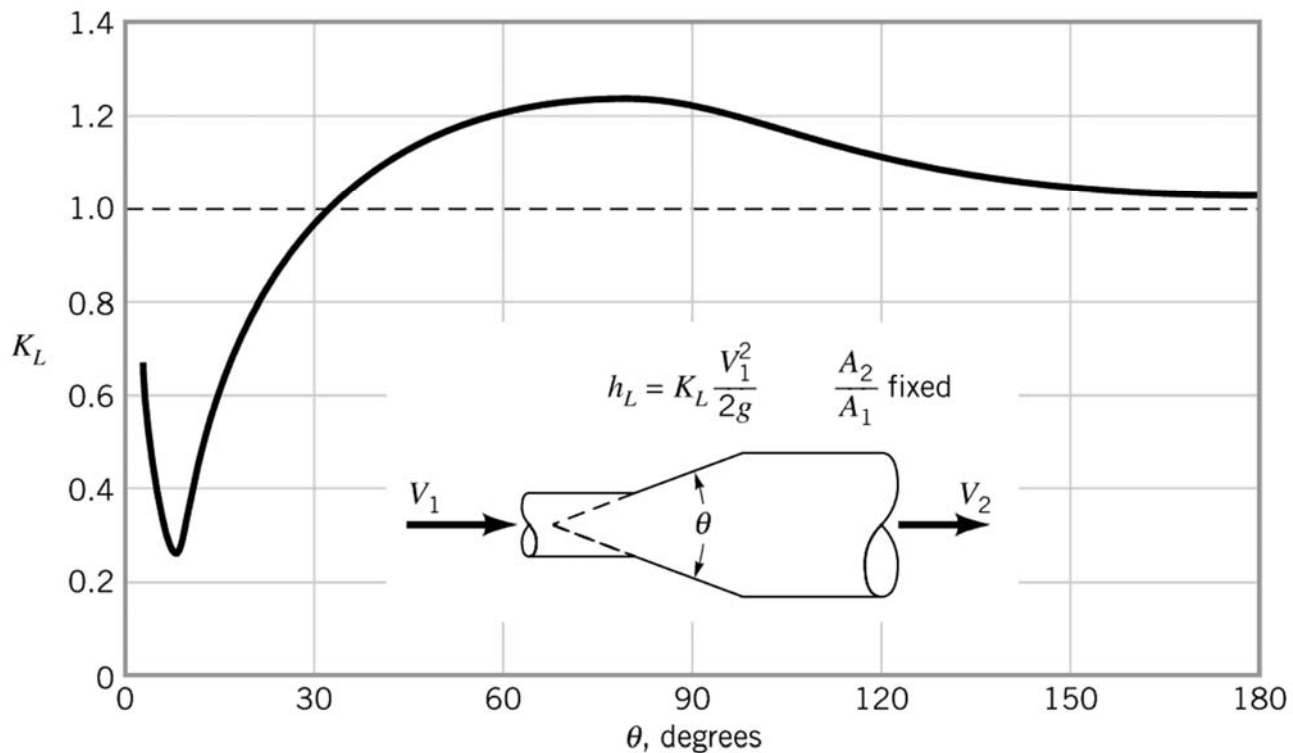
where we have used the fact that  $A_2 = A_3$ . This result, plotted in Fig. 8.27, is in good agreement with experimental data. As with so many minor loss situations, it is not the viscous effects directly (i.e., the wall shear stress) that cause the loss. Rather, it is the dissipation of kinetic energy (another type of viscous effect) as the fluid decelerates inefficiently.

The losses may be quite different if the contraction or expansion is gradual. Typical results for a *conical diffuser* with a given area ratio,  $A_2/A_1$ , are shown in Fig. 8.29. (A diffuser is a device shaped to decelerate a fluid.) Clearly the included angle of the diffuser,  $\theta$ , is a very important parameter. For very small angles, the diffuser is excessively long and most of the head loss is due to the wall shear stress as in fully developed flow. For moderate or large angles, the flow separates from the walls and the losses are due mainly to a dissipation of the kinetic energy of the jet leaving the smaller diameter pipe. In fact, for moderate or large values of  $\theta$  (i.e.,  $\theta > 35^\circ$  for the case shown in Fig. 8.29), the conical diffuser is, perhaps unexpectedly, less efficient than a sharp-edged expansion which has  $K_L = 1$ . There is an optimum angle ( $\theta \approx 8^\circ$  for the case illustrated) for which the loss coefficient is a minimum. The relatively small value of  $\theta$  for the minimum  $K_L$  results in a long diffuser and is an indication of the fact that it is difficult to efficiently decelerate a fluid.





## VARIAZIONI DI SEZIONE GRADUALE

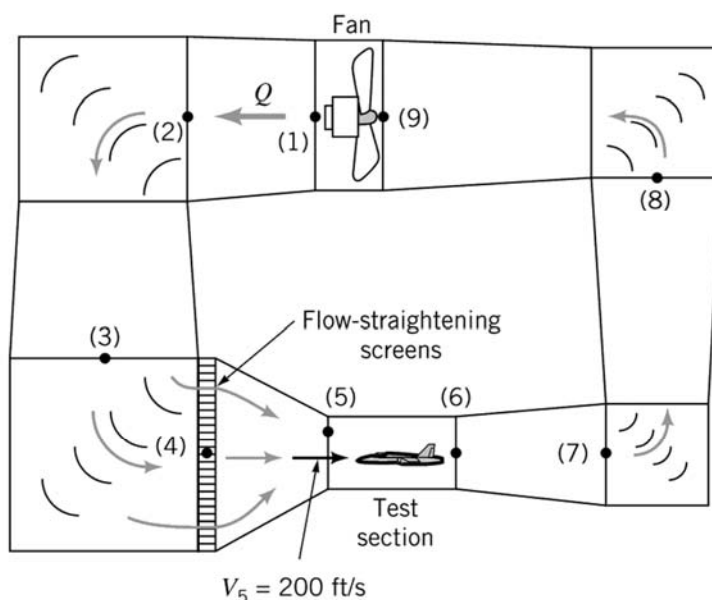


■ **FIGURE 8.29** Loss coefficient for a typical conical diffuser (Ref. 5).



## MOTI IN CONDOTTI ESERCIZI

Air at standard conditions is to flow through the test section [between sections (5) and (6)] of the closed-circuit wind tunnel shown in Fig. E8.6 with a velocity of 200 ft/s. The flow is driven by a fan that essentially increases the static pressure by the amount  $p_1 - p_9$  that is needed to overcome the head losses experienced by the fluid as it flows around the circuit. Estimate the value of  $p_1 - p_9$  and the horsepower supplied to the fluid by the fan.



Location	Area (ft <sup>2</sup> )	Velocity (ft/s)
1	22.0	36.4
2	28.0	28.6
3	35.0	22.9
4	35.0	22.9
5	4.0	200.0
6	4.0	200.0
7	10.0	80.0
8	18.0	44.4
9	22.0	36.4

■ **FIGURE E8.6**



## MOTI IN CONDOTTI ESERCIZI

The maximum velocity within the wind tunnel occurs in the test section (smallest area). Thus, the maximum Mach number of the flow is  $Ma_5 = V_5/c_5$ , where  $V_5 = 200 \text{ ft/s}$  and from Eq. 1.20 the speed of sound is  $c_5 = (kRT_5)^{1/2} = \{1.4(1716 \text{ ft} \cdot \text{lb/slug} \cdot ^\circ\text{R})[(460 + 59)^\circ\text{R}]\}^{1/2} = 1117 \text{ ft/s}$ . Thus,  $Ma_5 = 200/1117 = 0.179$ . As was indicated in **Chapter 3** and discussed fully in **Chapter 11**, most flows can be considered as incompressible if the Mach number is less than about 0.3. Hence, we can use the incompressible formulas for this problem.

The purpose of the fan in the wind tunnel is to provide the necessary energy to overcome the net head loss experienced by the air as it flows around the circuit. This can be found from the energy equation between points (1) and (9) as

$$\frac{p_1}{\gamma} + \frac{V_1^2}{2g} + z_1 = \frac{p_9}{\gamma} + \frac{V_9^2}{2g} + z_9 + h_{L_{1-9}}$$

where  $h_{L_{1-9}}$  is the total head loss from (1) to (9). With  $z_1 = z_9$  and  $V_1 = V_9$  this gives

$$\frac{p_1}{\gamma} - \frac{p_9}{\gamma} = h_{L_{1-9}} \quad (1)$$

Similarly, by writing the energy equation (Eq. 5.84) across the fan, from (9) to (1), we obtain

$$\frac{p_9}{\gamma} + \frac{V_9^2}{2g} + z_9 + h_p = \frac{p_1}{\gamma} + \frac{V_1^2}{2g} + z_9$$



## MOTI IN CONDOTTI ESERCIZI

where  $h_p$  is the actual head rise supplied by the pump (fan) to the air. Again since  $z_9 = z_1$  and  $V_9 = V_1$  this, when combined with Eq. 1, becomes

$$h_p = \frac{(p_1 - p_9)}{\gamma} = h_{L_{1-9}}$$

The actual power supplied to the air (horsepower,  $\mathcal{P}_a$ ) is obtained from the fan head by

$$\mathcal{P}_a = \gamma Q h_p = \gamma A_5 V_5 h_p = \gamma A_5 V_5 h_{L_{1-9}} \quad (2)$$

Thus, the power that the fan must supply to the air depends on the head loss associated with the flow through the wind tunnel. To obtain a reasonable, approximate answer we make the following assumptions. We treat each of the **four turning corners** as a mitered bend with guide vanes so that from Fig. 8.31  $K_{L_{\text{corner}}} = 0.2$ . Thus, for each corner

$$h_{L_{\text{corner}}} = K_L \frac{V^2}{2g} = 0.2 \frac{V^2}{2g}$$

where, because the flow is assumed incompressible,  $V = V_5 A_5 / A$ . The values of  $A$  and the corresponding velocities throughout the tunnel are given in Table E8.6.



## MOTI IN CONDOTTI ESERCIZI

We also treat the enlarging sections from the end of the test section (6) to the beginning of the nozzle (4) as a conical diffuser with a loss coefficient of  $K_{L_{dif}} = 0.6$ . This value is larger than that of a well-designed diffuser (see Fig. 8.29, for example). Since the wind tunnel diffuser is interrupted by the four turning corners and the fan, it may not be possible to obtain a smaller value of  $K_{L_{dif}}$  for this situation. Thus,

$$h_{L_{dif}} = K_{L_{dif}} \frac{V_6^2}{2g} = 0.6 \frac{V_6^2}{2g}$$

The loss coefficients for the conical nozzle between section (4) and (5) and the flow-straightening screens are assumed to be  $K_{L_{noz}} = 0.2$  and  $K_{L_{scr}} = 4.0$  (Ref. 13), respectively. We neglect the head loss in the relatively short test section.

Thus, the total head loss is

$$h_{L_{1-9}} = h_{L_{corner7}} + h_{L_{corner8}} + h_{L_{corner2}} + h_{L_{corner3}} + h_{L_{dif}} + h_{L_{noz}} + h_{L_{scr}}$$

or

$$\begin{aligned} h_{L_{1-9}} &= [0.2(V_7^2 + V_8^2 + V_2^2 + V_3^2) + 0.6V_6^2 + 0.2V_5^2 + 4.0V_4^2]/2g \\ &= [0.2(80.0^2 + 44.4^2 + 28.6^2 + 22.9^2) + 0.6(200)^2 \\ &\quad + 0.2(200)^2 + 4.0(22.9)^2] \text{ ft}^2/\text{s}^2/[2(32.2 \text{ ft/s}^2)] \end{aligned}$$



## MOTI IN CONDOTTI ESERCIZI

or

$$h_{L_{1-9}} = 560 \text{ ft}$$

Hence, from Eq. 1 we obtain the pressure rise across the fan as

$$\begin{aligned} p_1 - p_9 &= \gamma h_{L_{1-9}} = (0.0765 \text{ lb/ft}^3)(560 \text{ ft}) \\ &= 42.8 \text{ lb/ft}^2 = 0.298 \text{ psi} \end{aligned} \quad (\text{Ans})$$

From Eq. 2 we obtain the power added to the fluid as

$$\mathcal{P}_a = (0.0765 \text{ lb/ft}^3)(4.0 \text{ ft}^2)(200 \text{ ft/s})(560 \text{ ft}) = 34,300 \text{ ft} \cdot \text{lb/s}$$

or

$$\mathcal{P}_a = \frac{34,300 \text{ ft} \cdot \text{lb/s}}{550 (\text{ft} \cdot \text{lb/s})/\text{hp}} = 62.3 \text{ hp} \quad (\text{Ans})$$

With a closed-return wind tunnel of this type, all of the power required to maintain the flow is dissipated through viscous effects, with the energy remaining within the closed tunnel. If heat transfer across the tunnel walls is negligible, the air temperature within the tunnel will increase in time. For steady state operations of such tunnels, it is often necessary to provide some means of cooling to maintain the temperature at acceptable levels.



## MOTI IN CONDOTTI ESERCIZI

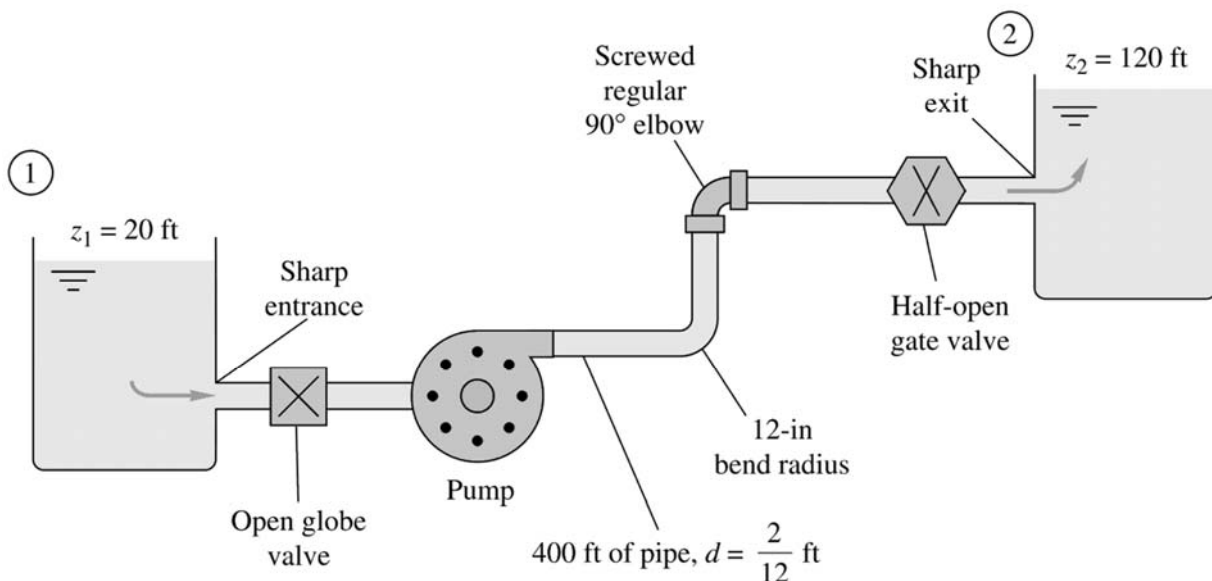
It should be noted that the actual size of the motor that powers the fan must be greater than the calculated 62.3 hp because the fan is not 100% efficient. The power calculated above is that needed by the fluid to overcome losses in the tunnel, excluding those in the fan. If the fan were 60% efficient, it would require a shaft power of  $\mathcal{P} = 62.3 \text{ hp}/(0.60) = 104 \text{ hp}$  to run the fan. Determination of fan (or pump) efficiencies can be a complex problem that depends on the specific geometry of the fan. Introductory material about fan performance is presented in **Chapter 12**; additional material can be found in various references (Refs. 14, 15, 16, for example).

It should also be noted that the above results are only approximate. Clever, careful design of the various components (corners, diffuser, etc.) may lead to improved (i.e., lower) values of the various loss coefficients, and hence lower power requirements. Since  $h_L$  is proportional to  $V^2$ , the components with the larger  $V$  tend to have the larger head loss. Thus, even though  $K_L = 0.2$  for each of the four corners, the head loss for corner (7) is  $(V_7/V_3)^2 = (80/22.9)^2 = 12.2$  times greater than it is for corner (3).



## MOTI IN CONDOTTI ESERCIZI

Water,  $\rho = 1.94 \text{ slugs/ft}^3$  and  $\nu = 0.000011 \text{ ft}^2/\text{s}$ , is pumped between two reservoirs at  $0.2 \text{ ft}^3/\text{s}$  through 400 ft of 2-in-diameter pipe and several minor losses, as shown in Fig. E6.16. The roughness ratio is  $\epsilon/d = 0.001$ . Compute the pump horsepower required.



## MOTI IN CONDOTTI ESERCIZI

Write the steady-flow energy equation between sections 1 and 2, the two reservoir surfaces:

$$\frac{p_1}{\rho g} + \frac{V_1^2}{2g} + z_1 = \left( \frac{p_2}{\rho g} + \frac{V_2^2}{2g} + z_2 \right) + h_f + \sum h_m - h_p$$

where  $h_p$  is the head increase across the pump. But since  $p_1 = p_2$  and  $V_1 = V_2 \approx 0$ , solve for the pump head

$$h_p = z_2 - z_1 + h_f + \sum h_m = 120 \text{ ft} - 20 \text{ ft} + \frac{V^2}{2g} \left( \frac{fL}{d} + \sum K \right) \quad (1)$$

Now with the flow rate known, calculate

$$V = \frac{Q}{A} = \frac{0.2 \text{ ft}^3/\text{s}}{\frac{1}{4}\pi(\frac{2}{12} \text{ ft})^2} = 9.17 \text{ ft/s}$$

Now list and sum the minor loss coefficients:

Loss	$K$
Sharp entrance (Fig. 6.21)	0.5
Open globe valve (2 in, Table 6.5)	6.9
12-in bend (Fig. 6.20)	0.15
Regular 90° elbow (Table 6.5)	0.95
Half-closed gate valve (from Fig. 6.18b)	2.7
Sharp exit (Fig. 6.21)	1.0
	$\sum K = 12.2$



Complementi di Gas

97

## MOTI IN CONDOTTI ESERCIZI

Calculate the Reynolds number and pipe-friction factor

$$\text{Re}_d = \frac{Vd}{\nu} = \frac{9.17(\frac{2}{12})}{0.000011} = 139,000$$

For  $\epsilon/d = 0.001$ , from the Moody chart read  $f = 0.0216$ . Substitute into Eq. (1)

$$\begin{aligned} h_p &= 100 \text{ ft} + \frac{(9.17 \text{ ft/s})^2}{2(32.2 \text{ ft/s}^2)} \left[ \frac{0.0216(400)}{\frac{2}{12}} + 12.2 \right] \\ &= 100 \text{ ft} + 84 \text{ ft} = 184 \text{ ft} \quad \text{pump head} \end{aligned}$$

The pump must provide a power to the water of

$$P = \rho g Q h_p = [1.94(32.2) \text{ lbf/ft}^3](0.2 \text{ ft}^3/\text{s})(184 \text{ ft}) = 2300 \text{ ft} \cdot \text{lbf/s}$$

The conversion factor is 1 hp = 550 ft · lbf/s. Therefore

$$P = \frac{2300}{550} = 4.2 \text{ hp} \quad \text{Ans.}$$

Allowing for an efficiency of 70 to 80 percent, a pump is needed with an input of about 6 hp.



Complementi di Gasdinamica – T Astarita

98

# MOTI IN CONDOTTI ESERCIZI

## Munson 8.8

Water at 60 °F flows from the basement to the second floor through the 0.75-in. (0.0625-ft)-diameter copper pipe (a drawn tubing) at a rate of  $Q = 12.0 \text{ gal/min} = 0.0267 \text{ ft}^3/\text{s}$  and exits through a faucet of diameter 0.50 in. as shown in Fig. E8.8a. Determine the pressure at point (1) if: (a) all losses are neglected, (b) the only losses included are major losses, or (c) all losses are included.

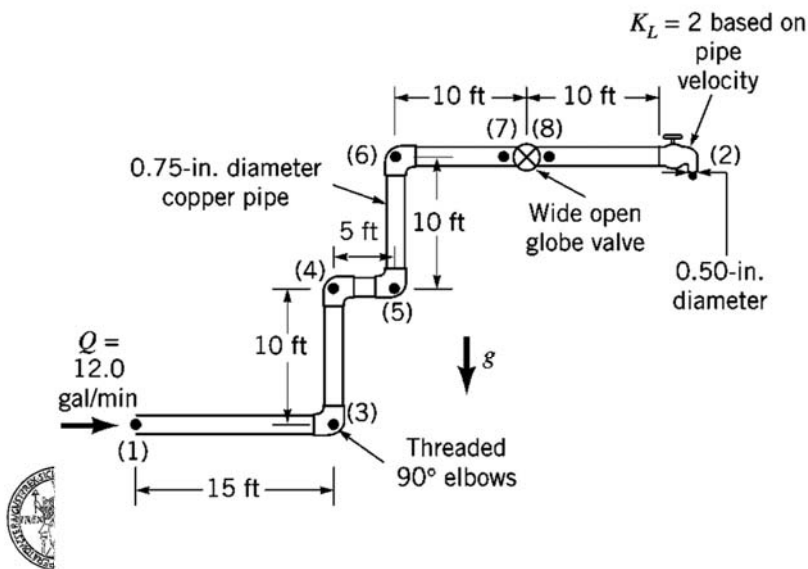
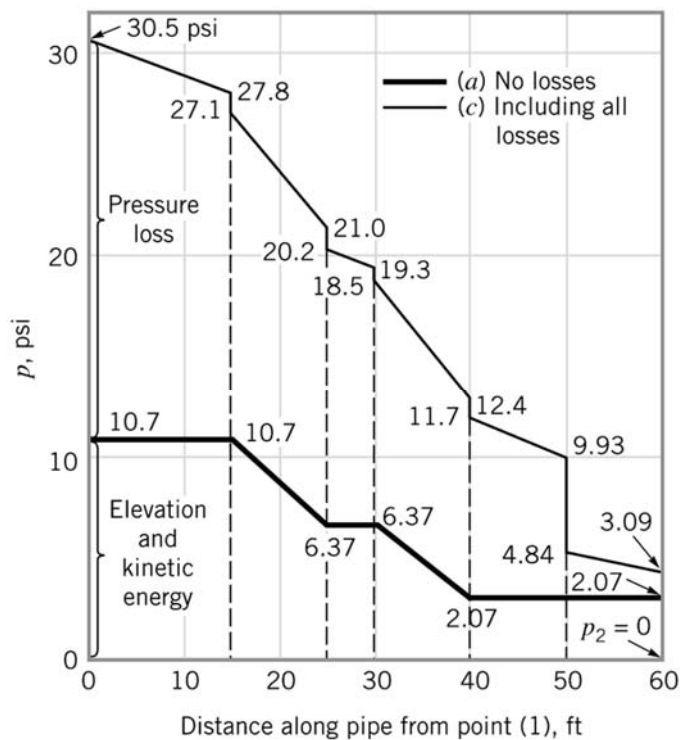
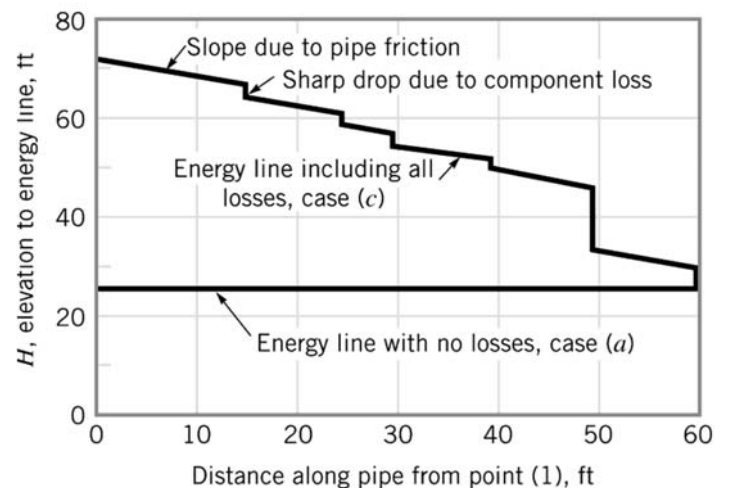


FIGURE E8.8a



## OTTI ESERCIZI



Location: (1) (3) (4) (5) (6) (7) (8) (2)

More detailed calculations will show that the pressure distribution along the pipe is as illustrated in Fig. E8.8b for cases (a) and (c)—neglecting all losses or including all losses. Note that not all of the pressure drop,  $p_1 - p_2$ , is a “pressure loss.” The pressure change due to the elevation and velocity changes is completely reversible. The portion due to the major and minor losses is irreversible.

## MOTI IN CONDOTTI ESERCIZI

### Munson 8.9

Crude oil at 140 °F with  $\gamma = 53.7 \text{ lb/ft}^3$  and  $\mu = 8 \times 10^{-5} \text{ lb} \cdot \text{s/ft}^2$  (about four times the viscosity of water) is pumped across Alaska through the Alaskan pipeline, a 799-mile-long, 4-ft-diameter steel pipe, at a maximum rate of  $Q = 2.4$  million barrels/day  $= 117 \text{ ft}^3/\text{s}$ , or  $V = Q/A = 9.31 \text{ ft/s}$ . Determine the horsepower needed for the pumps that drive this large system.

### Munson 8.10

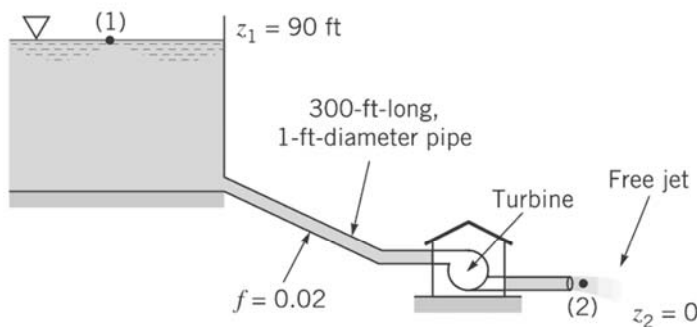
According to an appliance manufacturer, the 4-in.-diameter galvanized iron vent on a clothes dryer is not to contain more than 20 ft of pipe and four 90° elbows. Under these conditions determine the air flowrate if the pressure within the dryer is 0.20 inches of water. Assume a temperature of 100 °F and standard pressure.



## MOTI IN CONDOTTI ESERCIZI

### Munson 8.11

The turbine shown in Fig. E8.11 extracts 50 hp from the water flowing through it. The 1-ft-diameter, 300-ft-long pipe is assumed to have a friction factor of 0.02. Minor losses are negligible. Determine the flowrate through the pipe and turbine.



■ FIGURE E8.11



## MOTI IN CONDOTTI ESERCIZI

### Munson 8.12

Air at standard temperature and pressure flows through a horizontal, galvanized iron pipe ( $\epsilon = 0.0005$  ft) at a rate of  $2.0 \text{ ft}^3/\text{s}$ . Determine the minimum pipe diameter if the pressure drop is to be no more than  $0.50$  psi per  $100$  ft of pipe.

### Munson 8.13

Water at  $10^\circ\text{C}$  ( $\nu = 1.307 \times 10^{-6} \text{ m}^2/\text{s}$ , see Table B.2) is to flow from reservoir  $A$  to reservoir  $B$  through a cast-iron pipe ( $\epsilon = 0.26 \text{ mm}$ ) of length  $20 \text{ m}$  at a rate of  $Q = 0.0020 \text{ m}^3/\text{s}$  as shown in Fig. E8.13. The system contains a sharp-edged entrance and six regular threaded  $90^\circ$  elbows. Determine the pipe diameter needed.

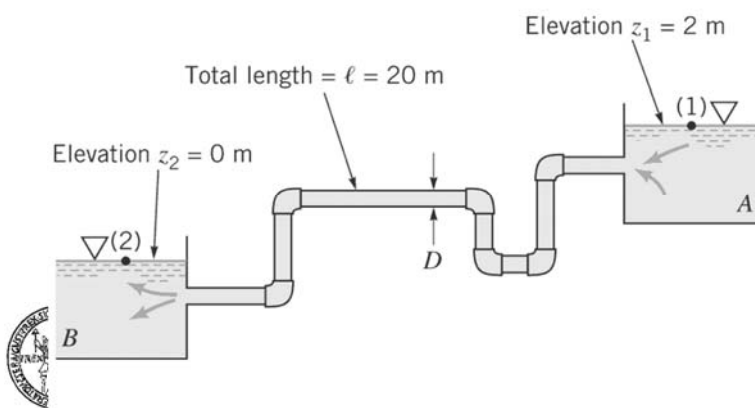
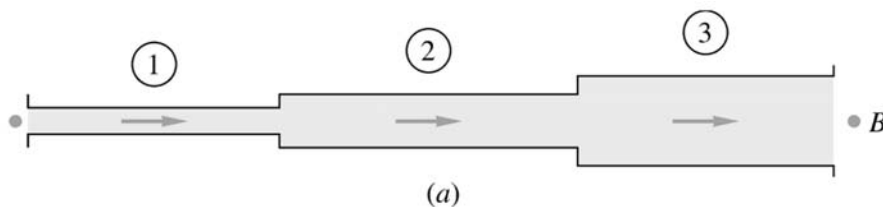


FIGURE E8.13

## MOTI IN CONDOTTI MULTIPLI



If you can solve the equations for one-pipe systems, you can solve them all; but when systems contain two or more pipes, certain basic rules make the calculations very smooth. Any resemblance between these rules and the rules for handling electric circuits is not coincidental.

Figure 6.24 shows three examples of multiple-pipe systems. The first is a set of three (or more) pipes in series. Rule 1 is that the flow rate is the same in all pipes

$$Q_1 = Q_2 = Q_3 = \text{const}$$

or

$$V_1 d_1^2 = V_2 d_2^2 = V_3 d_3^2 \quad (6.105)$$

Rule 2 is that the total head loss through the system equals the sum of the head loss in each pipe

$$\Delta h_{A \rightarrow B} = \Delta h_1 + \Delta h_2 + \Delta h_3 \quad (6.106)$$

In terms of the friction and minor losses in each pipe, we could rewrite this as





## MOTI IN CONDOTTI MULTIPLI

$$\Delta h_{A \rightarrow B} = \frac{V_1^2}{2g} \left( \frac{f_1 L_1}{d_1} + \sum K_1 \right) + \frac{V_2^2}{2g} \left( \frac{f_2 L_2}{d_2} + \sum K_2 \right) + \frac{V_3^2}{2g} \left( \frac{f_3 L_3}{d_3} + \sum K_3 \right) \quad (6.107)$$

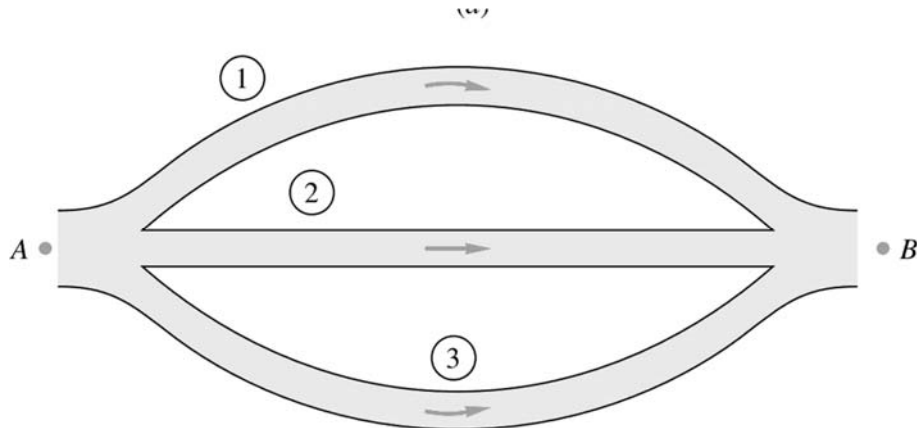
and so on for any number of pipes in the series. Since  $V_2$  and  $V_3$  are proportional to  $V_1$  from Eq. (6.105), Eq. (6.107) is of the form

$$\Delta h_{A \rightarrow B} = \frac{V_1^2}{2g} (\alpha_0 + \alpha_1 f_1 + \alpha_2 f_2 + \alpha_3 f_3) \quad (6.108)$$

where the  $\alpha_i$  are dimensionless constants. If the flow rate is given, we can evaluate the right-hand side and hence the total head loss. If the head loss is given, a little iteration is needed, since  $f_1, f_2$ , and  $f_3$  all depend upon  $V_1$  through the Reynolds number. Begin by calculating  $f_1, f_2$ , and  $f_3$ , assuming fully rough flow, and the solution for  $V_1$  will converge with one or two iterations. EES is ideal for this purpose.



## MOTI IN CONDOTTI MULTIPLI



The second multiple-pipe system is the *parallel*-flow case shown in Fig. 6.24b. Here the loss is the same in each pipe, and the total flow is the sum of the individual flows

$$\Delta h_{A \rightarrow B} = \Delta h_1 = \Delta h_2 = \Delta h_3 \quad (6.109a)$$

$$Q = Q_1 + Q_2 + Q_3 \quad (6.109b)$$



## MOTI IN CONDOTTI MULTIPLI

If the total head loss is known, it is straightforward to solve for  $Q_i$  in each pipe and sum them, as will be seen in Example 6.18. The reverse problem, of determining  $\sum Q_i$  when  $h_f$  is known, requires iteration. Each pipe is related to  $h_f$  by the Moody relation  $h_f = f(L/d)(V^2/2g) = fQ^2/C$ , where  $C = \pi^2 g d^5 / 8L$ . Thus each pipe has nearly quadratic nonlinear parallel resistance, and head loss is related to total flow rate by

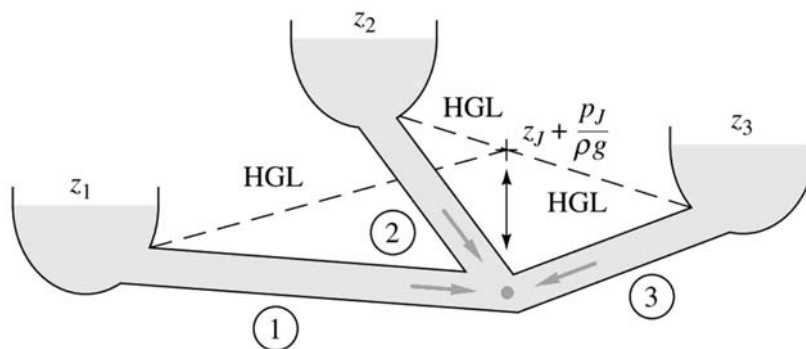
$$h_f = \frac{Q^2}{\left(\sum \sqrt{C_i/f_i}\right)^2} \quad \text{where } C_i = \frac{\pi^2 g d_i^5}{8L_i} \quad (6.109c)$$

Since the  $f_i$  vary with Reynolds number and roughness ratio, one begins Eq. (6.109c) by guessing values of  $f_i$  (fully rough values are recommended) and calculating a first estimate of  $h_f$ . Then each pipe yields a flow-rate estimate  $Q_i \approx (C_i h_f / f_i)^{1/2}$  and hence a new Reynolds number and a better estimate of  $f_i$ . Then repeat Eq. (6.109c) to convergence.

It should be noted that both of these parallel-pipe cases—finding either  $\sum Q$  or  $h_f$ —are easily solved by EES if reasonable initial guesses are given.



## MOTI IN CONDOTTI MULTIPLI



Consider the third example of a *three-reservoir pipe junction*, as in Fig. 6.24c. If all flows are considered positive toward the junction, then

$$Q_1 + Q_2 + Q_3 = 0 \quad (6.110)$$

which obviously implies that one or two of the flows must be away from the junction. The pressure must change through each pipe so as to give the same static pressure  $p_J$  at the junction. In other words, let the HGL at the junction have the elevation

$$h_J = z_J + \frac{p_J}{\rho g}$$



# MOTI IN CONDOTTI MULTIPLI

where  $p_J$  is in gage pressure for simplicity. Then the head loss through each, assuming  $p_1 = p_2 = p_3 = 0$  (gage) at each reservoir surface, must be such that

$$\begin{aligned}\Delta h_1 &= \frac{V_1^2}{2g} \frac{f_1 L_1}{d_1} = z_1 - h_J \\ \Delta h_2 &= \frac{V_2^2}{2g} \frac{f_2 L_2}{d_2} = z_2 - h_J \\ \Delta h_3 &= \frac{V_3^2}{2g} \frac{f_3 L_3}{d_3} = z_3 - h_J\end{aligned}\quad (6.111)$$

We guess the position  $h_J$  and solve Eqs. (6.111) for  $V_1$ ,  $V_2$ , and  $V_3$  and hence  $Q_1$ ,  $Q_2$ , and  $Q_3$ , iterating until the flow rates balance at the junction according to Eq. (6.110). If we guess  $h_J$  too *high*, the sum  $Q_1 + Q_2 + Q_3$  will be *negative* and the remedy is to reduce  $h_J$ , and vice versa.



## EXAMPLE 6.17

Given is a three-pipe series system, as in Fig. 6.24a. The total pressure drop is  $p_A - p_B = 150,000$  Pa, and the elevation drop is  $z_A - z_B = 5$  m. The pipe data are

Pipe	$L$ , m	$d$ , cm	$\epsilon$ , mm	$\epsilon/d$
1	100	8	0.24	0.003
2	150	6	0.12	0.002
3	80	4	0.20	0.005

The fluid is water,  $\rho = 1000$  kg/m<sup>3</sup> and  $\nu = 1.02 \times 10^{-6}$  m<sup>2</sup>/s. Calculate the flow rate  $Q$  in m<sup>3</sup>/h through the system.

## EXAMPLE 6.18

Assume that the same three pipes in Example 6.17 are now in parallel with the same total head loss of 20.3 m. Compute the total flow rate  $Q$ , neglecting minor losses.

## EXAMPLE 6.19

Take the same three pipes as in Example 6.17, and assume that they connect three reservoirs at these surface elevations

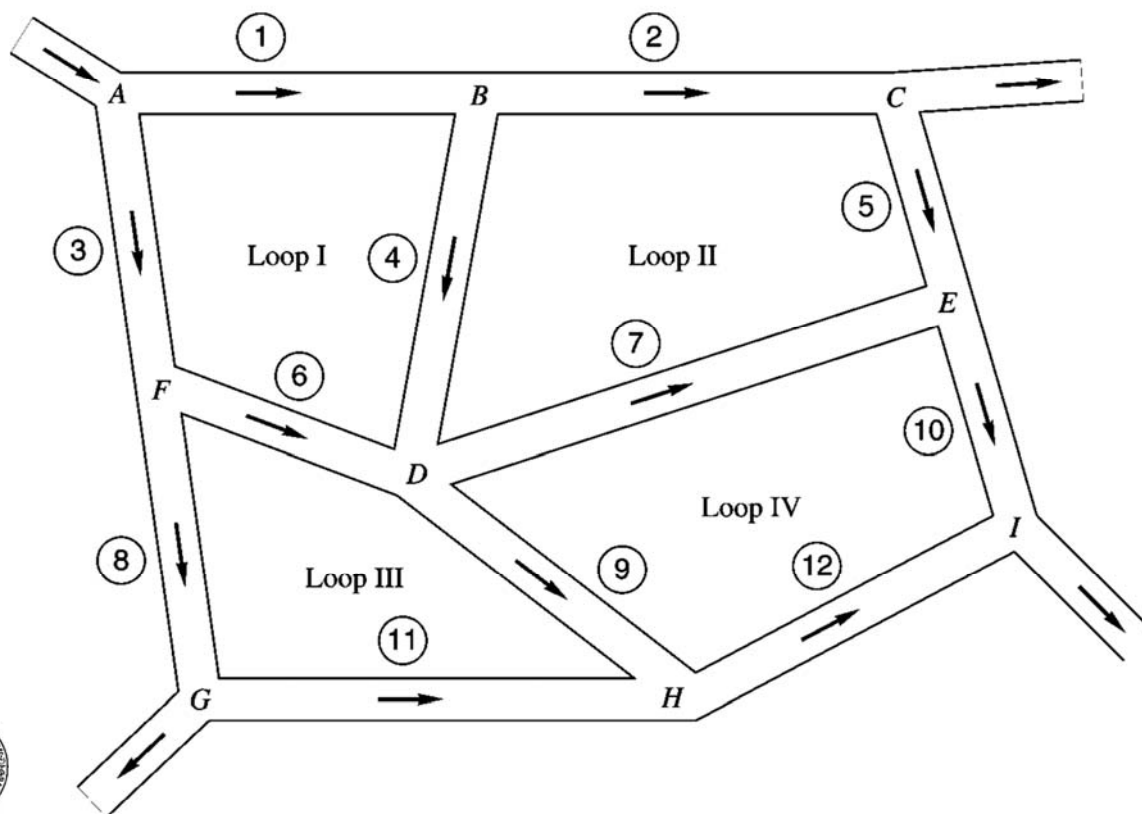
$$z_1 = 20 \text{ m} \quad z_2 = 100 \text{ m} \quad z_3 = 40 \text{ m}$$

Find the resulting flow rates in each pipe, neglecting minor losses.



## MOTI IN CONDOTTI MULTIPLI

The ultimate case of a multipipe system is the *pipng network* illustrated in Fig. 6.25. This might represent a water supply system for an apartment or subdivision or even a city. This network is quite complex algebraically but follows the same basic rules:



## MOTI IN CONDOTTI MULTIPLI

1. The net flow into any junction must be zero.
2. The net head loss around any closed loop must be zero. In other words, the HGL at each junction must have one and only one elevation.
3. All head losses must satisfy the Moody and minor-loss friction correlations.

By supplying these rules to each junction and independent loop in the network, one obtains a set of simultaneous equations for the flow rates in each pipe leg and the HGL (or pressure) at each junction. Solution may then be obtained by numerical iteration, as first developed in a hand-calculation technique by Prof. Hardy Cross in 1936 [17]. Computer solution of pipe-network problems is now quite common and covered in at least one specialized text [18]. Solution on microcomputers is also a reality. Some explicit numerical algorithms have been developed by Ormsbee and Wood [19]. Network analysis is quite useful for real water distribution systems if well calibrated with the actual system head-loss data.

# Hardy Cross Technique for hydraulic networks

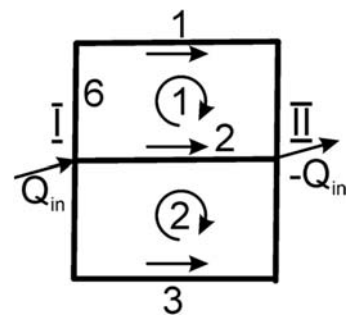
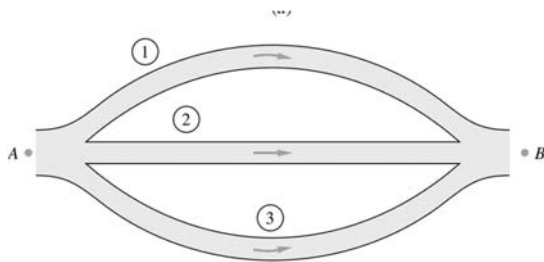
When three or more branches occur in a pipe flow system, it is called a network.

The Hardy Cross technique is a rational approach to the analysis employing an iterative procedure.

The Cross technique requires that the head loss terms for each pipe in the system should be expressed in the form:

$$h = h_f + h_c = kQ^2 \quad h_c = K_c \frac{V^2}{2g} = \frac{K_c}{2gA^2} Q^2 \quad h_f = f \frac{L}{D_e} \frac{V^2}{2g} = \frac{L}{D_e} \frac{f}{2gA^2} Q^2$$

Lets look at an easy example (pipes of Example 6.18).



# Hardy Cross Technique for hydraulic networks

1. The Cross iteration technique requires an initial estimates of the volume flow rate for each branch. Clearly at each junction the flow should be balanced. This step can be made easily by solving the underdetermined system of equations in the nodes (I and II).
- The fluid tends to follow the path of least resistance. Therefore, a pipe having a lower value of  $k$  will carry a higher flow rate than those having higher values. But in the present example we may simply assume:

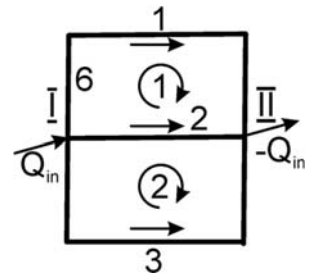
$$Q_i = \frac{Q_{tot}}{3}$$

2. Evaluate the head loss in each pipe (can be negative):

$$h_j = k_j Q_j^2$$

3. Evaluate the total head loss in each circuit, that should be equal to 0, with the correct sign  $s$  (positive when the flow is concordant with the circulation):

$$\sum_C s_j h_j = \sum_C s_j k_j Q_j^2$$



## Hardy Cross Technique for hydraulic networks

4. Correct the volume flow rate for each branch by a first order iteration for each circuit  $c$  (where the correction should be multiplied by  $s$ :

$$Q_j^{new} = Q_j + s_j \Delta Q_c$$

$$\sum_c s_j k_j (Q_j + s_j \Delta Q_c)^2 \rightarrow 0$$

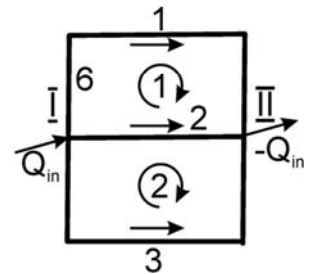
$$\sum_c s_j h_j = \sum_c s_j k_j Q_j^2$$

But

$$\sum_c s_j k_j (Q_j + s_j \Delta Q_c)^2 = \sum_c s_j k_j Q_j^2 \left( 1 + \frac{s_j \Delta Q_c}{Q_j} \right)^2 \cong \sum_c s_j k_j Q_j^2 \left( 1 + \frac{2s_j \Delta Q_c}{Q_j} \right) =$$

$$\sum_c s_j h_j \left( 1 + \frac{2s_j \Delta Q_c}{Q_j} \right) = 0 \rightarrow \Delta Q_c = \frac{-\sum_c s_j h_j}{\sum_c \frac{2h_j}{Q_j}} \quad (s_j)^2 = 1$$

5. Iterate steps 2 to 4 until convergence is found.



Complementi di Gasdinamica – T Astarita

## Hardy Cross Technique for hydraulic networks

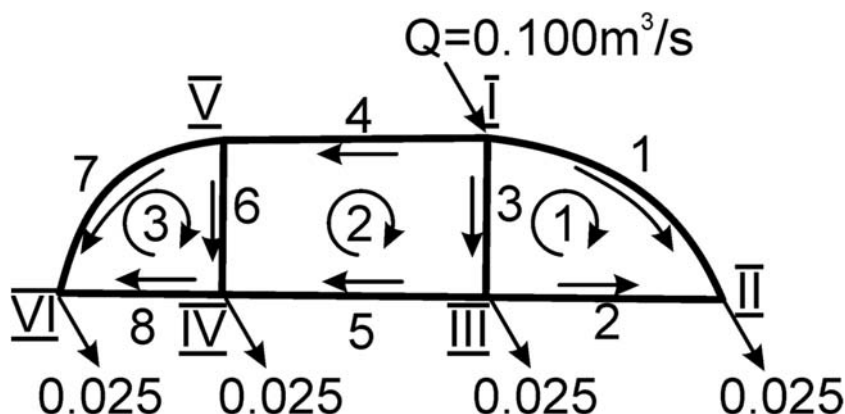
Now solve this problem with:

$$\nu = 1.15 \times 10^{-6};$$

$$L = [18 \ 15 \ 6 \ 15 \ 15 \ 6 \ 18 \ 15]'; \text{ meters}$$

$$\text{Eps} = [1 \ 1 \ 1 \ 1 \ 1 \ 1 \ 1 \ 1]' \times 1.5 \times 10^{-6};$$

$$D = [1 \ 1 \ 1 \ 1 \ 1 \ 1 \ 1 \ 1]' \times 2.907 \times 2.54 / 100;$$



Complementi di Gasdinamica – T Astarita

## MOTI

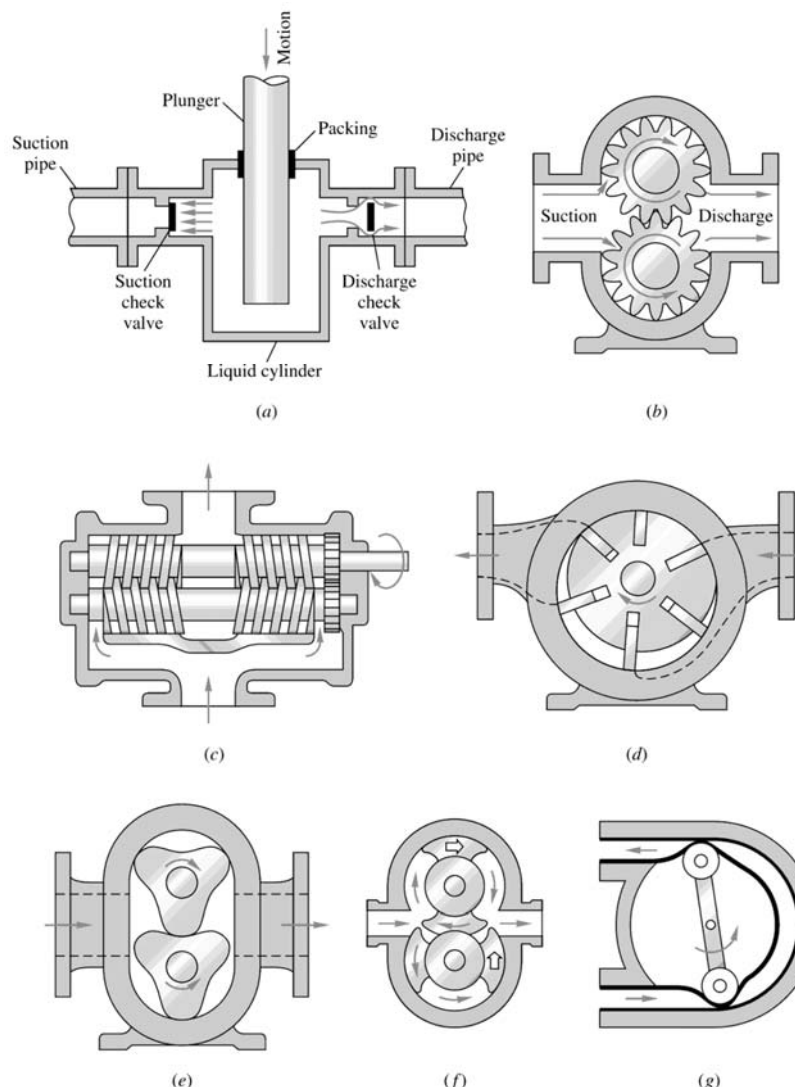
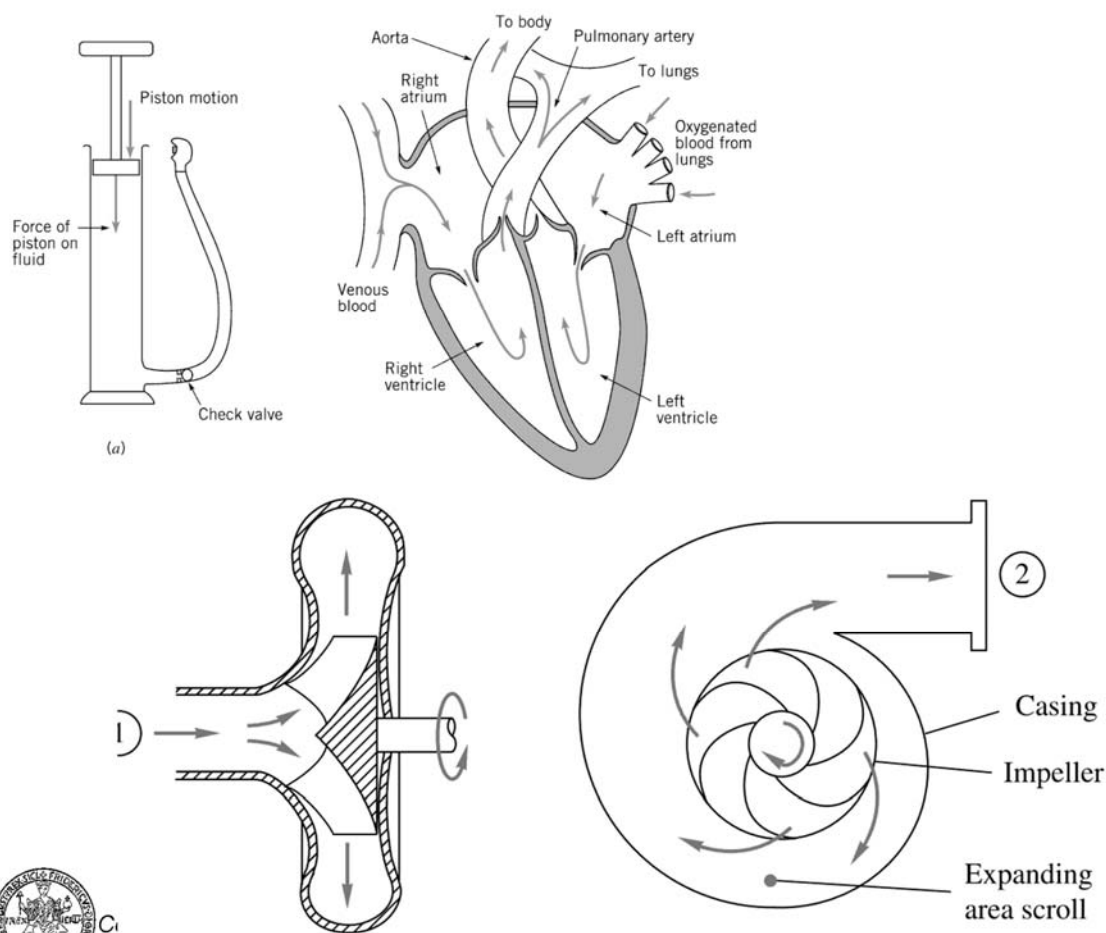


**Fig. 11.1** Schematic design of positive-displacement pumps: (a) reciprocating piston or plunger, (b) external gear pump, (c) double-screw pump, (d) sliding vane, (e) three-lobe pump, (f) double circumferential piston, (g) flexible-tube squeegee.

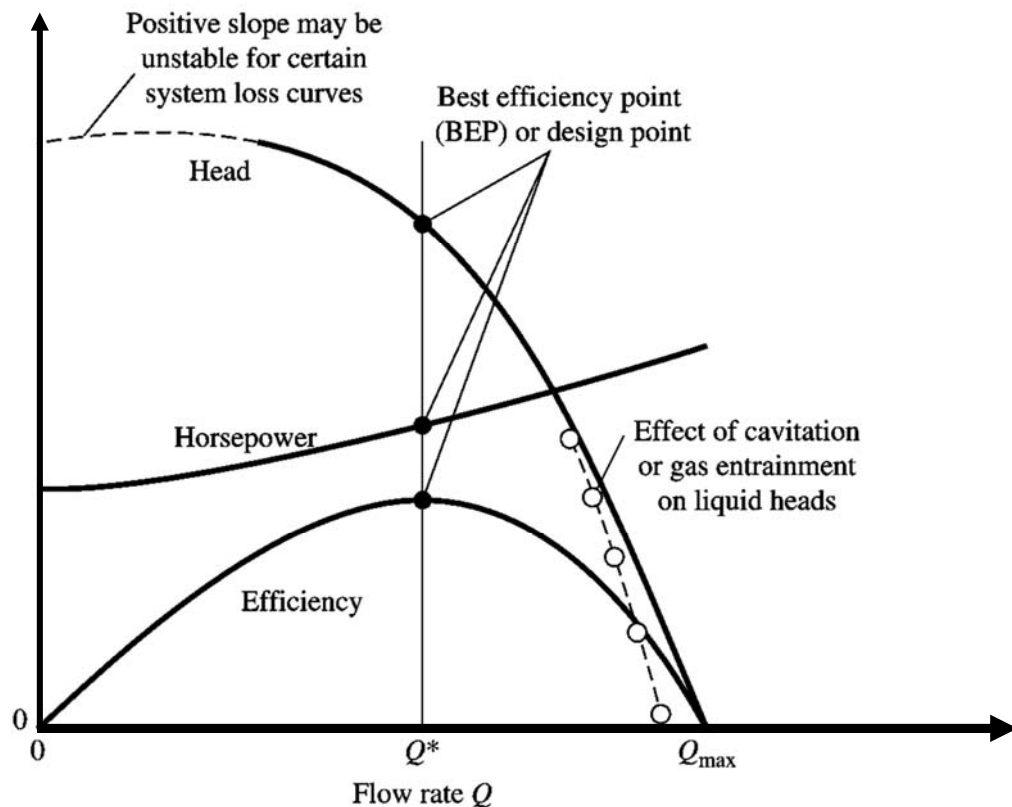


Complementi di Gasdinamica – T Astarita

## MOTI IN CONDOTTI



## Pompe centrifughe



## Pompe centrifughe

In the top of Fig. 11.7 is plotted the *net positive-suction head* (NPSH), which is the head required at the pump inlet to keep the liquid from cavitating or boiling. The pump inlet or suction side is the low-pressure point where cavitation will first occur. The NPSH is defined as

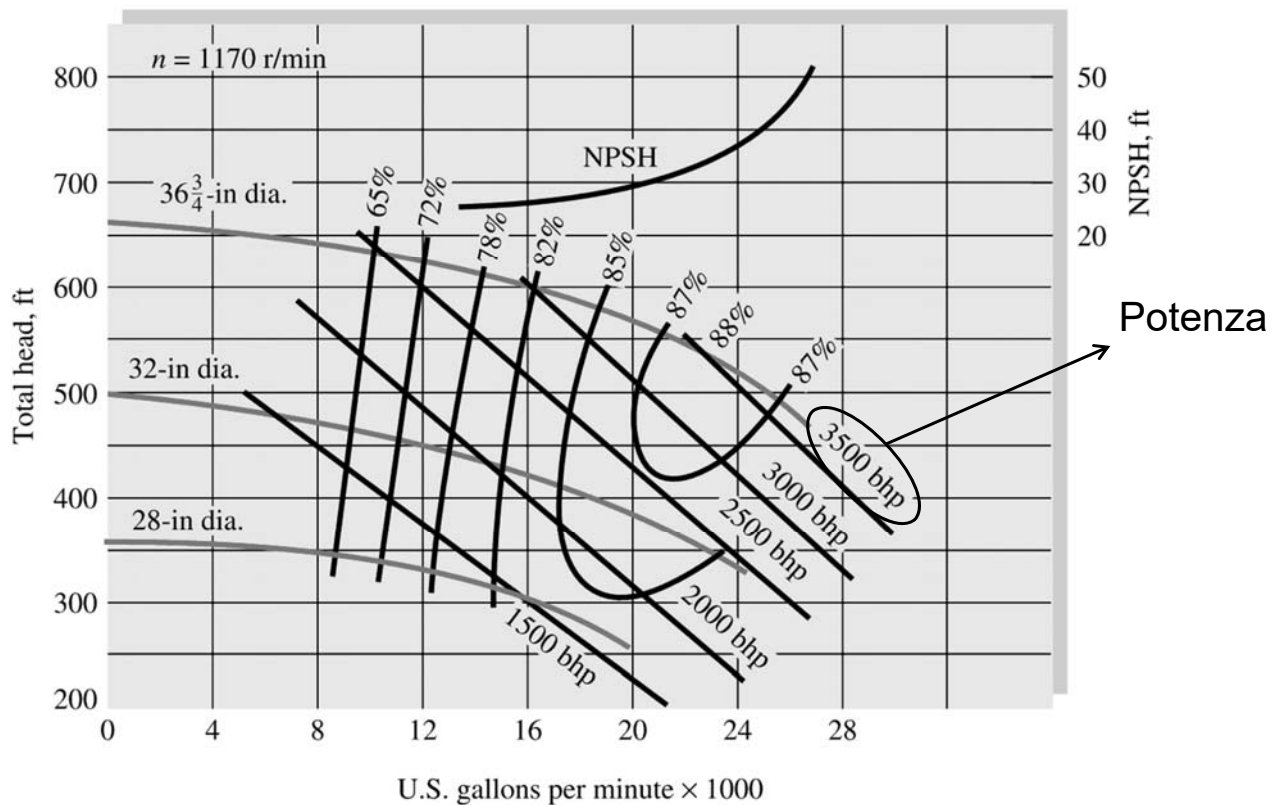
$$\text{NPSH} = \frac{p_i}{\rho g} + \frac{V_i^2}{2g} - \frac{p_v}{\rho g} \quad (11.19)$$

where  $p_i$  and  $V_i$  are the pressure and velocity at the pump inlet and  $p_v$  is the vapor pressure of the liquid. Given the left-hand side, NPSH, from the pump performance curve, we must ensure that the right-hand side is equal or greater in the actual system to avoid cavitation.





# Pompe centrifughe



## Accoppiamento

The ultimate test of a pump is its match with the operating-system characteristics. Physically, the system head must match the head produced by the pump, and this intersection should occur in the region of best efficiency.

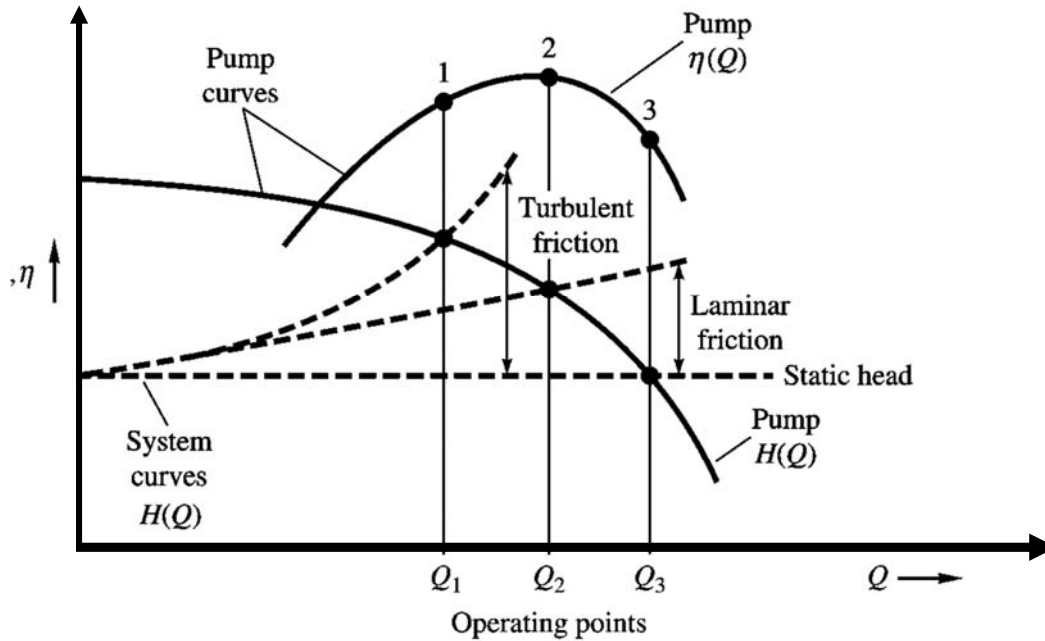
The system head will probably contain a static-elevation change  $z_2 - z_1$  plus friction losses in pipes and fittings

$$H_{\text{sys}} = (z_2 - z_1) + \frac{V^2}{2g} \left( \sum \frac{fL}{D} + \sum K \right) \quad (11.34)$$

where  $\sum K$  denotes minor losses and  $V$  is the flow velocity in the principal pipe. Since  $V$  is proportional to the pump discharge  $Q$ , Eq. (11.34) represents a system-head curve  $H_s(Q)$ . Three examples are shown in Fig. 11.17: a static head  $H_s = a$ , static head plus laminar friction  $H_s = a + bQ$ , and static head plus turbulent friction  $H_s = a + cQ^2$ . The intersection of the system curve with the pump performance curve  $H(Q)$  defines the operating point. In Fig. 11.17 the laminar-friction operating point is at maximum efficiency while the turbulent and static curves are off design. This may be unavoidable if system variables change, but the pump should be changed in size or speed if its operating point is consistently off design. Of course, a perfect match may not be possible because commercial pumps have only certain discrete sizes and speeds. Let us illustrate these concepts with an example.



# Accoppiamento



# Accoppiamento

## EXAMPLE 11.6

We want to use the 32-in pump of Fig. 11.7a at 1170 r/min to pump water at 60°F from one reservoir to another 120 ft higher through 1500 ft of 16-in-ID pipe with friction factor  $f = 0.030$ . (a) What will the operating point and efficiency be? (b) To what speed should the pump be changed to operate at the BEP?

## Solution

For reservoirs the initial and final velocities are zero; thus the system head is

$$H_s = z_2 - z_1 + \frac{V^2}{2g} \frac{fL}{D} = 120 \text{ ft} + \frac{V^2}{2g} \frac{0.030(1500 \text{ ft})}{\frac{16}{12} \text{ ft}}$$

From continuity in the pipe,  $V = Q/A = Q/[\frac{1}{4}\pi(\frac{16}{12} \text{ ft})^2]$ , and so we substitute for  $V$  above to get

$$H_s = 120 + 0.269Q^2 \quad Q \text{ in ft}^3/\text{s} \quad (1)$$

Since Fig. 11.7a uses thousands of gallons per minute for the abscissa, we convert  $Q$  in Eq. (1) to this unit:

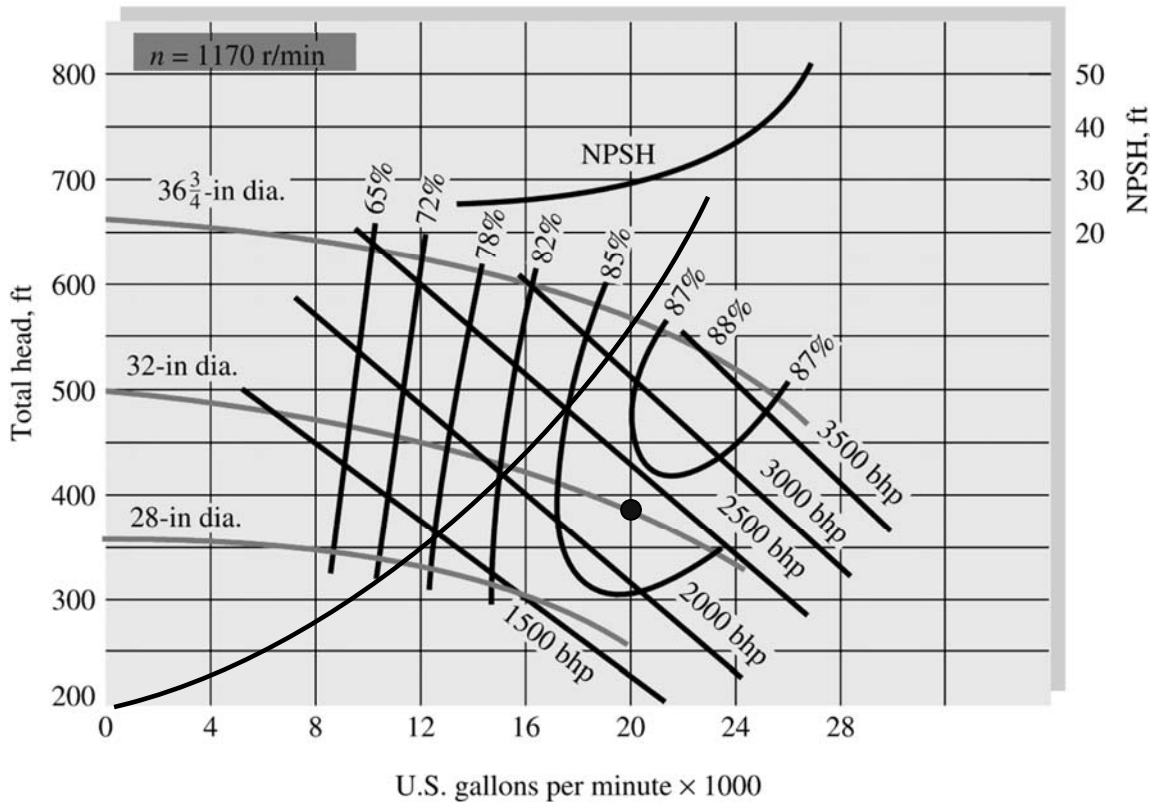
$$H_s = 120 + 1.335Q^2 \quad Q \text{ in } 10^3 \text{ gal/min} \quad (2)$$

We can plot Eq. (2) on Fig. 11.7a and see where it intersects the 32-in pump-head curve, as in Fig. E11.6. A graphical solution gives approximately

$$H \approx 430 \text{ ft} \quad Q \approx 15,000 \text{ gal/min}$$



# Pompe centrifughe



## Accoppiamento

The efficiency is about 82 percent, slightly off design.

An analytic solution is possible if we fit the pump-head curve to a parabola, which is very accurate

$$H_{\text{pump}} \approx 490 - 0.26Q^2 \quad Q \text{ in } 10^3 \text{ gal/min} \quad (3)$$

Equations (2) and (3) must match at the operating point:

$$490 - 0.26Q^2 = 120 + 1.335Q^2$$

or

$$Q^2 = \frac{490 - 120}{0.26 + 1.335} = 232$$

$$Q = 15.2 \times 10^3 \text{ gal/min} = 15,200 \text{ gal/min} \quad \text{Ans. (a)}$$

$$H = 490 - 0.26(15.2)^2 = 430 \text{ ft} \quad \text{Ans. (a)}$$

To move the operating point to BEP, we change  $n$ , which changes both  $Q \propto n$  and  $H \propto n^2$ . From Fig. 11.7a, at BEP,  $H^* \approx 386$  ft; thus for any  $n$ ,  $H^* = 386(n/1170)^2$ . Also read  $Q^* \approx 20 \times 10^3$  gal/min; thus for any  $n$ ,  $Q^* = 20(n/1170)$ . Match  $H^*$  to the system characteristics, Eq. (2),

$$H^* = 386 \left( \frac{n}{1170} \right)^2 \approx 120 + 1.335 \left( 20 \frac{n}{1170} \right)^2 \quad \text{Ans. (b)}$$

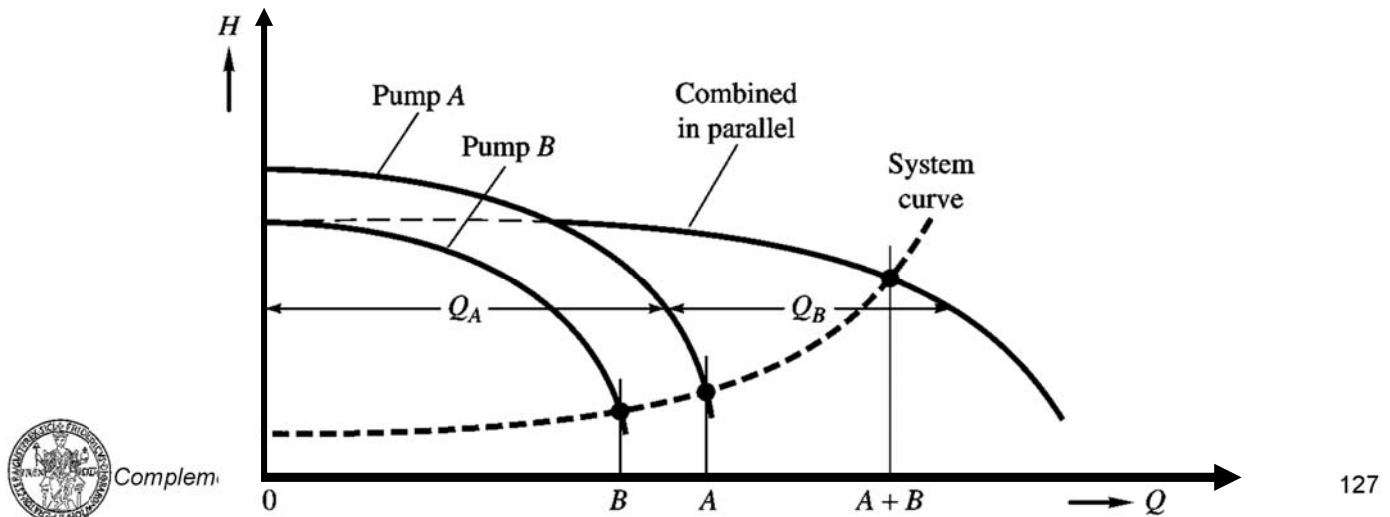


which gives  $n^2 < 0$ . Thus it is impossible to operate at maximum efficiency with this particular system and pump.

## Pompe in parallelo

If a pump provides the right head but too little discharge, a possible remedy is to combine two similar pumps in parallel, i.e., sharing the same suction and inlet conditions. A parallel arrangement is also used if delivery demand varies, so that one pump is used at low flow and the second pump is started up for higher discharges. Both pumps should have check valves to avoid backflow when one is shut down.

The two pumps in parallel need not be identical. Physically, their flow rates will sum for the same head, as illustrated in Fig. 11.18. If pump A has more head than pump B, pump B cannot be added in until the operating head is below the shutoff head of pump B. Since the system curve rises with  $Q$ , the combined delivery  $Q_{A+B}$  will be less than the separate operating discharges  $Q_A + Q_B$  but certainly greater than either one.



127

## Pompe in parallelo

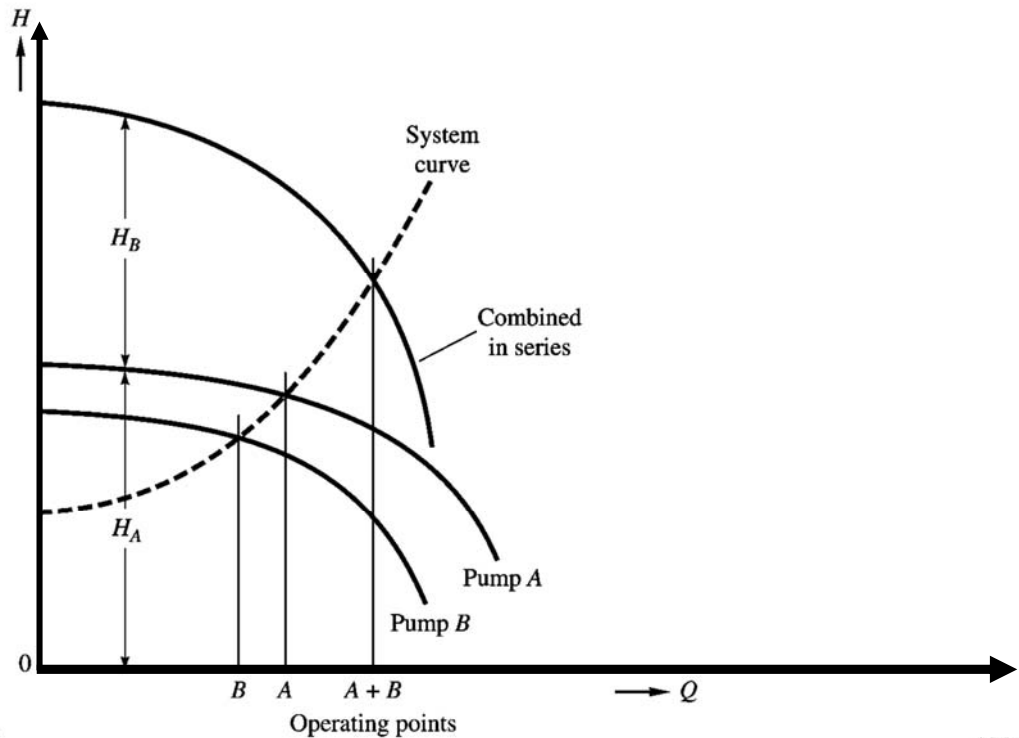
For a very flat (static) curve two similar pumps in parallel will deliver nearly twice the flow. The combined brake horsepower is found by adding brake horsepower for each of pumps A and B at the same head as the operating point. The combined efficiency equals  $\rho g(Q_{A+B})(H_{A+B})/(550 \text{ bhp}_{A+B})$ .

If pumps A and B are not identical, as in Fig. 11.18, pump B should not be run and cannot even be started up if the operating point is above its shutoff head.



## Pompe in serie

If a pump provides the right discharge but too little head, consider adding a similar pump in series, with the output of pump *B* fed directly into the suction side of pump *A*. As sketched in Fig. 11.19, the physical principle for summing in series is that the two heads add at the same flow rate to give the combined-performance curve. The two



## Pompe in serie

need not be identical at all, since they merely handle the same discharge; they may even have different speeds, although normally both are driven by the same shaft.

The need for a series arrangement implies that the system curve is steep, i.e., requires higher head than either pump *A* or *B* can provide. The combined operating-point head will be more than either *A* or *B* separately but not as great as their sum. The combined power is the sum of brake horsepower for *A* and *B* at the operating point flow rate. The combined efficiency is

$$\frac{\rho g (Q_{A+B}) (H_{A+B})}{550 \text{ bhp}_{A+B}}$$

similar to parallel pumps.

Whether pumps are used in series or in parallel, the arrangement will be uneconomical unless both pumps are operating near their best efficiency.

